



University of Ioannina

Department of Health Sciences

Faculty of Medicine

Biological Chemistry Laboratory

Inter-institutional Interdepartmental Program of
Postgraduate Studies
“Molecular and Cellular Biology and Biotechnology”

**Nuclear Envelope: Protein Interactions
and chromatin landscape.**

Tsomakian Konstantinos

Molecular Biologist

Master's Degree Thesis

April 2025,

Ioannina

Prologue

The current thesis work has been conducted in the laboratory of Biological Chemistry of the University of Ioannina under the supervision of Professor Anastasia Politou between the years 2022-2023. First of all I would like to express my sincere gratitude to Prof. Anastasia Politou for accepting me into her lab as a master's student and for kindly exposing me to knowledge and experiences that would otherwise have been impossible. I would also like to thank her for the excellent supervision during the entire course of my project. Additionally, I would like to express my gratitude to the post doctoral researcher of the lab Katerina Soupsana for always pushing me to become a better researcher and learn more. The supervision and technical assistance that Katerina provided to me were of major importance .

Furthermore, I would also like to express my deepest and kindest thanks to the rest of the lab members Dionisis, Evangelia, Eleni and Pavlina who welcomed me in the lab and kindly helped me any time I needed it.

Last but not least, I would also like to express my appreciation to my friends Dimitris, Panagiotis, Christina and Antonia as well as to my family for their unwavering support throughout this journey.

Contents

Contents.....	3
Abstract.....	6
Περίληψη.....	7
1. Introduction.....	9
1.1 The eukaryotic cell nucleus.....	10
1.1.1 Origin of the cell nucleus.....	10
1.1.2 The role of the Nuclear Envelope.....	12
1.1.2.1 Nuclear Envelope and cellular organization.....	12
1.1.2.2 Nuclear envelope and gene expression.....	13
1.1.2.3 Nuclear envelope and aging.....	13
1.1.3 Structure and dynamics of the Nuclear Envelope.....	14
1.2. Genome Organization.....	21
1.2.1 Low level genome organization.....	21
1.2.2 Chromatin Looping and TADs.....	21
1.2.3.1 Role of Histone Modifications in Genome Organization.....	23
1.2.3.2 Role of direct DNA modifications in Genome Organization.....	25
1.2.4 Higher Order Domains and Compartments.....	25
1.2.4.1 Lamina Associated Domains.....	25
1.2.4.2 Gene Regulation at the Nuclear Lamina.....	26
1.2.4.3 Nuclear Lamina and Genome Stability.....	27
1.2.4.4 Chromosome Territories.....	27
1.2.4.5 A and B compartments.....	28
1.2.4.6 Functional Phase Separation and Higher-Order Nuclear Organization.....	30
1.3. Nuclear envelope, nuclear periphery proteins and chromatin organization.....	31
1.3.1 LEM-Domain Proteins and Chromatin Organization.....	31
1.3.2 NPCs and Nucleoporins.....	32
1.3.3 LINC protein complex and Mechanotransduction in the Nuclear Envelope.....	34
1.3.4 The Nuclear Lamina.....	34

1.3.5 Lamin B Receptor (LBR).....	36
1.3.5.1 Structure and Function of Lamin B Receptor.....	36
1.3.5.2 Transmembrane Domains and Sterol Reductase Activity.....	38
1.3.5.3 LBR's Role in Genome Stability.....	39
1.3.6 PRR14 Protein.....	40
2. Materials and Methods.....	44
2.1 Cell culture.....	45
2.2 Plasmids.....	45
2.3 Transfection.....	45
2.5 Indirect Immunofluorescence.....	46
2.6 Confocal microscopy.....	47
2.7 Cell growth measuring.....	48
2.8 Heterochromatic foci measuring.....	48
2.9 Fluorescence Recovery After Photobleaching (FRAP).....	48
2.9.1 Experimental Procedure.....	48
2.9.2 FRAP Data analysis.....	49
2.10 SDS-PAGE.....	50
2.11 Western blot.....	50
2.12 Generation of stable cell lines.....	51
2.13.1 Cell lysis and sample preparation.....	51
2.13.2 Pre-clearance of the samples.....	52
2.13.3 Pulldown with streptavidin beads.....	52
3. RESULTS.....	53
3.1 Double knockout clones show significant growth impairment compared to control clones.....	55
3.2 Cholesterol supplementation fails to restore proliferation in LBR-LMNA/C double knockout clones.....	57
3.3 Loss of LBR and LMNA/C leads to asymmetric localization of nuclear periphery proteins without compromising nuclear envelope integrity.....	59
3.4 Heterochromatin organization is subtly affected by LBR and LMNA/C loss.....	63

3.5 Chromatin dynamics remain unchanged upon LBR and LMNA/C loss.....	65
3.7 Generation of stable cell lines expressing LBR or PRR14 fused with a biotin ligase.....	77
3.8 Pulldown of biotinylated proteins of the generated cell lines.....	86
4. Discussion.....	89
References.....	96

Abstract

In eukaryotic cells a dual membrane system separates the genetic information stored inside the cell nucleus from the rest of the cell. Wrapped around protein complexes, DNA takes the form of chromatin that can be divided into two main categories, active chromatin and inactive chromatin. In most eukaryotic cells active chromatin, also referred as euchromatin takes up the nuclear interior, while inactive chromatin also referred as heterochromatin takes up the nuclear periphery. Experiments by Salovei et al., have yielded two major findings regarding chromatin organization. First, the two key players responsible for tethering heterochromatin to the nuclear periphery are Lamin B Receptor (LBR) and A type lamins, as downregulation of these proteins leads to a reversed chromatin architecture. Second, this role of LBR and A type lamins is sequential with regards to development as LBR is mostly responsible for heterochromatin tethering to the nuclear periphery during early developmental stages, while A type lamins are responsible for heterochromatin tethering to the nuclear periphery on differentiated cells. Here, we used NIH/3T3 cells, generated by former lab members, where LBR or LMNA/C or both were deleted. Double KO clones were derived from LMNA/C KO cells as well as from LBR KO cells to account for the sequential manner that the two proteins function. We demonstrate that despite the mislocalization of several nuclear envelope proteins, nuclear integrity is maintained in cells lacking both LBR and LMNA/C. Our findings also suggest that the previously reported growth impairment is unlikely to be linked to LBR's sterol reductase activity. Moreover, while chromatin retains a generally conventional architecture, we observe a subtle shift toward an inverted-like configuration, accompanied by significant changes in gene expression and modest alterations in chromatin dynamics. The maintenance of conventional chromatin organization in the absence of these key envelope components points to the involvement of additional mechanisms governing chromatin topology. Furthermore, given the lack of compelling evidence implicating LBR or LMNA/C in specific biological processes, we support the prevailing view that these proteins primarily serve as general-purpose chromatin tethers rather than functioning in specialized cellular pathways. Finally, we successfully established stable cell lines for future identification of potential PRR14 and LBR interactors, as

well as the local proteome environment of these proteins, using the BioID2 proximity labeling system.

Περίληψη

Στα ευκαρυωτικά κύτταρα ένα σύστημα διπλής μεμβράνης διαχωρίζει το γενετικό υλικό το οποίο βρίσκεται μέσα στον πυρήνα από το υπόλοιπο κύτταρο. Το DNA είναι τυλιγμένο γύρω από πρωτεϊνικά σύμπλοκα σχηματίζοντας έτσι την χρωματίνη. Η χρωματίνη μπορεί να χωριστεί σε δύο υποκατηγορίες, την ενεργή και την μη ενεργή. Η ενεργή χρωματίνη η οποία αναφέρεται επίσης και ως ευχρωματίνη καταλαμβάνει κυρίως το εσωτερικό του πυρήνα, ενώ η μη ενεργή χρωματίνη η οποία αναφέρεται επίσης και ως ετεροχρωματίνη καταλαμβάνει κυρίως την πυρηνική περιφέρεια. Πειράματα από την Salovei et al., οδήγησαν σε δύο σημαντικά ευρήματα αναφορικά με την οργάνωση της χρωματίνης. Αρχικά ως βασικοί παράγοντες για την οργάνωση της χρωματίνης ταυτοποιήθηκαν ο LBR και οι A τύπου λαμίνες, καθώς απουσία αυτών η χρωματίνη αποκτά ανεστραμμένη οργάνωση. Επίσης βρέθηκε πως οι δύο αυτές πρωτεΐνες λειτουργούν σε χρονική σειρά κατά την ανάπτυξη όπου ο LBR είναι υπεύθυνος για την δεσμευση της ετεροχρωματίνης στον πυρηνική περιφέρεια στα αρχικά αναπτυξιακά στάδια, ενώ οι A τύπου λαμίνες είναι υπεύθυνες για την δεσμευση της ετεροχρωματίνης στον πυρηνική περιφέρεια σε διαφοροποιημένα κύτταρα. Στην παρούσα μελέτη χρησιμοποιήσαμε NIH/3T3 κύτταρα με απαλλοιφή είτε του LBR είτε των A τύπου λαμινών, είτε και των δύο. Λαμβάνοντας υπόψη την χρονική σειρά με την οποία οι δύο πρωτεΐνες λειτουργούν οι διπλά KO κυτταρικές σειρές είχαν κατασκευαστεί από προηγούμενα μέλη του εργαστηρίου είτε από LBR KO κύτταρα, είτε από LMNA/C KO κύτταρα. Στην παρούσα εργασία χρησιμοποιήσαμε τις παραπάνω κυτταρικές σειρές για να δείξουμε ότι παρά τον ασύμμετρο εντοπισμό αρκετών πρωτεϊνών της πυρηνικής περιφέρειας, η ακεραιότητα του πυρήνα διατηρείται σε κύτταρα που στερούνται τόσο του LBR όσο και των LMNA/C. Ακόμη, τα ευρήματά μας υποδεικνύουν ότι η προηγουμένως χαρακτηρισμένη καθυστέρηση της κυτταρικής ανάπτυξης είναι απίθανο να σχετίζεται με τη ενεργότητα αναγωγής του LBR. Επιπλέον, ενώ η χρωματίνη διατηρεί την συμβατική αρχιτεκτονική, παρατηρούμε μια λεπτή μετατόπιση προς μια "ανεστραμμένου τύπου" διαμόρφωση, η οποία συνοδεύεται από σημαντικές αλλαγές στην γονιδιακή έκφραση και μέτριες μόνο τροποποιήσεις στη δυναμική της

χρωματίνης. Η διατήρηση της συμβατικής οργάνωσης της χρωματίνης απουσία αυτών των βασικών συστατικών του περιβλήματος υποδηλώνει την ύπαρξη επιπρόσθετων μηχανισμών που ρυθμίζουν την τοπολογία της χρωματίνης. Επιπροσθέτως, δεδομένης της έλλειψης πειστικών αποδείξεων που να συνδέουν τον LBR ή τον LMNA/C με εξειδικευμένες βιολογικές διεργασίες, υποστηρίζουμε την επικρατούσα άποψη ότι αυτές οι πρωτεΐνες λειτουργούν κυρίως ως “αγκυρες” της χρωματίνης και όχι στο πλαίσιο ως στοιχεία εξειδικευμένων βιολογικών διεργασιών. Τέλος, δημιουργήσαμε επιτυχώς σταθερές κυτταρικές σειρές για τη μελλοντική ταυτοποίηση πιθανών αλληλεπιδρώντων των PRR14 και LBR, καθώς και του τοπικού πρωτεϊνικού περιβάλλοντος αυτών των πρωτεϊνών, χρησιμοποιώντας το σύστημα BioID2.

1. Introduction

1.1 The eukaryotic cell nucleus

1.1.1 Origin of the cell nucleus

The mammalian cell nucleus is the most profound cellular organelle and the one that defines eukaryotic cells. It is the cellular compartment where the genetic material is stored and separated from the rest of the cellular content by a set of two distinct yet connecting lipid layers that collectively form the nuclear barrier known as the nuclear envelope (D' Angelo and Hetzer, 2005). The origin of the nucleus is not clearly understood and possesses a still debated subject in the field of eukaryote evolution. Several models that attempt to describe the origin of the eukaryotic cell nucleus exist and in general can be divided into two main groups (**Figure 1**). First, there are models explaining the presence of the nucleus as a result of symbiosis between two organisms, where one symbiont turned into the nucleus and the other one into the cytoplasm and the outer cell structure. Alternative models suggest that the cell nucleus appeared as a result of extended differentiation in the internal membrane system of an individual cell by a autokaryogenesis process (Lisitsyana and Sheval, 2016).

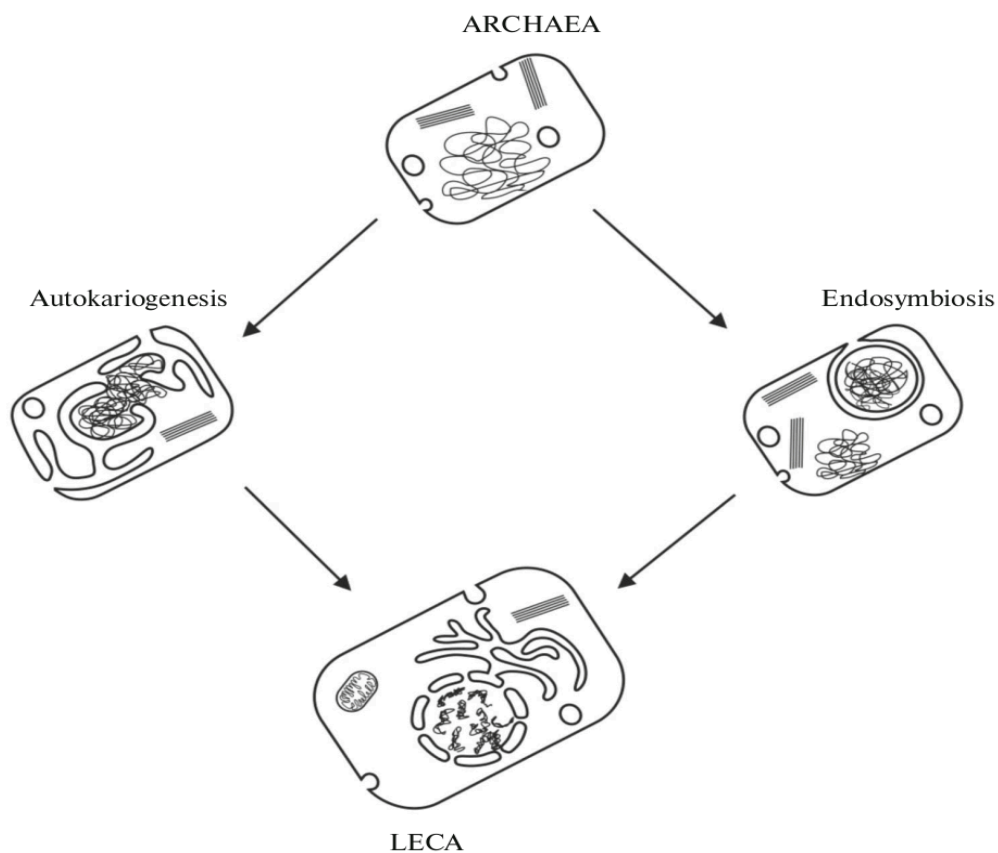


Figure 1: The two models describing the formation of the eukaryotic cell nucleus. Starting from archaea through an autokaryogenesis process where the DNA was engulfed in a membrane system or through endosymbiosis where the engulfment of another cell or virus resulted in the formation of the nucleus and the Last Eukaryotic Common Ancestor (LECA) (from Lisitsyna and Shevala 2016).

According to the theories supporting an endosymbiotic model, the cell nucleus appeared as a result of a cell to cell or cell to virus engulfment. Following a series of transformations, it is supposed that the engulfed cell or virus turned into the cell nucleus. Mereschkowsky was the first to propose an endosymbiotic model where a prokaryotic cell engulfed by an amoeboid cell turned into a cell nucleus (Mereschkowsky, 1905). Models explaining the formation of nucleus as a result of anaerobic syntrophy also exist. On the other hand, most of the studies supporting an autokaryogenesis model aim to explain the formation of the cell nucleus as a result of invaginations of the cell membrane that led to the formation of a separate organelle containing the genome (Cavalier-Smith, 2002). Additionally, models inspired by the endosporiosis process of the Gram-positive bacteria support that the formation of a nucleus could be explained by an abnormal cell division where the one daughter cell got trapped inside the other and eventually formed a nucleus (Lisitsyana and Sheval, 2016; Gould et al., 1979).

The advent of electron microscopy gave the opportunity to study finer cell structures in more detail and later experiments on oocytes of Triturus and Xenopus defined the nuclear boundary to what is today commonly accepted as a dual lipid membrane, the nuclear envelope (NE) (Watson 1955, Callan and Tomlin, 1950). The same experiments also revealed the existence of pores on the membrane, as they described the nuclear envelope having a continuous internal membrane and a porous external one. (Callan and Tomlin, 1950). Later work by Hartmann on nerve cells confirmed the presence of a double layered membrane separating the nuclear content from the rest of the cell but failed to describe any structures resembling pores (Hartman, 1953). Finally, as early as 1955, electron microscopy experiments carried out by Watson on several different organism specimens revealed that indeed the Nuclear Envelope consists of two membranes spanned by pores. Watson not only revealed that the nuclear pores penetrate both nuclear membranes but also that the two membranes are continuous one to the other and in certain specimens he studied, the external nuclear membrane appeared to be in continuity with the endoplasmic reticulum as well (**Figure 2**) (Watson, 1955)

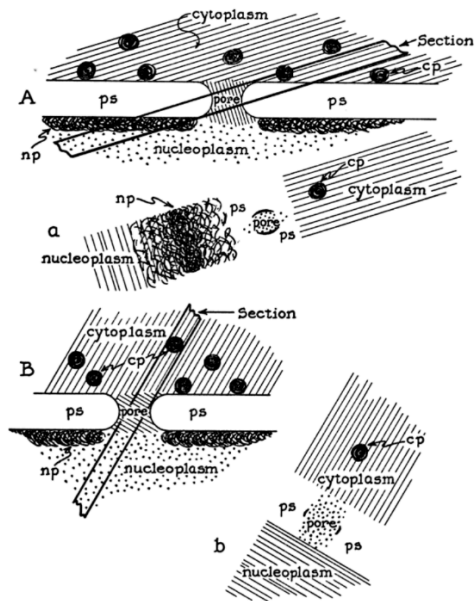


Figure 2: The first representation of the Nuclear Envelope as a double membraned layer spanned by pores penetrating both membranes (from Watson 1955).

1.1.2 The role of the Nuclear Envelope

As described above the nuclear envelope consists of a dual lipid membrane system, one facing the nuclear content and thus called inner nuclear membrane (INM), and one facing the cytoplasm and thus called outer nuclear membrane (ONM). Both INM and ONM are continuous with respect to each other whilst the ONM is also in straight continuity with the membranes of the cell's endoplasmic reticulum. However, apart from the obvious functionality that the nuclear envelope displays on separating and protecting the genome from the rest of the cell's content there are also several other functionalities that have been attributed to the nuclear envelope including roles in cell organization, regulation of gene expression and aging.

1.1.2.1 Nuclear Envelope and cellular organization

Several cell functions rely on proper nuclear localization inside the cell. Cell migration, division and overall development are all processes that require reorganization of the internal cell structures. (D' Angelo and Hetzer, 2005). The LiNC complex couples the nuclear envelope to the cytoskeleton and during migration the cell leverages this connection to fully rearrange the position of the organelles providing polarity to the cell, allowing it to exert the physical and spatial needs that the

migrating/envasing environment possesses (Calero-Cuenca et al., 2018). Firstly described in fibroblasts, the cytoskeleton through the actin based retrograde system of transportation leads to nuclear positioning at the leading edge of the migrating cell (R. Gomes et. al., 2005), whereas there are cases where during migration the nucleus stays at the back suggesting an important role of the cell nucleus positioning during migration (Zhen et al., 2002; Papakumar et al., 2004)

1.1.2.2 Nuclear envelope and gene expression.

The nuclear envelope functions as a regulator of gene expression mostly through its protein content. Requirements such as a specific epigenetic state and chromatin organization should be fulfilled in order for expression to occur. The proteome of the inner nuclear membrane and the underlying lamina meshwork create a suppressive environment for gene expression. In more detail, Lamin B Receptor and LMNA/C are considered the key players responsible for sequestering the inactive part of the genome at the nuclear periphery (Salovei et al., 2012). Gene expression is also regulated by the nuclear pore complexes in both direct and indirect manners. Indirectly NPC can regulate gene expression by giving access of regulatory proteins to the genome, whereas recent studies in both yeast and plants describe NPC as transcriptional hubs allowing the expression of genes in close proximity to the complex (Grossman et al. 2012, Raices and D'Angelo 2012; Henikoff and Smith et al. 2015). Finally, as previously mentioned the nuclear envelope can regulate gene expression by propagating mechanical stimuli through the LINC complex (Wong et al., 2021).

1.1.2.3 Nuclear envelope and aging

The presence of mutations in the LMNA/C gene in individuals with the premature aging syndrome Hutchinson-Gilford progeria (HGPS) suggests a direct role of the nuclear periphery in the mechanisms regulating aging (Lamis et al., 2022). Furthermore, the identification of such mutations increased the interest for further investigation of the relationship of the nuclear envelope and the associated proteins with the process of aging. Aging can be described as a functional decline of an organism that reflects several well-described defects/hallmarks to a cellular level including decreased

stemness, cellular senescence and genomic instability (Lopez-Otin et al., 2023). All these features are tightly bound to the proper function of the nuclear envelope. Reduced stemness of cells has been linked to nucleoplasmic protein sequestering at the nuclear periphery potentially indicating defects in the NE transport system and reduced NE integrity. Reduced chromatin dynamics after LMNA ablation leading to reduced differentiation capacity of mouse embryonic stem cells has been described as well (F. Martins et al. 2020). As expected, being the protective cell of the genome, loss of NE integrity can lead to genomic instability. NE ruptures expose the DNA to the cytoplasm promoting genomic instability (Vargas et al. 2012), whereas in migrating cancer cells nuclear deformation leads to decreased NE integrity (C.M. Denais et al. 2016). Finally, loss of expression of LBR, an integrated protein of the inner nuclear membrane is observed in senescent cells, a phenotype tightly related to cellular aging (Arai et al. 2019).

1.1.3 Structure and dynamics of the Nuclear Envelope

Structurally the nuclear envelope is an extension of the ER that forms two parallel lipid bilayers, one facing the nucleoplasm and thus called inner nuclear membrane (INM) and one facing the cytoplasm and thus called outer nuclear membrane (ONM). The INM and the ONM are separated by a ~40 nm long luminal space and fused in specified sites where supramolecular protein assemblies, the nuclear pore complexes (NPCs), span the envelope, providing a passing point for cargo targeted to and from the nucleus (**Figure 3**) (Hennen et al., 2020). The inner and outer membranes of the envelope, although considered as an extension of the ER, host their own lipid and protein content that distinguish the NE from the other membrane systems of the cell, ultimately providing to the nuclear envelope all the functionalities described above (Bahmanyar and Schlieker 2020).

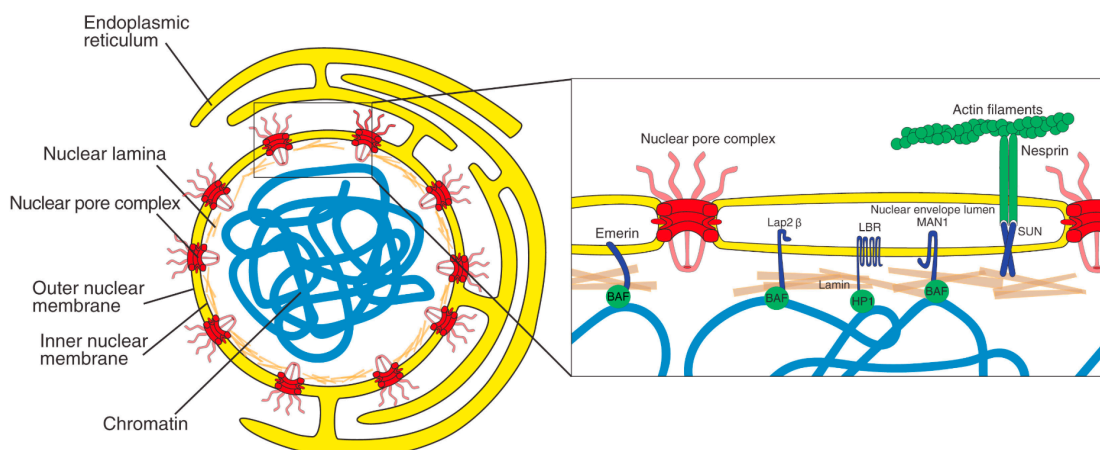


Figure 3: Schematic representation of the nuclear envelope. The nuclear envelope surrounds the genetic material (blue) and it is shown to be in direct continuity with the endoplasmic reticulum (yellow). Both the inner and outer nuclear membrane are also shown. Big macromolecular protein structures, the nuclear pores (red), penetrate the nuclear envelope connecting the cytoplasm with the nucleoplasm. (from Magistris and Antonin, 2018)

Regarding its content, the nuclear envelope is a dynamic structure undergoing several morphological reformations over the lifespan of the cell. The protein content as well as the lipid content of the two membranes of the envelope change during interphase, while the whole envelope gets disorganized during open mitosis and reorganized into two new fully functional NEs on the daughter cells. NE homeostasis during interphase is maintained by balancing the incorporation of new NE constituents (proteins and lipids) and the disposal of the defective ones. Most of the cell's lipid synthesis takes place at the ER, which is in straight continuity with the membranes of the nuclear envelope, suggesting that the lipid content of the NE is probably maintained by free diffusion of lipids from the ER and thus considering unlikely the existence of any specific lipid transfer system to the NE (Magistris and Antonin, 2018). Although this free diffusion system of lipids to the NE presumes to prevent any spatial segregation of lipids and the existence of any NE specific lipid environment, studies have shown the presence of unique lipids on the INM that support several NE related functions (Marschall et al., 2011; Hatch and Hetzer, 2014; J. Berg et al., 2002). Mass spectrometry analysis from van Meer shows that the ER and NE membranes mostly contain unsaturated glycerophospholipids and only a small portion of their precursor lipids (van Meer et al., 2008). Cholesterol and its intermediates are also found in very low levels, although the Lamin B Receptor, an INM integrated protein, has a key role in cholesterol biosynthesis (van Meer et al., 2008, Tsai et al., 2016). Collectively, the relative absence of cholesterol and its intermediates, whilst the abundance of unsaturated glycerolipids provide a loose packing to the ER/NE membranes that is suitable for protein exchange and incorporation of new proteins on the ER/NE membranes. Additionally, the specific lipid composition of ER/NE membrane has a crucial role in protecting the genome as overexpression of fatty acid elongase protein 2 (Elo2) to produce long chain fatty acids leads to the suppression of NE envelope ruptures on yeast, whereas the accumulation of long-chain sphingolipids precursors suppresses NE defects resulting from aneuploidy (Kinugasa et al., 2019, Hwang et al., 2019).

Nuclear Pore Complexes are the biggest and most profound constituents of the NE and are the structures that facilitate communication between the nucleoplasm and the cytoplasm. During

interphase, where the NE expands to host the replicating genome, the number of NPCs almost doubles. Additionally, new NPCs can be recruited to the NE in response to metabolic stimuli or during differentiation pointing to the existence of mechanisms that regulate this dynamic feature of the nuclear envelope (Doucet et al., 2010; Maul et al. 1971). Two different mechanisms of incorporating NPCs at the nuclear envelope have been described (**Figure 4**). A postmitotic one that refers to the NPCs targeted to NE during NE reformation upon cell division, and an interphase one where NPC assembly occurs after the new NE has been formed (Otsuka and Ellenberg 2017). During mitotic exit and within a few minutes, a large number of NPCs assemble at the nuclear envelope in parallel to NE sealing, whereas sporadic NPC assembly events that take about an hour occur during interphase (Otsuka et al., 2016, Otsuka et al. 2017). Regarding the postmitotic assembly process, experiments on *Xenopus* egg extracts have recognized a stepwise process where Nups, subunits of the NPC, reach the chromatin and subsequently assemble to a functional NPC with ELYS identified as a key protein in initiating the process (Rasala et al., 2008). Furthermore, live cell imaging and high-resolution electron tomography on different time intervals (one-minute intervals) of human cells, with respect to mitotic chromosome segregation, revealed that the rapid formation of nuclear pores during membrane sealing proceeds through the formation of prepores, approximately half the size of the mature pore complex that progressively collect the rest of the complex subunits and finally form the mature pore complex (Otsuka et al., 2017).

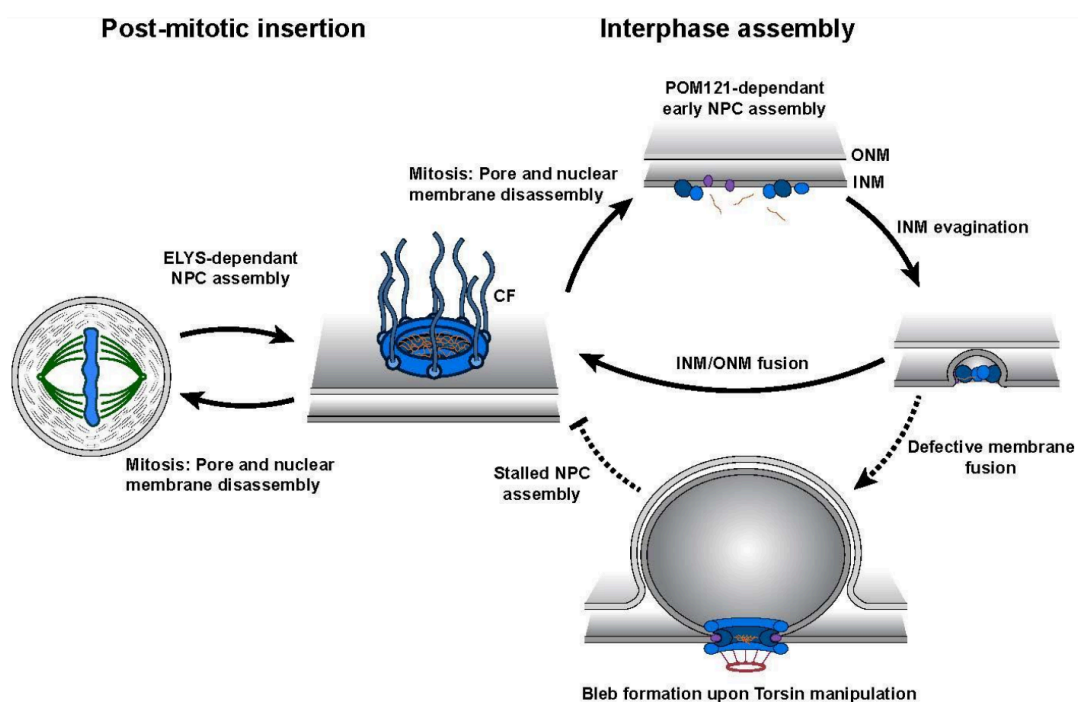


Figure 4: Schematic representation of the two distinct processes of nuclear pore complex assembly. Post mitotic NPC assembly involves the recruitment and incorporation of pre-existing NPCs on the forming nuclear envelope (left part of the image), while the interphase process involves the de-novo construction and integration of NPCs in continuous parts of the NE (right part of the image). (from Rampello et al., 2020)

On the other hand, the process of interphase NPC assembly is less well studied due to the sporadic nature of the process and the fact that the NPCs assembled during interphase are mixed with the postmitotic ones and thus not easily distinguishable (Otsuka and Ellenberg 2017). Interestingly, some of the proteins required for the interphase assembly process appear to be dispensable for the postmitotic process suggesting the presence of different mechanisms regulating the two processes (Otsuka et al. 2017). Mechanistically the incorporation of pores to the membrane requires the fusion of the inner and the outer membrane in the incorporation sites. Experiments on human and rat cells studying NPC assembly intermediates revealed that the interphase assembly proceeds through an inside-out mechanism where the INM grows in depth until it reaches and fuses with the ONM (Otsuka et al., 2016). Mechanistically this expanding structure of the INM is supported and probably initiated by an eight-fold symmetric nuclear ring protein complex/ NPC intermediate that underlies the INM (Otsuka et al., 2016). The cues that initiate this process although not directly identified, might be the recruitment of any of Nup153, Nup53, Pom21 or Sun1 as their targeting in the INM is required for the assembly of the pore complexes during interphase (Otsuka et al., 2017).

The most dynamic feature of the nuclear envelope is on display during cell mitosis. In the course of evolution eukaryotic cells have developed different strategies to enable proper division of the genetic material stored in the nucleus. Ranging from yeasts that deploy mechanisms of closed mitosis where the NE envelope stays in a somewhat intact state to humans where the NE completely breaks down to allow access of microtubules to the mitotic chromatin. Adding to that, a plethora of intermediate mitotic processes that can be described as semi-open mitosis have also been observed (**Figure 5**) (Magistris and Antonin 2018). After all checkpoints of G2 are met, the cell is committed to mitosis. In both cases of close and open mitosis the process proceeds through 4 well defined steps, prophase, metaphase anaphase and telophase. For open mitosis the breakdown of the NE starts in prophase and is completed in the transition to metaphase in a step called prometaphase. The cue that initiates the breakdown of the nuclear envelope has been recognized as the loss of the NPC exclusion barrier followed by the presence of large NE gaps (Laurel et al., 2011; Lenart and Ellenberg, 2003). Experiments on starfish oocytes and on mammalian cells where the entrance of dextrans is monitored during the course of mitosis reveal increased permeability during NE

breakdown. Although this is expected due to the breakdown itself the experiments in starfish oocytes show that this increase in permeability precedes both the appearance of NE discontinuities and the breakdown of the underlying lamina meshwork, suggesting that indeed the cue that initiates disassembly is related to the loss of the exclusion barrier of the pore complexes (Lenart and Ellenberg, 2003). This process that takes place during prophase triggered by NPC phosphorylation and loss of Nup98 lead to changes in NPC composition, structure and transport properties, thus allowing the cytoplasmic pool of tubulins to enter the nucleus and form the mitotic spindle microtubules (Ellenberg et al., 1997; Linder et al., 2017; Okada and Sato 2015). Mechanistically two different processes are responsible for the breakdown. Phosphorylation and subsequent depolymerization of the nuclear lamina as well as physical tearing of NE membranes by the microtubule cytoskeleton (Guttinger et al., 2009). Firstly, A type lamins start to be released into the nucleoplasm while disorganization of the meshwork that B type lamins form is observed later on and after the pore complexes are disassembled and the NE permeability barrier has been lost (Ungricht et al., 2015; Funakoshi et al., 2011).

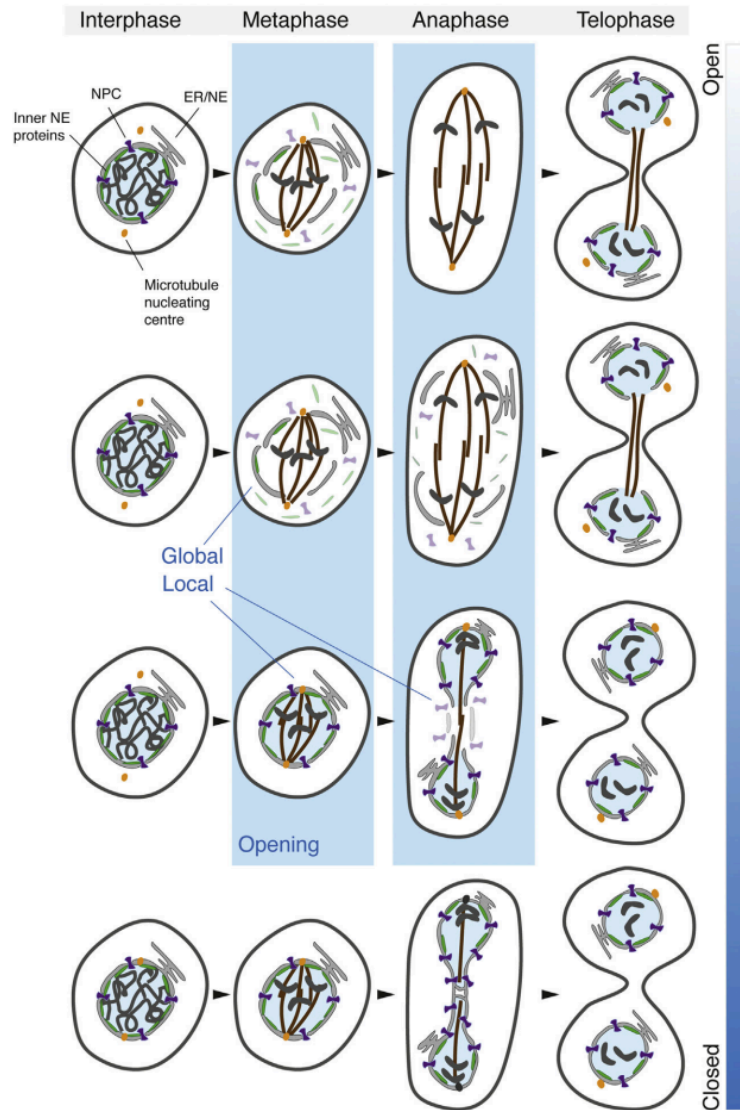


Figure 5. Schematic representation of the different types of mitosis regarding the structure of the nuclear envelope. Full breakdown of the nuclear envelope is observed in organisms that undergo open mitosis (upper part of the image), while in organisms that undergo closed mitosis the nuclear envelope stays intact (lower part of the image). Organisms where the nuclear envelope breaks down only partially during mitosis also exist (middle part of the image). (from Dey and Baum, 2021)

In late anaphase the sister chromatids of each chromosome have been separated and pulled to the two mitotic poles forming two distinct chromatin masses. At this stage the new nuclear envelopes start to reassemble through a process that includes chromatin decondensation, recruitment of NE membranes and NE components. At the end of telophase, the process has been completed and two new nuclei are formed (Ungrecht and Kutay, 2017). Finally, although lacking direct evidence

of the signals that initiates the assembly process an important cue responsible for the initiation of the assembly process seems to originate from the targeted localization of RanGTP on the surface of the chromatin and the dephosphorylation of nucleoporins and NE factors, the inactivation of CDK1 and the activation of the protein phosphatase 1 (PP1). Ran GTP is assumed to free NPC from inhibitory complexes while CDK1 deactivation inhibits mitotic activating signals and activation of PP1 leads to chromatin decondensation [111 from nature review] and organization of the lamina network (Schooley et al., 2015; Afonso et al., 2014, Vagnarelli et al., 2011; Wandke and Kutay 2013).

While the nuclear envelope membranes retreat to the ER during breakdown, they must be reassembled to new membranes for the daughter nuclei. NE reformation occurs through a process that involves the attraction of INM proteins, pore complexes and membranes from the tubular ER. The first step of this process is the reformation of the NE membrane through the binding of the tips of ER tubules to the decondensed chromatin (Anderson and Hetzer, 2007, Anderson and Hetzer, 2008). Among the candidate proteins that mediate this process are NDC1, POM121, SUN1 and Nups107-160 that are known to be located on curved regions of the membrane (Güttinger et al., 2009). Next, more NE material is recruited to the nascent membranes resulting in the conversion of the ER tubular membranes to flattened membrane patches on the chromatin (Anderson and Hetzer, 2007). Proteins of the reticulon family as well as the recruitment of INM proteins mostly control this process. Reticulon proteins have to be removed for the tubular structures to be flattened while INM proteins are needed to anchor the membrane patches to the chromatin (Anderson and Hetzer, 2007, Anderson and Hetzer, 2008). Especially the barrier of autointegration (BAF) has been shown to play a critical role in the recruitment of INM proteins carrying a LEM domain as shown in experiments in *C. Elegans* where depletion of VRK1 that phosphorylates BAF compromises NE formation and leads to LEM protein retention during mitosis (Gorjanacz et al., 2007). Interestingly, during the reformation process at the early telophase different regions of the chromatin attract different sets of NE proteins. While LBR, LAP2 β and lamin B take the peripheral chromatin regions, LAP2a, BAF, emerin and a small portion A type lamins initially take the core regions that face the spindle (Dechat et al., 2004; Haraguchi et al., 2008). Finally, the biggest portion of the lamin mass is acquired only when the nuclei have been competent for nuclear transport (Newport et al., 1990).

1.2. Genome Organization

1.2.1 Low level genome organization

In eukaryotic cells, genome organization starts at the fundamental level of DNA wrapped around proteins called histones, to form bigger structures, the nucleosomes that create a “beads-on-a-string” chromatin structure. Each nucleosome consists of approximately 147 base pairs of DNA that is wrapped around a set of 8 histones comprising the full nucleosome. This type of organization around the histones allows the DNA to adopt a compact yet dynamic structure that can either favor or prevent interactions with other proteins (Krietenstein et al., 2020; Hughes et al., 2015).

Recently, the advent of Next Generation Sequencing (NGS) techniques that allow a high-resolution sight to the genome, such as Micro-C (a variation of Hi-C), have allowed scientists to monitor chromatin resolution to nucleosome level, thus providing a more detailed view of the specific arrangement of nucleosomes inside the nucleus. Hsieh et al. used Micro-C to demonstrate single nucleosome placing to chromatin and nucleosome absence to functional elements such as promoters and enhancers [Hsieh et al. 2020]. Moreover, they also demonstrated that DNA wrapped around histones do not facilitate any long ranged higher conformation rather a zig-zag like structure that spans only a few nucleosomes. Interestingly in the same study they demonstrated that active genes exhibit increased nucleosome spacing and thus allowing for protein accessibility, which facilitates transcription factor binding, indicating the importance of nucleosome positioning in gene regulation. (Hsieh et al., 2020)

1.2.2 Chromatin Looping and TADs

Although a high degree of packaging is achieved by nucleosomes, a higher order of packaging of mammalian DNA is required to fit the entire genome into the narrow space of the NE. In order for chromatin to be further packaged, it is organized first into loops and later into larger topologically associated domains. Structurally, genomic loops are conserved functional features of the genomes across organisms that can range from kbs to Mbs (Dekker and Misteli 2015). At their simplest form they can associate functional elements of the genome to exert gene regulation. More complex loops are found as well. For example, several functional elements can come in close proximity through looping and form super-enhancers or even include entire gene clusters that need to be co-regulated

such as developmental gene clusters whose expression should be precisely regulated (Vermunt et al., 2019) (**Figure 6**).

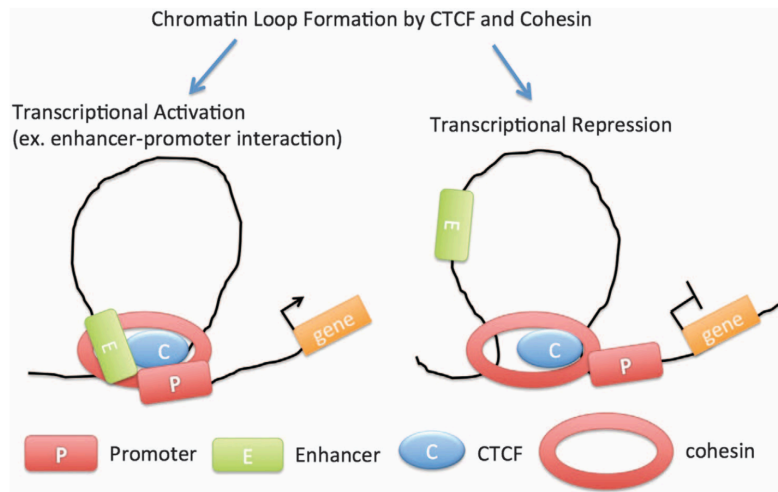


Figure 6: Formation of chromatin loops and their effect in gene expression. Loops can bring in close proximity functional elements resulting in transcriptional activation (left part of the image) or can isolate activating elements from gene promoters resulting in transcriptional repression (right part of the image). (from Kim et al., 2015)

Scaling up, topologically associated domains are formed by architectural proteins that define their boundaries (**Figure 7**). Firstly identified via in situ hybridization and then confirmed via genome wide conformation assays, TADs span several kb to Mb of genomic distance (Cremer and Cremer, 2010, Lieberman-Aiden et al., 2009;). Cohesin and the CCCTC-binding factor (CTCF) are the proteins that mainly drive TAD formation. Cohesin is a protein complex belonging to the structural maintenance of chromosome (SMC) protein family that creates loops through a loop extrusion mechanism (Yoori Kim and Hangtao Yu 2020). Briefly, cohesin anchors chromatin and starts extruding loops. As extrusion proceeds bigger and bigger loops are formed. The process stops when cohesin meets a CTCF bound in the chromatin (Yoori Kim and Hangtao Yu 2020). CTCF is a transcription factor that binds to CCCTC motifs in the genome and as expected ChIP experiments demonstrate CTCF enrichment in the borders of TADs. Due to its non palindromic binding motif CTCF binds to chromatin to two different directions and interestingly TADs are demarcated by two convergent CTCF motifs.(Tom van Schaik et al. 2022, Elzo de Wit et al.2015, Dixon et al. 2012, Nora et. Al. 2012)

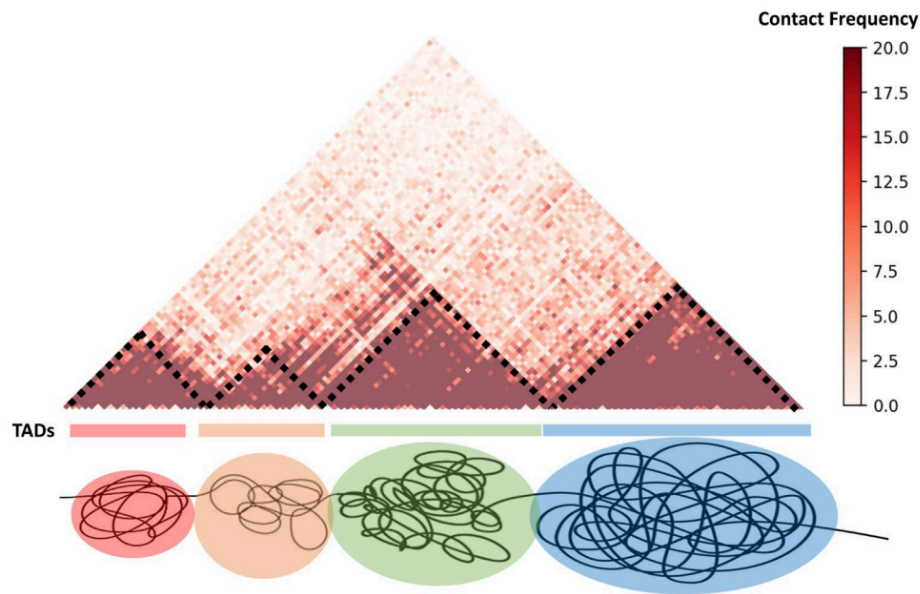


Figure 7: Schematic representations of chromatin conformation representing different contact frequency rates. Highly interacting genomic regions (deep red) form distinct genomic domains termed topologically associated domains (TADs). (from Joon Wei et al., 2022)

1.2.3.1 Role of Histone Modifications in Genome Organization

Apart from the information stored in genomic sequences there is an extra layer of information that determines gene expression. Namely, histone code includes a set of post translational modifications in histones that through their physicochemical properties regulate chromatin accessibility and transcription factor binding. Histones can be structurally divided into two parts, the defined histone fold domain that contains the regions responsible for interactions with the DNA and other histones and an N-terminal disordered tail that extends outside of the histone core and is prone to various chemical modifications (L. Mariño-Ramírez et al. 2005). The main chemical modifications found in histones are acetylation, phosphorylation and methylation. Acetyltransferases, kinases and methyltransferases respectively are the enzymes that deposit these modifications to the tails of histones (D. Rossetto et al. 2012). In general acetylation is related to chromatin openness because the addition of the acetyl group neutralizes the charge of the lysine residue that is added on, leading to an increase in nucleosome spacing, whereas methylation and phosphorylation are deposited predominantly on lysines, arginines and serines, tyrosines and threonines, respectively, and can be related to both repressive and activating events. Phosphorylation adds a negative charge to the

residue that marks, whereas methylation although does not alter the charge it can change the steric interactions of the residues because there can be up to three methyl groups added to the residue (D. Rossetto et al. 2012). For instance, phosphorylation of serine 10 of histone H3 or methylation of lysine 4 of the same histone results in chromatin relaxation and transcriptional activation of genes. Conversely, methylation of lysine 9 or lysine 27 of histone H3 results in chromatin condensation and transcriptional repression. Collectively, these chemical modifications can be read to alter the organization of the genome. For example, methylated lysines on histone 3 are recognized by the heterochromatin protein 1 through its bromodomain and compact chromatin whereas activating marks can be recognized by the chromatin remodelling complex SWI-SNF to regulate nucleosome positioning and form an open chromatin state (A. Kumar and H. Kono 2020). Finally there are several other modifications that occasionally occur such as ribosylation, ubiquitination and sumoylation and are related to more specific processes (**Figure 8**).

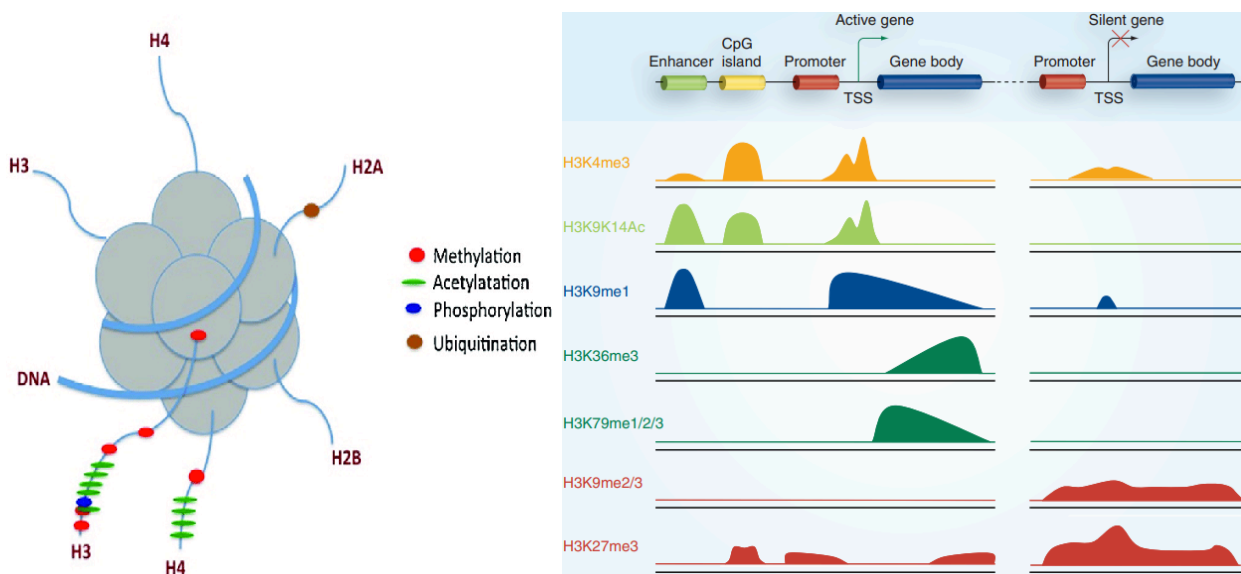


Figure 8: A) Representation of the DNA wrapped around the histone octamer forming a nucleosome. Histone tails are flanking outside the core histone structure and are chemically modified with methyl (red), acetyl (green) phosphate and ubiquitin (brown) groups (From Sahu et al., 2020). B) Distribution of different histone modification across the gene body and different functional elements regulating transcription (from Lim et al., 2010)

1.2.3.2 Role of direct DNA modifications in Genome Organization

In addition to histone modifications, direct DNA methylation is also a way to repress specific genes. DNA methylation occurs at specific cytosine nucleotides that precede guanine nucleotides, resulting in the creation of C-G dinucleotides (CpG). DNA methylation is a way to silence genes and establish cell type specific gene expression (A. M. Deaton and A. Bird 2011). Additionally it suppresses the movement of transposable elements such as LINEs within the genome promoting genome integrity. Interestingly the methylation pattern is maintained during DNA replication by the action of an enzyme that recognizes the methylated parent strand and catalyzes the same modifications in the daughter strand. However, these modifications are reversible as the methyl group can be oxidized by TET family members and replaced through the action of repair mechanisms. (F. M. Piccolo and A. G. Fisher 2014).

1.2.4 Higher Order Domains and Compartments

1.2.4.1 Lamina Associated Domains

Lamina-associated domains (LADs) are large genomic regions that interact with the nuclear lamina, covering up to 40% of the genome. LADs typically contain gene-poor, heterochromatic regions marked by repressive histone modifications mostly H3K9me2 and H3K27me3, that lack transcriptional activity (van Steensel and Belmont, 2017) (**Figure 9**). These domains play a key role in organizing the genome into functional compartments, namely A and B (further described later) thus separating active parts of the genome from inactive ones (Briand and Collas, 2020).

LADs can be subdivided into two types. Constitutive LADs (cLADs), which are consistently associated with the nuclear lamina across cell types, and facultative LADs (fLADs), which exhibit cell-type-specific and developmentally regulated interactions with the nuclear lamina. This separation of LADs allows cells to maintain low levels of transcription in genomic regions that threaten chromosomal integrity, such as transposable elements (LINEs/SINEs), while also providing the ability for cells to dynamically alter their gene expression profile in response to differentiation signals (Kind et al., 2015; Guelen et al., 2008).

LADs were firstly identified via DamID (DNA adenine methyltransferase identification), a sequencing based experimental process that allows monitoring of genomic regions that are in close proximity to the lamina meshwork. Following their identification DamID and ChIP-seq have been

extensively used, revealing that LADs are stable yet exhibit dynamic changes under certain conditions, such as during the cell cycle or in response to DNA damage (Kind et al., 2013). An example that showcases the dynamic nature of LADs is cell mitosis where LADs are released from the lamina, only to re-establish contact upon cell cycle progression into interphase. (Kind and van Steensel, 2010).

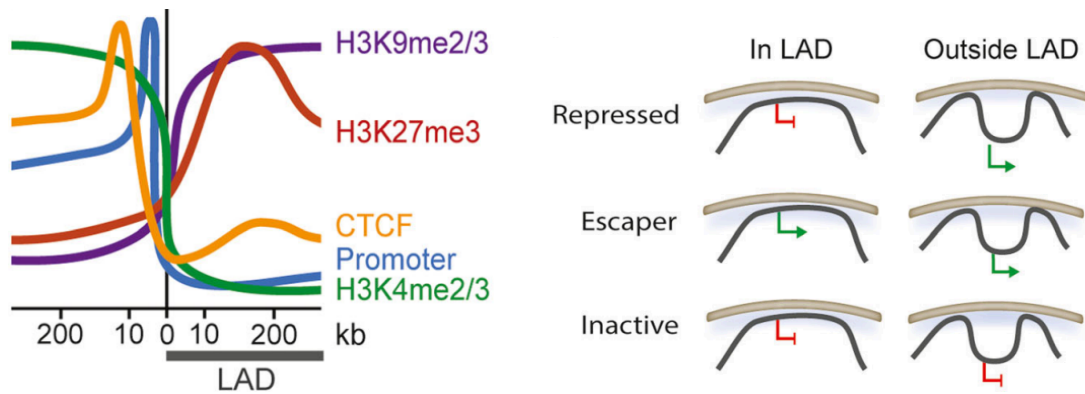


Figure 9: **A)** Changes in histone modification distributions between LADs and non-LADs. LADs are enriched for suppressive marks (H3K9me2/3 and H3K27me3) whereas chromatin regions outside LADs are enriched for activating modifications (H3K4me2/3). CTCF responsible for the formation of loops peaks at LAD borders. **B)** Schematic representation of active and inactive transcription with respect to the nuclear topology (inside LADs and outside LADs) (Briand and Collas 2020).

1.2.4.2 Gene Regulation at the Nuclear Lamina

As mentioned above, interactions between LADs and the nuclear lamina have significant implications for gene regulation, mostly linking LADs to transcriptional repression (Guelen et al., 2008). Experiments where expression loci were purposely tethered to the nuclear periphery resulted in expression silencing and reversely expression loci that were transposed from the periphery to the nuclear interior resulted in expression increase (Finlan et al., 2008). However there are also opposing experiments that demonstrate that the tethering of a loci to the periphery is not always adequate for expression silencing. Interestingly, Padeken et al. have shown links between cell type-specific regulatory elements and a particular subset of LADs that are solely marked with H3K9me2 and not H3K9me3 named KODs (H3K9me2 only domains) (Padeken et al., 2022). Overall if the correlation between expression silencing and nuclear periphery tethering demonstrates causation as well is a still highly debatable question in the field.

1.2.4.3 Nuclear Lamina and Genome Stability

Several functions regarding genome stability maintenance, chromatin organization and DNA repair, particularly in the case of double strand break (DSB) repair, have been attributed to nuclear lamina. Regarding the role of nuclear lamina in double strand break repair it has been demonstrated that lamins are able to interact with DNA repair proteins, making the nuclear periphery a focal point for damage recognition and repair (M. Shokrollahi et al. 2024). Furthermore, damaged LADs are capable of dissociating from the nuclear lamina in order to reach repair factors. Once repair is complete these domains can retreat back to the nuclear periphery overall showcasing the highly dynamic nature of the chromatin domains (Tenga and Medalia, 2020).

Mutations in genes that encode lamins disrupt genome stability and have been linked to a series of disorders all together known as laminopathies. Mutations in the gene that encode A type lamins cause progeria syndrome that is characterized by accelerated cell aging, while mutations in the genes that encode B type lamins lead to another type of diseases called leukodystrophies characterized by increased neuron demyelination (Shimi et al., 2015; Harhour et al., 2018; Briand and Collas, 2020). Altogether, the presence of such disorders highlights the importance of lamins in nuclear integrity and cellular health.

1.2.4.4 Chromosome Territories

Interphase chromosomes are not randomly distributed within the nucleus. Instead they occupy distinct regions of the nuclear interior named chromosome territories. These territories were firstly identified by in situ fluorescence experiments that utilized probes that bind to repetitive sequences, specific for each chromosome, thus allowing to stain chromosomes with different fluorescent substances in order to reveal their different nuclear topology (**Figure 10**) (Bolzer et al., 2005). Later, the advent of high throughput sequencing approaches to studying chromatin conformation such as Hi-C confirmed that chromosomes organize into distinct domains by demonstrating that intra chromosomal interactions are higher compared to the inter chromosomal ones (Lieberman-Aiden et al., 2009). However, these territories are not static domains. Instead there are examples in both differentiating and malignant cells where genes are able to reposition inside the chromosome territory (Williams et al. 2006; K. J. Meaburn et al 2009). Interestingly, the

boundaries of the territories are not sharply defined. Instead, the edges of neighboring chromosome territories interact, forming overlapping domains called intermingling or kissing chromosomes (Branco and Pombo, 2006; Cremer and Cremer, 2010). In many cases this type of interactions lead to the formation of membraneless functional structures such as the nucleolus where the genes encoding the rRNAs are distributed across five different chromosomes that come close to exert the formation of the nucleolus or the genes for the olfactory receptors that are also distributed across several chromosomes and through interactions come together to form the olfactosome (McStay, 2016; Lomvardas et al., 2006; Monahan et al., 2017). Other structures regulating gene expression between loci of neighboring chromosomes have been proposed to result from interactions between neighboring territories (Barutcu et a., 2022)

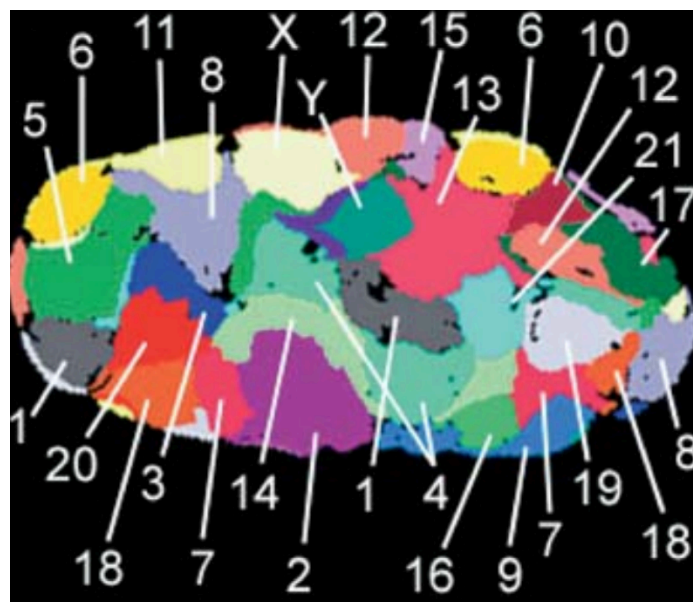


Figure 10: Map of the human chromosomes represented as chromosome territories. (from Bolzer et al., 2005)

1.2.4.5 A and B compartments

On the top level of the genome organization hierarchy, chromatin can be divided into as little as two compartments (**Figure 11**). Since 2009 when Lieberman et al. proposed the Hi-C method for capturing interactions between genomic loci 3D genomic interactions can be visualized in the two dimensional space as interaction frequencies across bins of the genome (Lieberman-Erez et al.,

2009). This type of visualization of the architecture of the genome results in a plaid like pattern that when overlaid with epigenetic features reveals the presence of two mutually exclusive chromatin compartments, one corresponding to the active early replicating part of the genome named compartment A and one corresponding to the inactive late replicating part of the genome named compartment B (Lieberman-Erez et al. 2009).

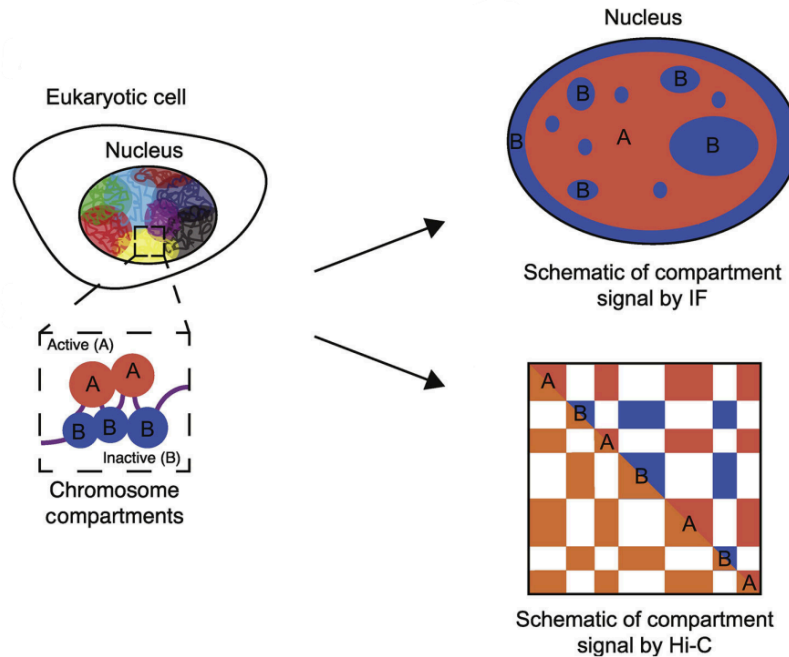


Figure 11: Schematic representation of the A and B compartments of chromatin. B compartment occupies mostly the nuclear periphery whereas A compartment occupies mostly the nuclear interior . (from Hildebrand and Dekker, 2020)

In nuclei following the conventional nuclear architecture compartment B occupies mostly the peripheral heterochromatin anchored to the nuclear lamina and the nuclear envelope as well as the heterochromatic layer that covers the nuclei, overall containing mostly gene-poor, A/T rich regions and LINE transposable elements. On the other hand, compartment A covers the active part of the genome and occupies mostly the interior of the nucleus (T. Misteli 2020). Recently, optimizations on the Hi-C protocol that allow for identification of higher resolution interactions as well as the advent of new computational tools that integrate epigenetic data for compartment identification have revealed the presence of subcompartments in both compartment A and B (S.S.P. Rao et al. 2014). Rao et al used unsupervised clustering methods on deeply sequenced Hi-C libraries on 9 different human cell lines and found that at least 6 subcompartments exist, two for compartment A and four for compartment B. While both A1 and A2 exhibit early replication and are correlated to activating histone marks, A1 finishes replication first and A2 is more correlated to the repressive

mark H3K9me3 compared to A1. B1 corresponds to facultative heterochromatin due to its correlation to H3K27me3. B2 contains mostly pericentromeric heterochromatin located at the nuclear lamina and the NADs, whereas B3 is only enriched in LADs and not in NADs. Finally, B4 corresponds to a small part of the human chromosome 19 (11 Mb) and is extremely enriched in KRAB-ZNF genes, a family of genes encoding transcription factors carrying the transcriptional repressor KRAB domain (**Figure 12**) (Rao et al. 2014)

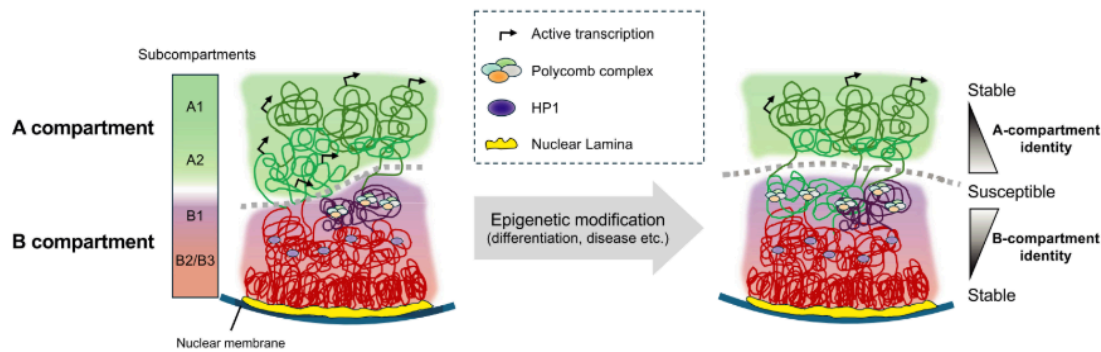


Figure 12) Compartmentalization of the chromatin into two distinct compartments. A compartment (green) takes the interior and is open for transcription whereas B compartment (red) segregates along with HP1 towards the nuclear periphery and transcription is less often compared to the A compartment(From Rao et al., 2014).

1.2.4.6 Functional Phase Separation and Higher-Order Nuclear Organization

Finally, by analogy with the cytoplasm, the nucleoplasm also contains nuclear bodies that perform distinct functions and compartmentalize the nucleus. The nuclear bodies are not surrounded by a membrane but maintain their coherence due to interactions mostly between RNA and proteins or just between proteins. They are dynamic structures as they constantly exchange their biomolecules with biomolecules of the nucleus. The most characteristic and profound nuclear body is the nucleolus, which is the center of transcription and processing of ribosomal RNAs as well as the center of assembly of ribosomal subunits. The polycomb bodies, which are specialized in the coordinated repression of genes of the same or different chromosomal regions, as well as the Cajal bodies, which are specialized in the assembly and processing of ribonucleoprotein complexes such as snRNPs. In addition to the characteristic nuclear bodies mentioned above, there is a wide variety of other bodies that help perform various nuclear functions and coordinate the transcription of different genetic loci (Mao et al., 2011).

1.3. Nuclear envelope, nuclear periphery proteins and chromatin organization.

1.3.1 LEM-Domain Proteins and Chromatin Organization

NE proteins, including LEM-domain proteins and nucleoporins, contribute significantly to nuclear structure and function, interfacing with chromatin, and the cytoskeleton (Hetzer and Wentze, 2009). LEM-domain proteins, such as emerin, LAP2, MAN1, and LEM2, are key INM components of the nuclear envelope that directly link nuclear structure to gene regulation. These proteins have the ability to bind chromatin mostly through interactions with the barrier-to-autointegration factor (BAF), tethering heterochromatin to the nuclear periphery and forcing gene repression and genome stability (Berk et al., 2013) (**Figure 13**). Emerin, for example, a conserved LEM-domain protein, is able to interact both with chromatin through BAF, the core components of the nuclear co-repressor (NCoR) complex and directly with HDAC3 leading to deacetylation of histone lysine residues, and thus stabilizing repressive chromatin domains at the nuclear periphery (Berk et al., 2013, Wong et al., 2021, Moser et al., 2020).

Additionally, LEM2 has specialized functions in nucleotide excision repair (NER), recruiting repair proteins to the nuclear periphery, which facilitates damage recognition and repair. This function demonstrates how NE proteins link genome stability to chromatin organization and highlight the broader role of LEM-domain proteins in coupling repair pathways with nuclear structure (Moser et al., 2020; Haraguchi et al., 2008).

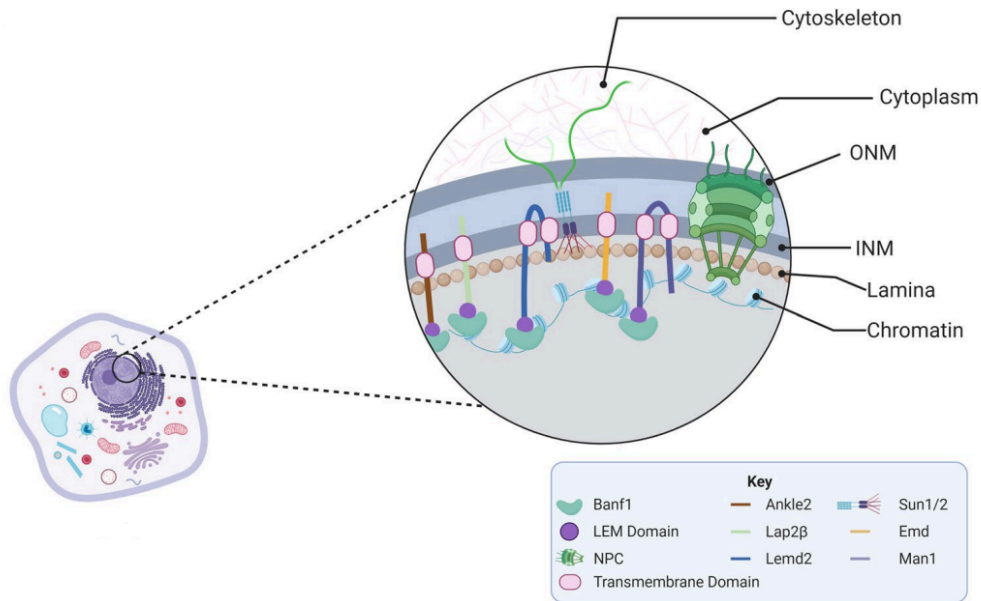


Figure 13: Schematic representation of the LEM domain containing proteins in the nuclear periphery. INM integrated proteins with a LEM domain flanking in the nuclear interior interact with heterochromatin or lamins (interaction not shown) through BAF and subsequently sequester heterochromatin to the nuclear periphery (edited from Rose et al., 2022)

1.3.2 NPCs and Nucleoporins

Nuclear pore complexes (NPCs) are the largest protein complexes found in the NE. NPCs are symmetric structures, serving as gateways for regulated nucleocytoplasmic transport. NPCs are composed of about 30 different nucleoporins (Nups), which firstly assemble into distinct subcomplexes all together building a functional pore that creates a selective transport channel through the nuclear envelope. The most profound NPC structures include cytoplasmic filaments, a central scaffold, and the nuclear basket. The FG-repeat Nups build the central channel form a hydrophobic barrier, selectively allowing small molecules to freely diffuse while larger macromolecules require active transport via the nuclear transport mechanism (**Figure 14**) (Knockenbauer and Schwartz, 2016, Wentz and Rout, 2010).

The NPC's modular architecture allows the complex to respond to different transport demands while maintaining nuclear integrity. This adaptability is achieved through structural components like the Y-complexes within the scaffold, which stabilize NPC architecture and facilitate its dynamic interactions with transport factors (Hoelz et al., 2016). Recently cryo-electron microscopy

has provided high-resolution insights into NPC structure, elucidating how the arrangement of Nups enables selective permeability and transport efficiency across the NE (Beck and Hurt, 2017; Kim et al., 2018).

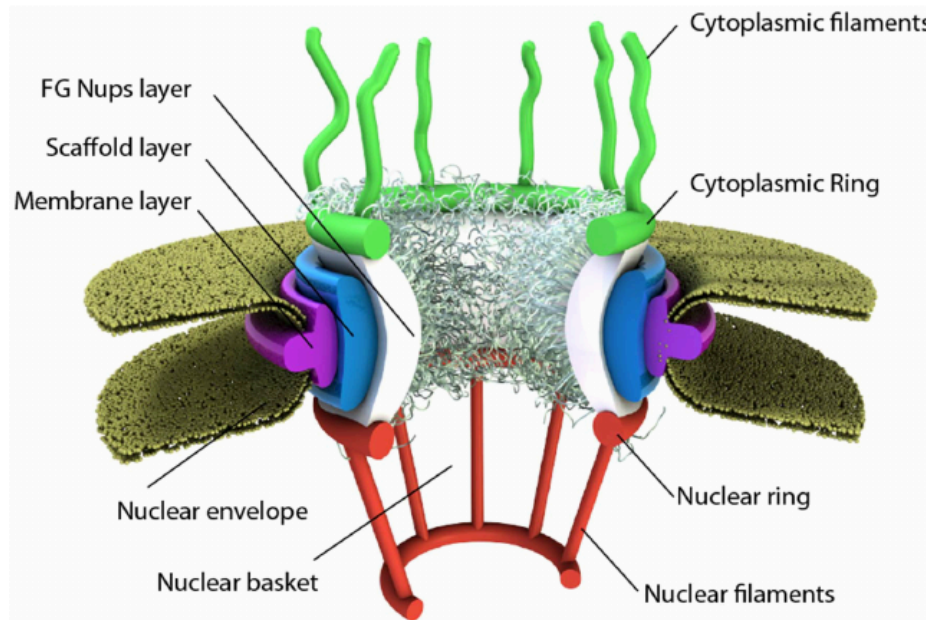


Figure 14 : Structure of nuclear pore complex. A scaffold is formed supporting the protein complex in the membrane. The FG nups (white) are shown with the FG (Phenylalanine-Glycine) disordered parts of them exposed to the pore forming the pore barrier. A set of cytoplasmic filaments and nuclear filaments extend to the cytoplasm and the nucleoplasm respectively (From Azimi et al., 2013).

Beyond their transport roles, it has been shown that NPCs play significant regulatory roles in gene expression by organizing chromatin and supporting active transcription. Interestingly it has been demonstrated that nucleoporins like Nup153 and Nup98 associate with transcriptionally active chromatin regions beneath the pore complex, enhancing the expression of nearby genes and creating an area of active transcription in the nuclear periphery. Imaging experiments performed by Capelson et al. have demonstrated that Nup98 colocalizes with phosphorylated RNAPol2 showcasing the correlation of active transcription to tethering genomic loci to NPCs (Capelson et al., 2010). Furthermore, NPCs are also known to interact with the histone acetyltransferase SAGA and mRNA export factors Sac3-Thp1 suggesting a model where actively transcribed genes located nearby the NPCs are processed and directly targeted to the nucleoplasm (Sood and Brickner, 2014; Roopa Luthra et al. 2007).

Furthermore, NPCs are shown to be implicated in the regulation of specific gene clusters. One such example is Nup98 where it is shown to influence the expression of genes involved in cell cycle progression and immune response by recruiting transcription factors and chromatin remodelers, such as the Trithorax complex, to target genomic loci. This recruitment results in increased chromatin accessibility and as a result transcriptional activation, underscoring the importance of NPCs in gene expression with regard to differentiation and cellular stress (Franks et al., 2016; Gozalo et al., 2020).

1.3.3 LINC protein complex and Mechanotransduction in the Nuclear Envelope

Mechanotransduction is the conversion of mechanical stimulation into intracellular signaling, which in turn allows cells to adapt their cytoskeleton and behavior accordingly. This connection between the cytoskeleton and nuclear interior is mediated through an interaction with the linker of the nucleoskeleton and cytoskeleton (LINC) complex. Correspondingly, the LINC complex transmits external forces across to NE thereby affecting nuclear shape, stiffness (Lombardi et al., 2011) and gene expression is downregulated or up-regulated alike. Mechanotransductive signaling requires NE proteins (emerin). In the presence of external mechanical signals emerin interacts directly with lamin A/C and actin filaments causing changes in chromatin structure as well as transcriptional regulation. Through regulating nuclear stiffness, soft material mechanosensitive proteins modulate chromatin accessibility to alter transcriptional and differentiation outcomes in response to mechanical environments. It is not surprising, then, that defects in NE proteins that contribute to a tissue's ability to experience its mechanical environment and vice versa are also common drivers of disease states such as muscular dystrophy or cardiomyopathy (Kirby and Lammerding 2018; Miroshnikova et al., 2022).

1.3.4 The Nuclear Lamina

Underlying the inner nuclear membrane (INM) is a thick, filamentous layer called the nuclear lamina (NL), which is primarily made up of type V intermediate filament proteins called lamins. This structural network influences processes including gene regulation, nuclear placement, and cellular differentiation by providing to the nucleus mechanical stability and establishing functional interactions with chromatin (**Figure 15**). The spatial organization of the genome is largely dependent on the nuclear lamina as a huge portion of the genome is directly interacting with the

lamina meshwork. Interactions between lamins and genomic regions build up lamina-associated domains (LADs), which help to compartmentalize chromatin into active and repressive states (Gruenbaum et al., 2005; Kind and van Steensel, 2010).

The LMNA/C, LMNB1, and LMNB2 genes encode the A- (lamins A and C) and B-type (lamins B1 and B2) lamins respectively that make up the nuclear lamina. B-type lamins are generally expressed in all somatic cells and are related in both structural support and cell-specific tasks, whereas A-type lamins are mostly expressed in differentiated cells (Nazer, 2022, Salovei et al 2012). Under the nuclear envelope, the lamin network creates a scaffold that connects nuclear mechanics to chromatin structure, gene expression, and DNA repair mechanisms (Shimi et al., 2015).

Lamin filaments are arranged in a meshwork with a diameter of around 3.5 nm, as demonstrated by cryo-electron microscopy and super-resolution imaging. This meshwork gives the nuclear lamina its distinct mechanical characteristics. In addition to providing physical stress protection for the nucleus, this structure facilitates mechanotransduction within the cell by integrating cytoskeleton signals through the linker of nucleoskeleton and cytoskeleton (LINC) complex (Tenga and Medalia, 2020; Kirby et. al., 2018).

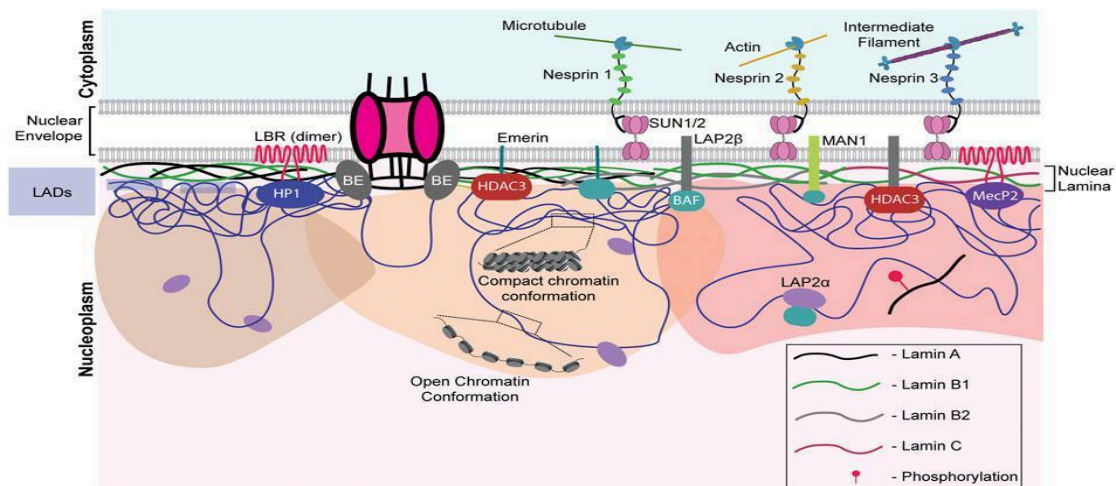


Figure 15: Schematic representation of the interactions taking place at the nuclear periphery. A lamina meshwork is organized beneath the nuclear envelope. LEM domain proteins such as MAN1 LAP2 and Emerin interact with BAF and the nuclear lamina and heterochromatin as well. LBR is shown here as a dimer binding heterochromatin through HP1 or with MeCP2. The mechanotransduction system connecting tubulins to the nucleoskeleton through nesprin and SUN 1 / 2 is also shown (From Balaji et al.,2020).

1.3.5 Lamin B Receptor (LBR)

The Lamin B Receptor (LBR) is an integral protein of the inner nuclear membrane (INM) with key roles in processes including nuclear organization, expression silencing, chromatin tethering to the nuclear periphery, and cholesterol metabolism. It has the ability to anchor heterochromatin to the nuclear envelope, a function that directly impacts genome stability, transcriptional regulation, and cellular differentiation. It was firstly described by Worman and Georgatos in 1988 and further studies on the structure of the protein and the phenotypes induced by its absence have underscored the interplay of the protein in several processes while also linking its absence to a variety of diseases (Worman et al. 1988, Olins et al., 2010, Hirano et al., 2012). LBR is synthesized in the ER and carries two sequence motifs comprising a nuclear localization signal. The translocation of LBR from the ER to the INM is achieved through a diffusion-retention mechanism. Through diffusion LBR proteins firstly reach the outer nuclear membrane and next through lateral diffusion via the peripheral pores of the NPCs are targeted to the inner nuclear membrane to which they are retained through interactions with several nuclear components such as the chromatin, the nuclear lamina and other proteins (Smith et al., 1993; Soulmann et al., 1993; Ellenberg et al., 1997).

1.3.5.1 Structure and Function of Lamin B Receptor

The structure of LBR comprises an N-terminal nucleoplasmic domain and eight transmembrane domains anchoring the protein to the inner nuclear membrane, and a sterol reductase domain at the C-terminus end (**Figure 16**). Interestingly, the N-terminal domain that carries the bipartite NLS and only one of the transmembrane domains are adequate to localize LBR in the INM (Giannios et al., 2017). Mutations on the gene of LBR affecting different parts of the produced protein show that each domain contributes uniquely to LBR's diverse functions, allowing it to act both as a structural anchor and as an enzymatic regulator within the nuclear membrane (Nikolakaki et al., 2017). Regarding the chromatin binding roles of LBR early pulldown experiments targeting LBR led to isolation of chromatin marked with the H3K9me3 and H3K29me3 histone marks (Makastori et al., 2004)

The N-terminal domain of LBR contains two distinct chromatin-binding regions and a protein binding one. Starting from the N terminal end of LBR's structure there is a Tudor domain, a domain enriched with arginine and serine residues named arginine-serine-rich (RS) domain and a globular domain.

Tudor domains were firstly described in drosophila as domains that acquire an antiparallel b-fold structure that allows for recognition of methylated lysine and arginine residues (Hirano et al., 2012). Multidimensional NMR spectroscopy experiments by Liokatis et al. revealed the antiparallel b sheet structure that the ovarian 60 first residues acquire, while follow up structural homology searches of the same region revealed high similarity to previously known tudor domains of other proteins (Liokatis et al. 2012). In LBR the tudor domain along with the RS region allow the protein to recognize and interact with H4K20me2, a mark commonly associated with heterochromatin resulting in tethering H4K20me2 heterochromatin to the nuclear envelope (Hirano et al., 2012, Solovei et al., 2013, Liokatis et al 2012). Furthermore, it is assumed that this interaction of LBR along with its ability to multimerize in the nuclear periphery gives the protein the ability to compact chromatin leading to its repression (Nikolalkaki et. al 2017).

On the other hand, RS domains were first described in oocytes and are shown to be present in many proteins controlling intron splicing where RS domains are important for establishing protein-protein interactions (Shepard et al., 2009). Similarly in LBR the RS domain comprises a disordered region of the LBR protein structure (Liokatis et al 2012) that is responsible for establishing protein protein interactions with the interacting proteins being mostly Methyl Cp2 protein, lamin B and other LBR molecules. FRAP experiments on LBR demonstrated different kinetics of the protein leading to the assumption that LBR is not uniformly distributed in the nuclear periphery (Giannios et al., 2017). Later experiments showcased the ability of LBR to oligomerize forming insoluble protein clusters, possibly explaining the difference in FRAP kinetics as the difference between oligomerized and non oligomerized LBR molecules. The human LBR RS domain consists of four consecutive RS dipeptides whereas the avian one consists of five repeats. All Serine residues of the repeats are prone to phosphorylation by the SRPK1 kinase and the Akt1 and Akt2 kinases. Furthermore, Sellis et al. approaching the oligomerization of LBR with molecular dynamics simulations demonstrated that the phosphorylation of the RS domains results in formation of an Arg-claw like structure where the phosphorylation groups are exposed to the periphery (Sellis et al. 2012). Additionally, experiments by Nikolakaki et al. demonstrated that phosphorylation of the RS domain of RS domain containing proteins leads to their dissociation, all together leading to the conclusion that

oligomerization of LBR molecules is regulated by the phosphorylation state of its RS domain (Nikolakaki et al., 1996).

Lastly the N terminal domain of LBR carries also a globular domain which is responsible for the interactions with the heterochromatin protein 1, thus tethering H3K9me3 marked heterochromatin to the nuclear periphery. Deletion of either the tudor or the globular domain of the LBR resulted in reduced transcriptional repression mediated by LBR (Nikolakaki et al., 2017).

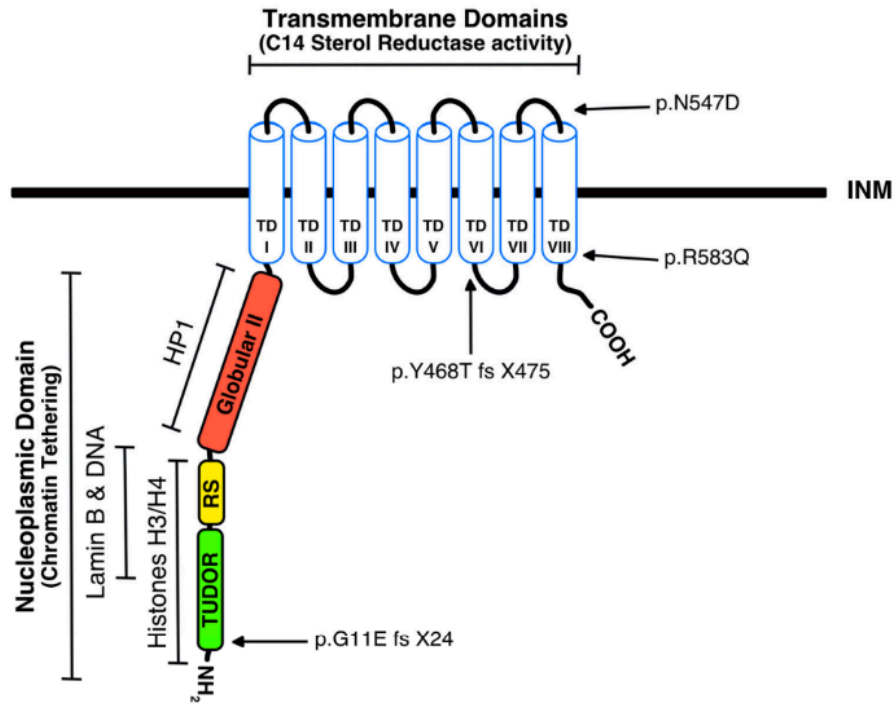


Figure 16: Schematic representation of the structure and associated functions of the Lamin B receptor. Eight transmembrane domains on the C-terminal end span the Inner Nuclear Membrane and are responsible for the Sterol reductase activity of LBR. The N terminal part of the protein hosts a region with arginine-serine repeats prone to phosphorylation and responsible for LBR oligomerization while also implicated along with a TUDOR domain with the interactions of LBR with MeCP2 and lamin B. A globular domain also exists responsible for interactions with heterochromatin protein 1 (from Nikolakaki et al., 2017).

1.3.5.2 Transmembrane Domains and Sterol Reductase Activity

LBR's C-terminal sterol reductase domain has eight transmembrane segments that contribute to its enzymatic activity, essential for cholesterol biosynthesis. This domain enables LBR to function in sterol metabolism, specifically through the reduction of the C14-unsaturated bond of lanosterol. (Olins et al., 2010).

Although TM7SF2 also is able to catalyze this specific reduction step that LBR mediates, mutations in the sterol reductase domain of LBR have been suggested to disrupt cholesterol metabolism, causing several diseases in humans with the most well studied being the Pelger-Huët anomaly (PHA) and Greenberg skeletal dysplasia, whereas analogous homozygous mutation in mice cause skin impairments of a phenotype known as ichthyosis. PHA is characterized by abnormal nuclear shape in blood cells, where nuclear mechanics are affected due to dysfunctional LBR whereas Greenberg is a fatal syndrome characterized by bone abnormalities. These pathologies underscore LBR's essential structural and functional roles within the nuclear membrane. (Bickmore and van Steensel, 2013)

1.3.5.3 LBR's Role in Genome Stability

Much attention has been drawn lately to the link of LBR and cellular senescence. Cellular senescence refers to a cell state of irreversible growth arrest. This phenotype is characterized by genomic instability, a characteristic secretory phenotype (SASP) and can be induced either due to aging, oncogene activation or even by exposure to specific chemicals such as thymidine (Huang et al., 2022). Studies have shown that LBR downregulation is associated with increased chromatin dynamics and the release of heterochromatin from the nuclear periphery, leading to genomic instability promoting senescence pathways. In senescent cells, the detachment of heterochromatin from the nuclear periphery is accompanied by a reduction in LBR expression, contributing to changes in nuclear shape and chromatin reorganization that are hallmarks of cellular aging (Arai et al. 2019).

The connection between LBR and cellular senescence is also evident in cancer. Reduced LBR expression has been linked to genomic instability in tumor cells, suggesting that LBR functions as a tumor suppressor by preserving nuclear structure and preventing DNA damage. This role in tumor suppression underscores the importance of LBR in safeguarding nuclear integrity across different cell types and stages of cellular life (Lukášová et al., 2017).

1.3.6 PRR14 Protein

Recent studies have highlighted proline-rich protein 14 (PRR14) as a protein that is important in heterochromatin organization within the nucleus, mostly through interactions with HP1 and Lamin A/C. More specifically, PRR14 has been directly linked to heterochromatin tethering to the nuclear periphery through interactions with the nuclear lamina (Poleshko et al., 2013; Kiseleva et al., 2023). PRR14 was firstly identified via a screening based method to detect epigenetic silencing factors as a transcriptional repressor (Poleshko et al., 2010) and later as a protein that colocalizes with the A type lamins during interphase (Poleshko et al., 2013). The peptide sequence of PRR14 consists of 585 amino acids with high proline content (Poleshko et al 2013). As expected, due to the high proline content of the protein, computational algorithms revealed that PRR14 is mostly disordered with only a few structured regions mostly responsible for its interactions with HP1 and lamina (Poleshko et al., 2013). Previous biochemical and proteomic studies have already demonstrated interactions between PRR14 and HP1 although to that point no interaction of the protein with A type lamins had been assessed (Nozawa et al., 2010; Rual et al., 2005).

Following its identification, multiple mutation and deletion experiments targeting different regions of the PRR14 protein sequence have revealed different functional parts of the protein. Regarding the structure of PRR14 the protein hosts distinct domains responsible for both lamina and chromatin association (**Figure 17**). Similarly to LBR, PRR14 is synthesized at the endoplasmic reticulum and its sequence hosts a bipartite nuclear localization signal that targets the protein to the nuclear interior. In the middle of the protein sequence an 120 amino acid long lamina binding domain (LBD) exists that can be reduced to a minimal LBD of 52 residues (231-282) that is evolutionary conserved beyond mammals. The LBD includes two distinct lamina binding motifs that are both needed for proper lamin localization of PRR14. Interestingly phosphorylation sites in these lamina binding motifs exist and missense mutations leading to changes in the phosphorylation targets resulted in increased PRR14 localization at the nuclear periphery demonstrating the phosphoregulated properties of PRR14 (Dunlevy et al 2020). Adding to that, FRAP experiments on wild type PRR14 and phospho-ablated PRR14 cells revealed higher recovery rates of the first, all together pointing to a notion of a highly dynamic phospho-regulated protein whose dynamics are tightly connected to the phospho-regulated nature of mitotic entry and mitotic exit.

Regarding its binding to heterochromatin, PRR14 carries two different variations of the LxVxL motif that heterochromatin protein 1 recognizes through its chromoshadow domain. Specifically,

there is a main LAVVL motif on the N terminal end of the protein that mostly mediates the interactions with HP1 but there is also an LVVML motif approximately 100 residues downstream of the first motif that also has the ability to interact with HP1. Interestingly, PRR14 is able to interact with all HP1 isoforms (α , β , γ). However, overexpression experiments of the protein and parallel visualization of the three HP1 isoforms demonstrated a much higher affinity of the PRR14 protein with the α and β isoforms.

Finally, the C terminal region of the protein carries probably the only ordered region of the protein with high similarity to the Tantalus protein family that also includes a Protein Phosphatase 2 Subunit A (PP2A) recognition motif. Mutations targeting this motif that disrupt PP2A binding result in mislocalization of the PRR14 leading to increased PRR14 in the nucleoplasm compared to the wild type one, overall suggesting a regulatory mechanism between the tantalus domain, PP2A and the phospho-regulated lamin binding domains of PRR14.

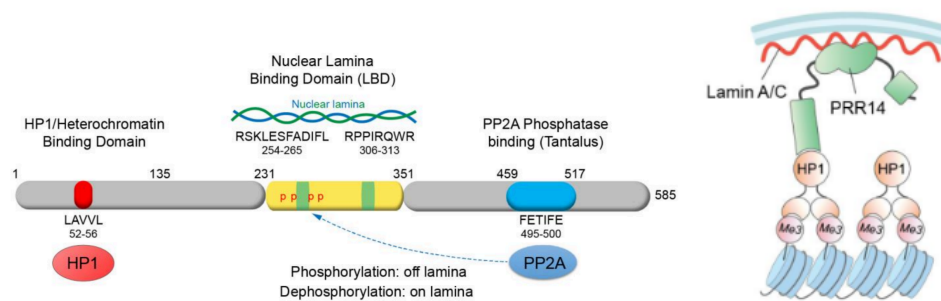


Figure 17: A) Schematic representation of the structure of the PRR14 protein. A bipartite nuclear localization signal targets the protein inside the nucleus while two Lamina binding domains (yellow) are responsible for interactions of PRR14 with A type lamins. An HP1 binding site (red) is responsible for interactions with HP1 and finally a tantalus domain carrying a binding site for the Protein Phosphatase 2 Subunit A (blue) regulates the phosphorylation of the protein (from Dunlevy et al., 2020). **B)** Mechanism connecting the structure of PRR14 on tethering heterochromatin to the nuclear periphery (from Kiseleva et al., 2023).

Regarding its overall distribution, super resolution microscopy demonstrated that a layer of PRR14 molecules are organized beneath the inner nuclear membrane following the distribution of A type

lamins thus creating somewhat of an anchoring layer for H3K9me3 marked heterochromatin (**Figure 9**). Additionally, regarding PRR14 dynamics, FRAP experiments on NIH/3T3 cells with profound heterochromatic foci enriched in PRR14 depleted of its lamina binding domain reveal high recovery rates suggesting a dynamic nature of the PRR14-HP1 interaction during interphase. On the other hand upon entering to mitosis and as the nuclear lamina gets disrupted, PRR14 also becomes phosphorylated and reestablishes contact with chromatin via HP1 during anaphase while later on the HP1 bound chromatin along with PRR14 bind to the newly organized nuclear lamina during telophase, showcasing a potential role of PRR14 in re-establishing the peripheral heterochromatin following mitotic exit (Poleshko et al., 2014, Poleshko et al., 2023).

Lastly, new data connect PRR14 to the biology of cancer, namely through its role in the PI3K/Akt/mTOR pathway. Some malignancies, such as lung cancer, have been shown to overexpress PRR14, which stimulates tumor growth by triggering PI3K signaling through interactions with GRB2. According to Yang et al., this pathway promotes cellular proliferation and resistance to apoptosis, which aids in oncogenesis and implies that PRR14 acts as an oncogene in malignancies linked to deregulation of the PI3K pathway. (Yang, M., et al. 2016)

Aim of the study

In the current thesis work we aim to explore the impact of LBR and LMNA/C loss—individually and in combination—on nuclear envelope architecture, chromatin dynamics and organization and transcriptional regulation. More specifically we want to integrate previous studies of the group regarding the growth of cells lacking LMNA/C, LBR or both as well as investigate whether non symmetrical distribution of peripheral proteins upon LMNA/C and LBR loss compromise nuclear envelope integrity. Additionally, we aim to assess changes in chromatin dynamics and organization following the loss of LBR, LMNA/C, or both and follow with transcriptome wide approaches to identify corresponding changes in gene expression. Finally we aim to identify potential compensatory factors that may act in response to LBR depletion, focusing on interactors of both LBR and the PRR14 protein.

2. Materials and Methods

2.1 Cell culture

NIH/3T3 cells were used for the experiments. NIH/3T3 cells were cultured in Dulbecco's Modified Eagles Medium (DMEM) - High Glucose with Sodium Pyruvate (Gibco, 41966-029), supplemented with 2 mM L-glutamine (Biosera, MS014N100P), 2mM (2mM, penicillin) (A201) 10% or 15% fetal bovine serum (FBS) (Gibco, 10270-106). In order to ensure their growth, the cells were maintained in an incubator with appropriate humidity at 37°C with simultaneous administration of 5% CO₂.

Cells were transferred to new plates every 2 days, when the plate confluency reached approximately 80%. The cell transfer procedure involved washing the cells twice with Dulbecco's buffered saline (DPBS) (Biosera, MS018S1002) and detaching them from the plate surface using a trypsin/EDTA solution (Biosera, MS00WA100M), diluted 1:2). The trypsin is then inactivated by adding fully supplemented growth medium and an appropriate amount of cells are transferred to new cell culture plates.

Long-term storage of the cells is made possible by detaching them from the culture plate using trypsin, centrifuging at 1000 rpm for 3 minutes and resuspending them in freezing medium, which contained 30% v/v FBS and 10% v/v dimethyl sulfoxide (DMSO) in DMEM. Finally, the cells are transferred to cryovials, slowly frozen at -80°C and stored in liquid nitrogen.

The recovery of cells from nitrogen is done by rapid thawing in a 37°C water bath, addition of fresh medium at an appropriate temperature and transfer to new cell culture dishes. At the same time, in order to avoid mycoplasma contamination, all cell lines are checked at regular intervals.

2.2 Plasmids

The plasmids used in this thesis have been designed and constructed by the former post doctoral fellow of the laboratory Katerina Soupsana. For FRAP experiments, pPycagip-eGFP-huHP1a was produced using standard cloning procedures, while pPycagip-birA-mLBR-HA, pPycagip-birA-mPRR14-HA and pPycagip-ATG-HA were generated using the In-fusion cloning kit from Takara Bio following manufacturer's protocol.

2.3 Transfection

Transfection of NIH/3T3 cells was performed using polyethylenimine (PEI). PEI is a positively charged synthetic polymer that can form complexes with the negatively charged phosphate groups of the DNA backbone and thereby introduce exogenous DNA into cells via endocytosis. Specifically, 2 µg of plasmid DNA (for a 35 mm dish) was diluted in 25 µl of free DMEM (Mixture 1) and 0.9 liters of PEI working solution (9 µg PEI in 500 liters of sterile cell culture water (Biosera, MS00Q2100A)) was diluted in 75 µl of free DMEM (Mixture 2). Mixture 1 and mixture 2 were combined in a third tube, mixed by pipette and incubated for 30 minutes at room temperature.

The cells were seeded in culture dishes one day before the day of transfection, in order to reach a plate filling percentage of approximately 50% at the time of transfection. In addition, immediately before the transfection procedure, the culture medium was replaced with fresh medium. For a 35 mm dish, 1 ml of fresh complete growth medium was used. Mixture 3 was added dropwise. A 4.5 hour incubation at 37°C followed. At the end of the incubation period, the medium was changed again. This time, 2 ml of fresh complete growth medium was added to the cells and incubated for 24-48 hours at 37°C, depending on the experiment.

2.4 Generation of stable cell lines

Generation of stable cell lines started by transfecting cells with one of pPycagip-birA-mLBR-HA, pPycagip-birA-mPRR14-HA or pPycagip-ATG-HA plasmid harboring a puromycin resistance gene. Cells harboring the plasmid were selected with addition 1 µg/ml puromycin (ThermoFischer). Cells were initially tested for efficacy of biotinylation and proper protein localization before selection. Proper protein localization was assessed after puromycin selection as well. Next, from each selected cell line cells were counted and diluted to achieve a concentration of one cell per well on a 96-well plate. Finally, seeded cells were grown to give raise to full clones. Final clones were assayed for proper protein expression localization and efficient biotinylation via western blotting and indirect immunofluorescence.

2.5 Indirect Immunofluorescence

To perform immunofluorescence experiments, cells were cultured on glass coverslips (#N1.5) until the desired plate filling was reached. They were then washed three times with PBS and fixed for 5-10 minutes at room temperature using a fixing solution containing 1-4% formaldehyde (FA)

diluted in PBS. The concentration of FA and the duration of incubation depended on the antibody used. After fixing the cells, two more washes were performed with PBS followed by incubation in Quench buffer (0.07 g glycine in 50 ml PBS) for 10 minutes at room temperature. The samples were washed once more with PBS and then incubated in blocking buffer (150 mM NaCl, 20 mM Hepes pH 7.4, 2 mM MgCl₂, 0.5% Fish Skin Gelatin, 0.2% Triton-X100, 0.1 mM at room temperature 1 mM). Primary antibodies diluted in blocking buffer were then added to the samples and incubated in a humidified chamber, protected from light for 1 hour. The samples were then washed three times with blocking buffer and in the last wash the samples were incubated in the blocking solution for 15 min. Then, the secondary antibodies were added, incubated and removed from the samples following the same protocol as the primary ones. A PBS wash step followed and the samples were incubated with TO-PRO 3 iodide solution (642/661) (Invitrogen, T3605) (diluted 1:10000 in PBS) for 1 hour at room temperature, protected from light. Finally, the samples were rinsed again five times with PBS and mounted on slides using an anti-fade mounting medium (Vectashield, H 1000). The samples were stored until examination at 4°C, protected from light.

Full details of the antibodies used can be found in Tables 1. All antibodies were previously tested for specificity and optimal fixation and dilution conditions.

Antibody	Species	Concentration	Reference
a-LMNB2	Rabbit	1:200	ProteinTech 10895-1-AP
a-HA	Rat	1:200	Roche 11-867-423-001
Anti-Rabbit IgG, Alexa Fluor 488	Goat	1:400	Invitrogen A11008
Anti-Mouse IgG, Alexa Fluor 568	Goat	1:400	Invitrogen A11004
Anti-Rat IgG, Alexa Fluor 568	Goat	1:200	Invitrogen A-11081
Streptavidin-488	-	1:100	Thermo S32354

Table 1: List of antibodies used in immunofluorescence experiments

2.6 Confocal microscopy

In all FRAP experiments, images were acquired with a Leica SP5 TCSII confocal microscope using an argon laser at 10% of maximum intensity, a solid-state diode laser (561 nm), a HeNe laser (633 nm) and a HCX PL APO CS 63X/1.4 oil or HCX PL APO CS 100X/1.4 oil objective. Bidirectional scanning at 400Hz was applied to acquire images and the sequential acquisition mode was used. Images were acquired as Z-stacks with 0.42 μm intervals and the line average was set to 2 or 4 (depending on the sample being observed). Image resolution was 512 x 512 pixels. All confocal images were processed using LAS X, and Fiji software.

2.7 Cell growth measuring

For cell growth assessment of the cells, cells were counted with a Neubauer hemocytometer and 5000 cells were seeded at day 0. Viable cells were counted using the same approach with trypan blue (ThermoFisher 0.4%) in 3x24 hour intervals after seeding.

2.8 Heterochromatic foci measuring

For heterochromatic foci measuring, cells were stained with DAPI and confocal images spanning the whole nucleus were acquired using Leica SP5 TCSII confocal microscope. The z-step used was 0.21 μm . Produced confocal images were imported to Fiji image analysis software where X and Y dimensions were measured on maximum projection, The Z dimension was considered as the number of z-steps from foci top to bottom multiplied by the step size.

2.9 Fluorescence Recovery After Photobleaching (FRAP)

2.9.1 Experimental Procedure

FRAP experiments were performed with a Leica SP5 TCSII confocal microscope using the Argon laser at 10% of maximum power and a HCX PL APO CS 63X/1.4 oil objective. The pinhole and zoom factor were adjusted to 1.57 Airy Units and 10-12, respectively. The image resolution was set to 256x256 pixels (8bit). The 488 nm laser line was at 15%, with an emission detection range of 500-550 nm. The regions of interest (ROI) were circular, 1 μm in diameter, and were bleached

using the 488 nm laser line at 100% of maximum power. Bidirectional scanning was applied at a rate of 1400Hz.

Before applying three bleaching pulses, 50 images were acquired (1 image every 0.113 sec). Upon completion of the experiment, 350 images were acquired every 0.113 sec. At the end of the experiment, the following ROIs were also recorded:

- a) unbleached ROI (unfrap) - a circular ROI of 1 μ m diameter in a similar area,
- b) the entire nucleus, and
- c) background - a circular ROI of 1 μ m diameter outside the nucleus.

The samples were maintained at a constant temperature of 37°C and their medium was changed to Minimum Essential Eagle's Medium (Sigma Aldrich, M3024).

2.9.2 FRAP Data analysis

Raw FRAP data were initially corrected for background fluorescence and photobleaching based on Kang et al., 2012. In more detail from raw FRAP data the background corrected signal was acquired by subtracting the fluorescence signal of a background region from the frap region and dividing by the fluorescence signal obtained by the unfrap region subtracted again by the background fluorescence.

$$F_{corrected}(t) = \frac{F_{frap}(t) - F_{bk}}{F_{unfrap}(t) - F_{bk}}$$

Finally the background corrected measurements were scaled to 0-1 using the following formula:

$$F(t) = \frac{F_{corrected}(t) - F_0}{F_i - F_0}$$

where $F_{corrected}(t)$ represents the background corrected signal at time point t , F_0 initial fluorescence of the bleached area prior bleaching and F_i the mean intensity of the bleached area prior bleach.

Given the normalized FRAP intensities the recovery halftime ($t_{1/2}$), the Mobile fraction and the diffusion coefficient(D_a) could be computed. $t_{1/2}$ is computed as the time point at which the bleached area had recovered half of its final intensity, M_f is computed as the average of the final recovered signal over the initial signal on the steady state, and D_a as proposed by Kang et al., 2012 using the following formula:

$$D_{confocal} = \frac{r_n^2 + r_e^2}{8 * t_{1/2}}$$

where r_n is the nominal radius of the bleached spot as defined by the user (in this case $r_n=0.5\mu\text{m}$) and r_e is the effective radius of a post bleach profile (here $r_e=0.5755\mu\text{m}$, as determined by colleagues in previous experiments)

Statistical analysis of the FRAP data was performed by Gerta Qamili (Dr. Mpatsidis group, Department of Mathematics, University of Ioannina). K-sample test was used to infer statistically significant changes arising from the FRAP data.

2.10 SDS-PAGE

For protein electrophoresis 13.5 % bis-acrylamide SDS-PAGE was used. Prior to that, cells were left to grow in approximately 90% confluence and subsequently washed with PBS, scraped off in trypsin solution (1:1 in PBS) and resuspended in Laemmli 2X sample buffer (10mM Tris-HCl pH 7, 4.6% SDS, 20% glycerol, 0.1%w/v bromophenol blue, 50mM DTT). Samples were denatured at 100 °C for 5 minutes and stored at -20 °C. Sample electrophoresis was performed at 180V in Electrode Buffer (0.025M Tris-Base, 0.192M glycine, SDS 0.1%)

2.11 Western blot

After sample electrophoresis, proteins were transferred onto a nitrocellulose membrane under the influence of an electric field in a tank filled with transfer buffer (1:2:7 parts of electrode buffer, methanol and ddH₂O). Following transfer, the nitrocellulose membrane was incubated in washing buffer (20 mM Tris-HCl pH 7.4, 155 mM NaCl, 0.1% Tween-20) and then blocked either overnight at 4°C or for 1.5 hour in RT in blocking buffer (5% skim milk powder dissolved in washing buffer). After removing the blocking buffer, the membrane was left O/N to incubate with the primary antibody. Next, four 10-minute washes were performed with washing buffer and the membrane was incubated with the secondary antibody for 1 hour at RT under gentle agitation. A full list of the antibodies used can be found in table 2. Finally, six washes of 5 minutes each were performed before detecting protein bands using enhanced chemiluminescence (ECL) for signal visualization. In the case of streptavidin the membrane was left to incubate with streptavidin conjugated with HRP and bands were directly visualized.

Antibody	Species	Concentration	Reference
a-HA	Rat	1:4000	Roche 11-867-423-001
a-rat HRP	Goat	1:3000	Proteintech SA00001-15
a-tubulin	Mouse	1:5000	Sigma T5168
a-mouse HRP	Goat	1:1000	Proteintech SA00001-1
Streptavidin-HRP	-	1/4000	Proteintech SA00001-0

Table 2: List of antibodies used in immunoblotting experiments.

2.12 Generation of stable cell lines

Generation of stable cell lines started by transfecting cells with one of pPycagip-birA-mLBR-HA, pPycagip-birA-mPRR14-HA or pPycagip-ATG-HA plasmid harboring a puromycin resistance gene. Cells harboring the plasmid were selected with addition 1 μ g/ml puromycin (ThermoFischer). Cells were initially tested for efficacy of biotinylation and proper protein localization before selection. Proper protein localization was assessed after puromycin selection as well. Next, from each selected cell line cells were counted and diluted to achieve a concentration of one cell per well on a 96-well plate. Finally, seeded cells were grown to give raise to full clones. Final clones were assayed for proper protein expression localization and efficient biotinylation via western blotting and indirect immunofluorescence.

2.13 Pulldown of biotinylated proteins

2.13.1 Cell lysis and sample preparation

For each replicate 2x100mm culture dishes of around 80% confluency were used. Upon adequate confluency levels cells were treated with 50 μ M biotin for 16 hours. An 20x biotin solution was produced and diluted to serum free medium prior to addition to the cell culture. Two washing steps with PBS followed and subsequently cells were lysed using 540 μ l lysis buffer(5M urea, 50 mM Tris pH 7.4,Protease inhibitors (EDTA-Free) and 1 mM DTT). For enhanced cell lysis and detachment

from the dish surface a cell scraper was used. Following cell lysis 0.1 μ l of Pierce Universal Nuclease (Thermo, 88700). was added on each dish and left to incubate for 10 minutes. 20% of Triton X was added to final concentration 1%. 5 cycles of sonication followed with settings of: 30 seconds at 30% cycle duty and output level 3. 1260 extra μ l of lysis buffer were added to achieve a total volume of around 2 ml. Subsequently the sample where transferred to eppendorf tubes, centrifuged (16500 x g for 10 minutes at 4°C) and the supernatant was transferred to a 5 ml falcon tube.

2.13.2 Pre-clearance of the samples

A pre-clearing step was performed to eliminate biotinylation of non-specific proteins. 200 μ l of gelatin sepharose beads(GE Healthcare, 17095601) were washed with 200 μ l of lysis buffer. Beads were centrifuged at 800 x g for 3 minutes and the supernatant was rejected. Beads were resuspended at 500 μ l of lysis buffer and the same step of centrifugation/resuspension was repeated and beads were resuspended in 1 ml sample this time. Samples were incubated under rotation with the beads for 2 hours at 4°C. Finally, to remove the beads, samples were centrifuged at 800 x g for 5 minutes and the supernatant was transferred to new tubes.

2.13.3 Pulldown with streptavidin beads

50 μ l of streptavidin conjugated sepharose beads(GE Healthcare, 17511301) were washed twice with lysis buffer as described above. Next, streptavidin beads were resuspended in 1ml sample lysate and left to incubate under rotation for 4 hours. The final step was to wash off the biotinylated proteins from the beads. A 5 minute centrifugation is performed to pull down the beads and subsequently the beads were resuspended in 1ml wash buffer (8 M urea in 50 mM Tris pH 7.4) and left incubate under rotation for 8 minutes. This washing step is repeated six times and the final pellet is resuspended in 50 μ l 50 mM ammonium bicarbonate containing 1mM biotin and finally flash freezed at -80.

3. RESULTS

Background

This thesis work is part of a long term project focused on the role of LBR in nuclear envelope architecture and chromatin organization. To this end, former lab members Dr. Katerina Soupsana, Panagiotis Martzios and Tassou Vasiliki have generated all the KO clones used to perform the experiments described in the current thesis. In more detail, the Crispr-Cas9 nickase system was utilized in order to target LBR and LMNA/C genes leading to improper repair of the double stranded breaks, overall resulting in no functional gene products of the two genes (**Figure 17**). Two different biological replicates were obtained following LMNA/C KO and two following LBR KO. Next, the same guide RNAs were used to target either LBR on LMNA/C KO cells or LMNA/C on LBR KO cells. This second step of gene deletion resulted in double KO cells that were either LBR derived (deleting LMNA/C from LBR KO cells) or LMNA/C derived (deleting LBR from LMNA/C KO cells). Again two biological replicates were obtained from each double KO clone. Following this approach of serial deletion of the genes allows us to incorporate the sequential mechanism that LBR and LMNA/C possess in tethering heterochromatin to the nuclear periphery, described by Salovei et al..

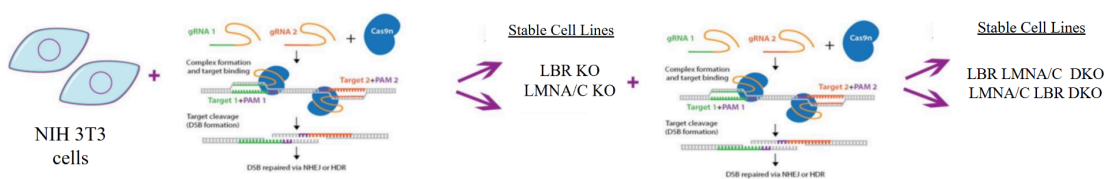


Figure 17: Schematic representation of the order that gene deletions were performed to obtain the cells used in this study.

In total the following KO clones were generated in NIH-3T3 mouse cells:

LBR KO1: Cells lacking the expression of LBR (first replicate)

LBR KO2: Cells lacking the expression of LBR (second replicate)

LMNA/C KO1: Cells lacking the expression of LMNA/C (first replicate)

LMNA/C KO2: Cells lacking the expression of LMNA/C (second replicate)

LBR DKO1: LBR KO1 cells where LMNA/C was additionally deleted (LMNA/C-LBR DKO) (first replicate)

LBR DKO2: LBR KO1 cells where LMNA/C was additionally deleted (LMNA/C-LBR DKO) (second replicate)

LMNA/C DKO1: LMNA/C KO1 cells where LBR was additionally deleted (LBR-LMNA/C DKO) (first replicate)

LMNA/C DKO2: LMNA/C KO1 cells where LBR was additionally deleted (LBR-LMNA/C DKO) (second replicate)

Following the establishment of these stable cell lines, all clones lacking the expression of LBR demonstrated significantly slower growth compared to the rest of the clones. In order to compensate for this reduced growth rate, clones lacking LBR were cultured in medium supplemented with 15 % FBS while the rest of the cells were cultured in medium with 10% FBS. Wild type NIH-3T3 cells were cultured in both 15% and 10% FBS and used as controls accordingly. All experiments described in this result section are part of the current thesis unless explicitly stated otherwise.

3.1 Double knockout clones show significant growth impairment compared to control clones.

Considering the importance of LBR and LMNA/C in establishing proper genome architecture and maintaining the correct expression profile necessary for normal cellular function—along with recent studies linking reduced LBR expression to a non-proliferative senescent state- we first sought to determine whether the ablation of LBR, LMNA/C or both has any significant effect on key cellular processes. One such process is the ability of the cell to maintain its proliferation state. To do so we monitored cell proliferation over the span of three days after seeding 5000 cells of each clone at day zero (**Figure 18**). Interestingly cells carrying only loss of LBR show similar proliferation rates to control clones whereas additional deletion of LMNA/C leads to decrease in cell proliferation. However, deletion of LMNA/C leads to controversial results with one of the biological replicates growing slightly slower compared to control clones while the other replicate exhibiting a very significant drop in proliferation. Similarly with the LBR-LMNA/C DKO clones LMNA/C-LBR DKO clones grow significantly slower compared to the control clones. Overall, both LBR-LMNA/C and LMNA/C-LBR knockout cells demonstrate slower growth. These results could potentially

indicate an interaction effect of LMNA/C and LBR loss where deletion of only one is not sufficient to stall proliferation but sequential deletion of both results in reduced proliferation.

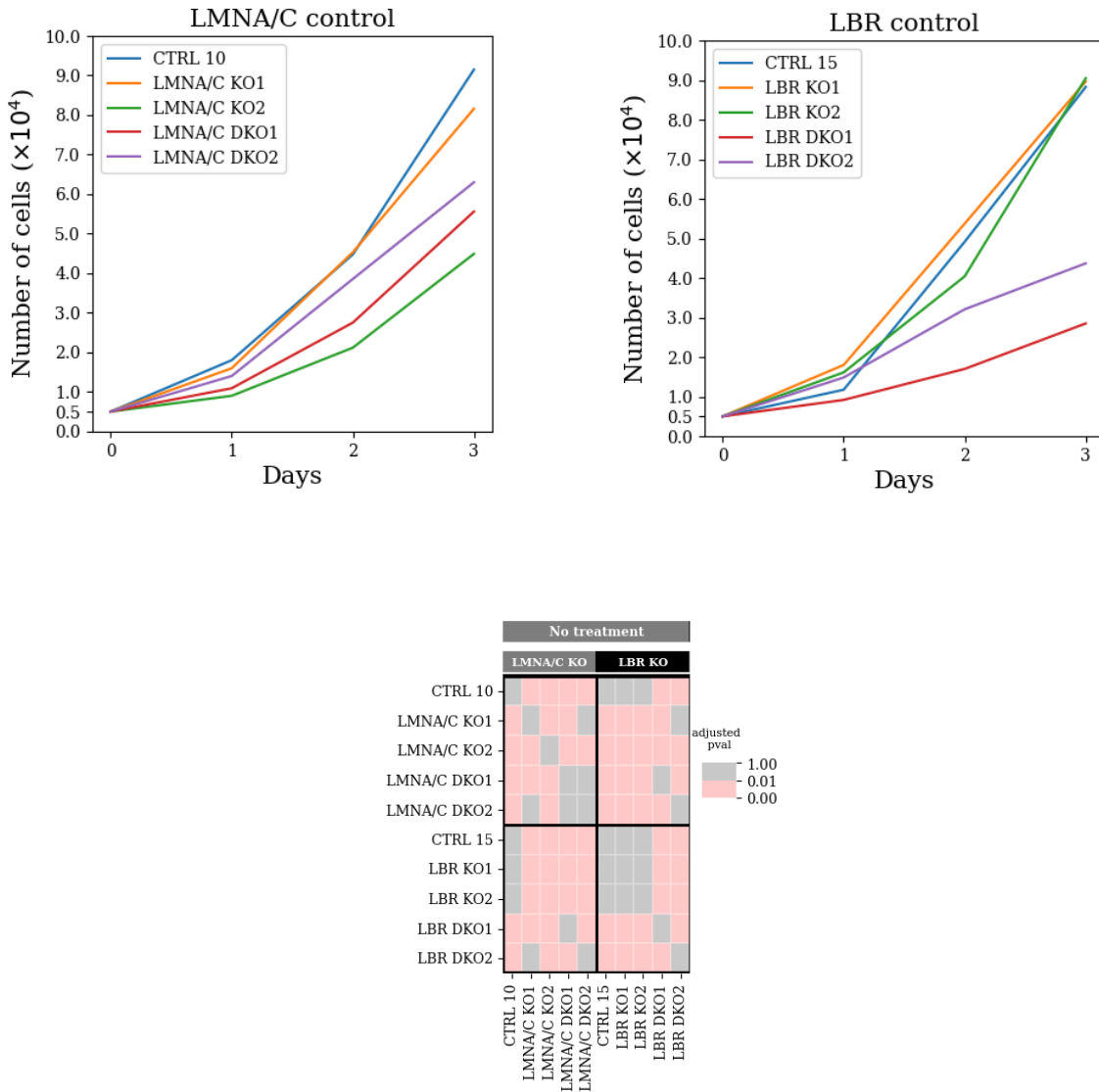


Figure 18: Cell growth of single and double KO clones compared to control cells. 5000 cells were seeded at day 0 and cells were daily counted for the following three days. X axis represents the time in days and Y axis represents the number of cells measured (10.000). The heatmap represents statistical significance of the compared clones with a p value cutoff of 0.01. Pairwise comparisons where the p-value is below the p-value cutoff are colored pink whereas comparisons where the p-value is greater than the p-value cutoff are colored grey. Experiments were performed by P. Martzios and K. Tsomakian.

3.2 Cholesterol supplementation fails to restore proliferation in LBR-LMNA/C double knockout clones.

LBR is involved in several critical cellular functions, including nuclear envelope assembly and the tethering of heterochromatin to the nuclear periphery. It has also been proposed to possess enzymatic activity responsible for reducing the C14 unsaturated bond in lanosterol, thereby contributing to cholesterol biosynthesis; however, this role remains incompletely characterized and is not yet well documented (Nikolakaki et al., 2017). Indirect evidence supporting this function primarily arises from pathological phenotypes observed in both humans and mice with deficiencies in LBR's sterol reductase activity. Additionally, the loss or downregulation of LBR expression has been associated with non-proliferative senescent cells and poorly proliferating bone marrow cells (Gaines et al., 2008; En et al., 2020). Nonetheless, it is likely that LBR plays an auxiliary or redundant role in cholesterol biosynthesis, with the primary enzymatic function attributed to TM7SF2. Given these considerations, we aimed to determine whether impaired cholesterol biosynthesis due to LBR loss, in combination with the absence of LMNA/C, contributes to the reduced proliferative capacity observed in our double knockout clones. To investigate this, we sought to assess whether the absence of the LBR associated cholesterol biosynthesis along with the absence of LMNA/C are the factors triggering the reduced cell proliferation state observed in our double knockout clones. To test this hypothesis we again seeded 5000 cells of each clone and monitored their growth over the span of three days. However, to test the above hypothesis this time we supplemented all clones with exogenous cholesterol. All experiments were performed twice, once for 5 µg/ml cholesterol and once for 10 µg/ml. Due to its lipid nature cholesterol cannot be diluted in water and subsequently in cell culture medium. We used ethanol to dilute cholesterol and considered as control cells supplemented with the same concentration of ethanol in the absence of exogenous cholesterol (5 µl). Measurements demonstrate that ethanol by itself leads to significant reduction in cell proliferation (**Figure 19**). Comparing the ethanol measurements with the control measurements the exact same pattern is observed in LBR single knockout clones and in LBR-LMNA/C double knockout clones (**Figure 19**). Similarly LMNA/C-LBR double knock out clones retain their proliferation lag compared to their controls. Interestingly however both LMNA/C clones this time grow slower compared to NIH control cells. When culturing cells with 5 µg/ml cholesterol in the case of LBR single knockouts cells seem to grow slower compared to NIH control cells while LBR-LMNA/C cells grow even slower again with agreement to a pattern where double knockout clones grow slower compared to control clones (**Figure 19**). Regarding LMNA/C, although no valid conclusion can be extracted from the

data given that NIH10 cells completely failed to grow, an interesting twist is observed where LMNA/C-LBR double knockout clones grow faster compared to LMNA/C single knockout clones (**Figure 19**).

Next, to determine whether higher concentrations of cholesterol can yield higher proliferation of our KO clones we cultured cells with 10 µg/ml cholesterol (**Figure 19**). In the case of LBR knockout clones the same pattern as the control cells is observed again. Cells lacking the expression of LBR grow with similar rates as control cells and LBR-LMNA/C DKO clones grow slower. On the other hand, cells lacking only the expression of LMNA/C show a similar trend to proliferate slower than both control and DKO cells. LMNA/C-LBR DKO cells again grow slower when compared to control cells. Summing up, the external addition of cholesterol to cells lacking the expression of either LBR, LMNA/C or both could not recover the reduced proliferation rate resulted from the KOs and seemed to cause opposing effects on LMNA/C KO clones, suggesting that the LBR's putative role in cholesterol biosynthesis itself is not responsible for the reduced proliferation of our KO clones. However, the strong effect of ethanol alone on the proliferation of all tested cell lines prevents drawing definitive conclusions.

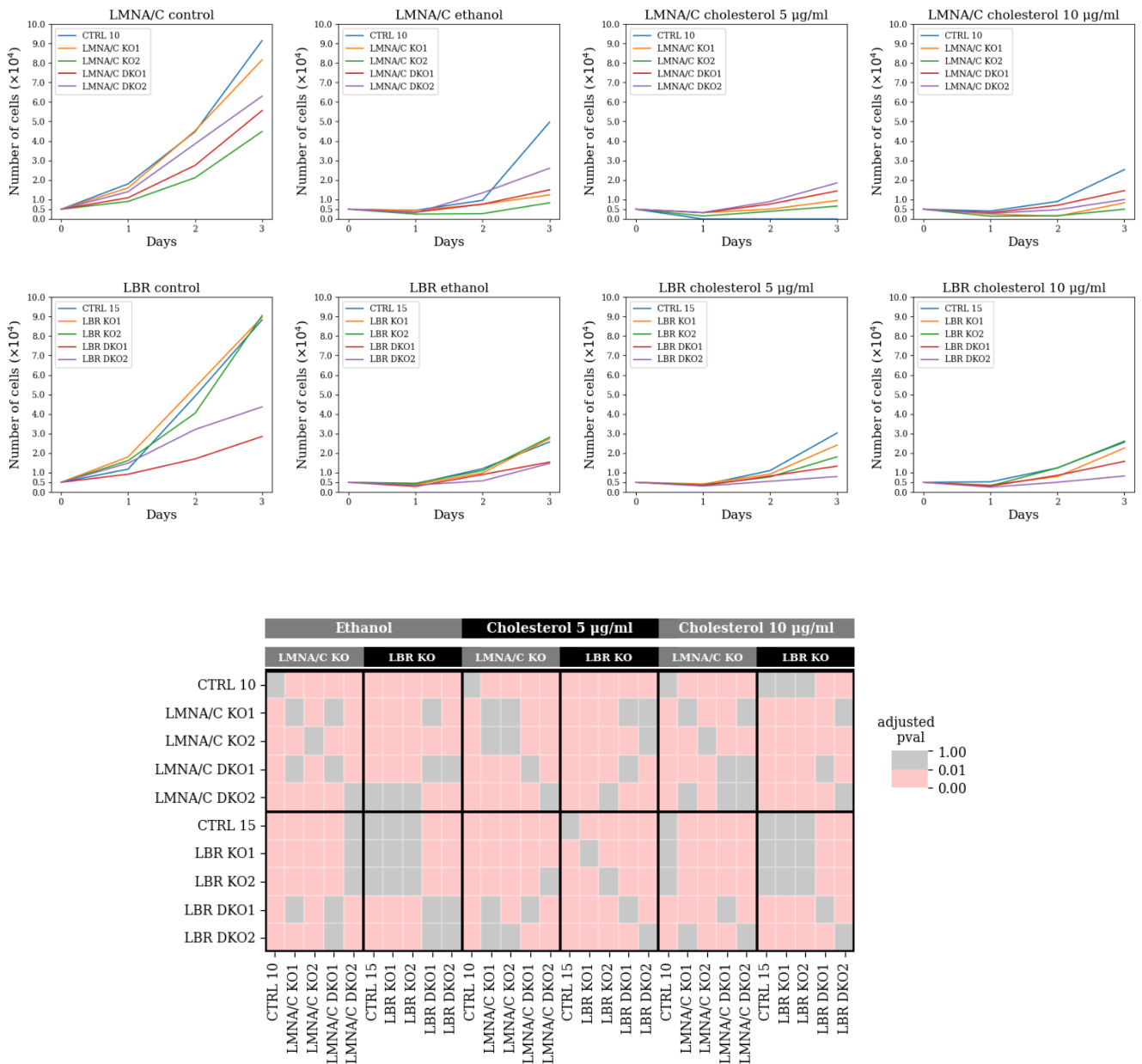


Figure 19: Cell growth of control, single and double KO cells supplemented with ethanol, 5 µg/ml and 10 µg/ml of cholesterol. Cells were counted over the span of three days. External addition of cholesterol is not sufficient to recover cell proliferation of double knockout cells. For the line plots X axis represents the time in days and Y axis represents the number of cells measured (5,000). For the heatmap statistically significant comparisons are colored red while not significant comparisons are colored grey.

3.3 Loss of LBR and LMNA/C leads to asymmetric localization of nuclear periphery proteins without compromising nuclear envelope integrity

As described in the introduction, LMNA/C plays a key role in nuclear integrity and proper genome architecture while being tightly linked to cell division. Lamins undergo phosphorylation, leading to the disorganization of the lamina meshwork, a crucial step for mitosis. A-type lamins degrade first, followed by B-type lamins. The absence of LMNA/C in mice causes developmental retardation and muscular dystrophy, along with mislocalization of emerin, a key nuclear periphery protein. Additionally, mutations in LMNA/C (R482Q or R482W) result in abnormal fat distribution, as seen in Dunnigan-type familial partial lipodystrophy (FPLD). Fibroblasts from FPLD patients show defects in B-type lamins, emerin, nuclear pore complexes, and LAP2 β , with regions lacking chromatin (Ungricht et al., 2015).

To investigate whether such phenotype could be reproduced in our single and double KO clones, members of our lab (P. Martzios, unpublished results) examined the distributions of nuclear periphery proteins in all control, single and double knockout clones. The localization of Lamin B1, LAP2b and nuclear pore complexes was assessed. **Figure 20** illustrates an example of these asymmetries, where a pronounced asymmetrical distribution of nuclear pore complexes is observed in LBR-LMNA/C double KO clones.

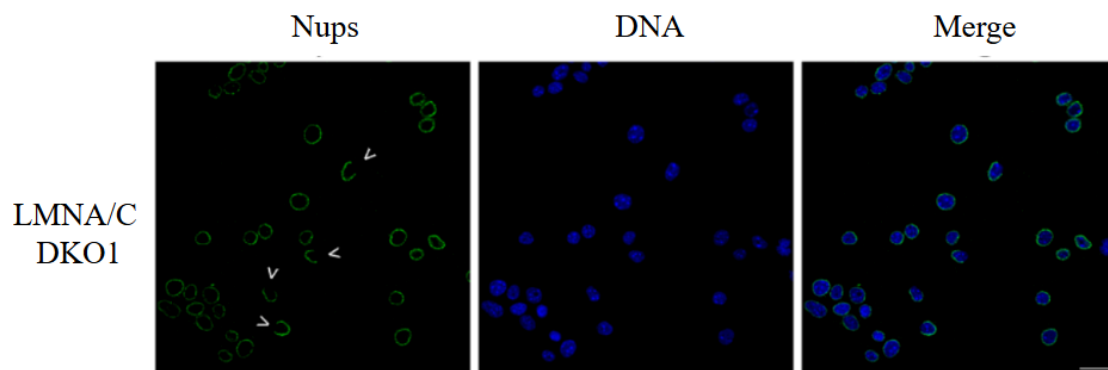


Figure 20: Asymmetrical distribution of nuclear pore complexes in LBR-LMNA/C double KO clones. Lap2b and Lamin B1 follow the exact same distribution in subpopulations of all cell populations lacking LMNA/C expression. Scale bar: 8 μ m. (P. Martzios, unpublished results).

While NIH control cells and LBR single KO clones exhibit proper distribution of all three proteins, LMNA/C single KO cells and both LBR-LMNA/C and LMNA/C-LBR double KO cells contain a subpopulation of cells with non symmetrical yet overlapping distribution of the three proteins tested, consistent with the findings of Vigoroux et al.

Although immunofluorescence results clearly show no DNA dye leakage from the envelope regions where the asymmetries occur, we aimed to further confirm that these regions of the nuclear envelope represent only protein mislocalization and non symmetrical distribution of the tested proteins rather than nuclear ruptures, we overexpressed histone H1 based on the rational being that overexpression of a histone isoform would lead to saturation of all available chromatin binding sites and, in the presence of nuclear ruptures, any unbound histone would eventually diffuse freely into the cytoplasm. To visualize the asymmetrical regions of the nuclear envelope alongside H1, we stained cells with Lamin B1 as well. First, we tested NIH control cells and LBR single KO cells where asymmetries are not observed. (**Figure 21**). The results confirm Lamin B1 localization at the nuclear rim and the exclusive retention of overexpressed histone H1 within the nuclear boundaries, as expected.

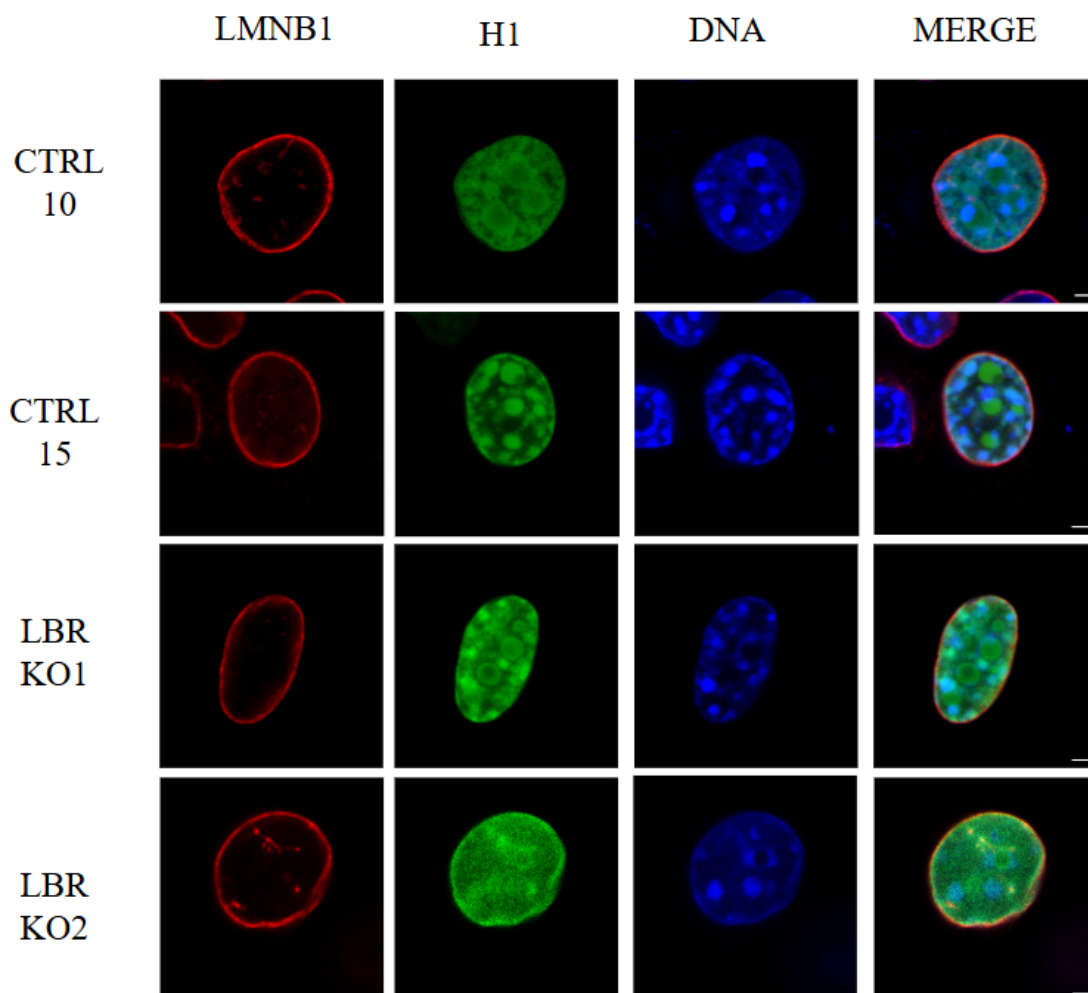
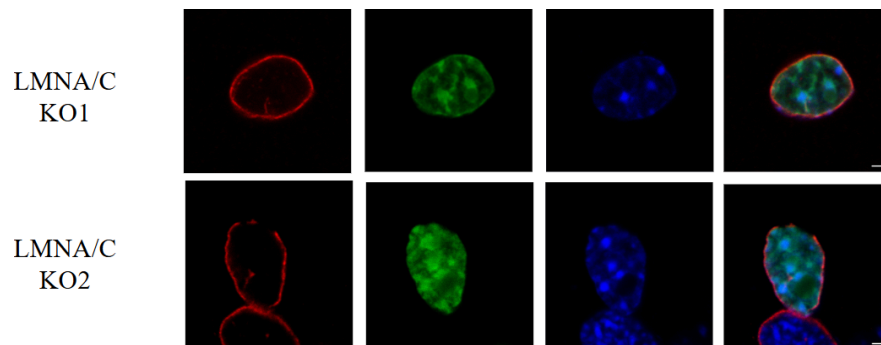


Figure 21: IF of lamin B1 along with H1 on cells with no evident defects on NE protein distribution. In all control and LBR single KO clones, lamin B1 is localized, as expected at the nuclear rim, while the over-expressed H1 is retained inside the nucleus. Scalebar 2 μ m.

where asymmetries are present (**Figure 22**). The results clearly demonstrate that H1 remains confined within the nuclear envelope in regions of asymmetries across all affected clones.

These findings collectively suggest that nuclear envelope integrity is preserved, with no major defects present, following the loss of LBR, LMNA/C or both, indicating that the altered distribution of these proteins is regulated by a mechanism that does not compromise nuclear membrane integrity.



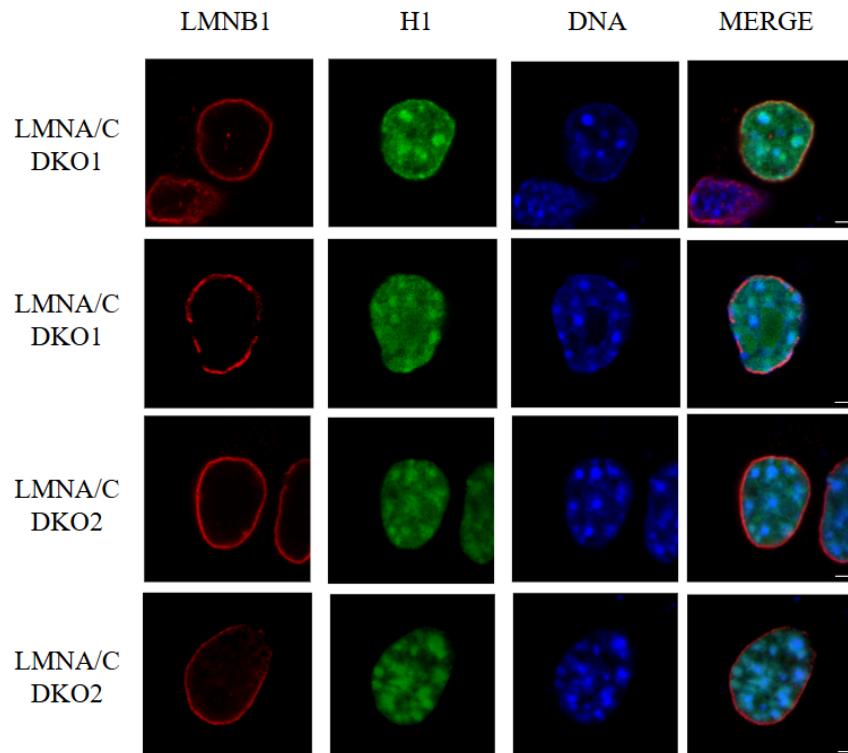
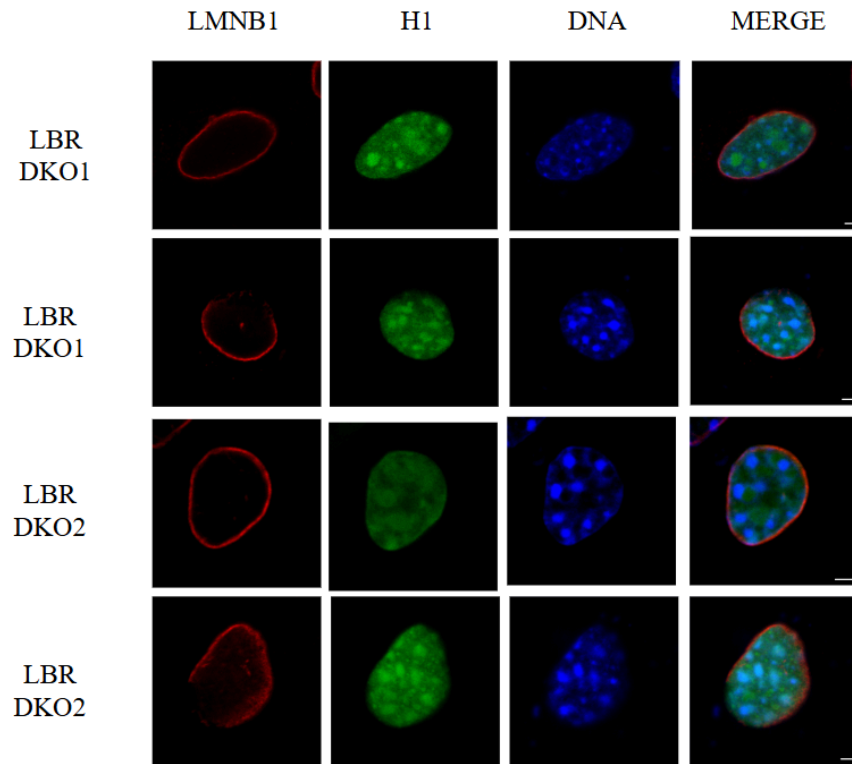


Figure 22: Immunofluorescence (IF) of Lamin B1 and Histone H1 in Cells with Nuclear Envelope (NE) Protein Distribution Defects. The upper panel shows LMNA/C single KO clones, comparing cells with no observed asymmetries to those where asymmetries are present (scale bar: 2 μm). The middle panel presents LBR-derived double KO clones, highlighting both conditions-cells without asymmetries and those exhibiting asymmetries (scale bar: 2 μm). Similarly, the bottom panel depicts LMNA/C-derived double KO clones, showing cells without asymmetries alongside those with asymmetrical protein distribution (scale bar: 2 μm).

3.4 Heterochromatin organization is subtly affected by LBR and LMNA/C loss.

Conventional genome organization has been correlated with the expression of at least one of the LBR or LMNA/C genes across various tissues. Notably, mouse myoblasts with conventional genome organization adopt a reversed architecture when depleted of both proteins. Similarly rod shaped cells of nocturnal animals that naturally exhibit a reversed genome organization lack expression of both proteins. These findings emphasize the critical role of LBR and A-type lamins in maintaining the conventional genome architecture (Salovei et al., 2013).

Given the significance of LBR and LMNA/C in genome organization we sought to determine whether the depletion of any or both of these proteins affects the genome organization in NIH cells. It should be noted that in mouse cells pericentromeric chromatin is organized into heterochromatin-dense foci inside the nucleus that appear as densely stained regions when cells are stained for DNA. To assess changes in heterochromatin organization we measured and compared the number and size of these heterochromatic foci in NIH control cells, LBR single KO cells, LMNA/C single KO cells, LBR-LMNA/C double KO cells and LMNA/C-LBR double KO cells. All three spatial dimensions (x, y, z) of the foci were measured using confocal microscopy with a z-step of 0.21 μm . A focus was defined as any nuclear region exhibiting a significant change in DAPI staining intensity compared to its surrounding area.

Regarding the size of the heterochromatic foci, LMNA/C-LBR double KO clones have significantly larger foci compared to NIH 10% control cells. LBR-LMNA/C double KO cells also tend to have larger heterochromatic foci but the difference is not statistically significant (p value cutoff 0.05). Both double LMNA/C-LBR and LBR-LMNA/C cells exhibit significantly larger heterochromatic foci compared to LBR single KO cells. Additionally, further deletion of LBR in LMNA/C-depleted cells leads to a significant increase in foci size (**Figure 23**).

Similar to the size findings, there is no significant difference in the number of heterochromatic foci between control cells and either single KO clone. However, when both LBR and LMNA/C are deleted, double KO clones show a significant decrease in the number of heterochromatic foci.

These findings suggest that the deletion of LBR or LMNA/C alone is not sufficient to induce any significant difference in the size and number of heterochromatic foci. This aligns with a study by Salovei et al., which demonstrated that the presence of at least one of the two proteins is sufficient to maintain the conventional genome architecture and prevent large-scale heterochromatin reorganization.

However, the additional deletion of LBR in LMNA/C depleted cells (or vice versa) leads to increase in the size of heterochromatic foci and decrease in their number, resulting in heterochromatin clustering and a shift in nuclear architecture. This suggests that the absence of both proteins compromises genome organization to a certain extent, but not dramatically.

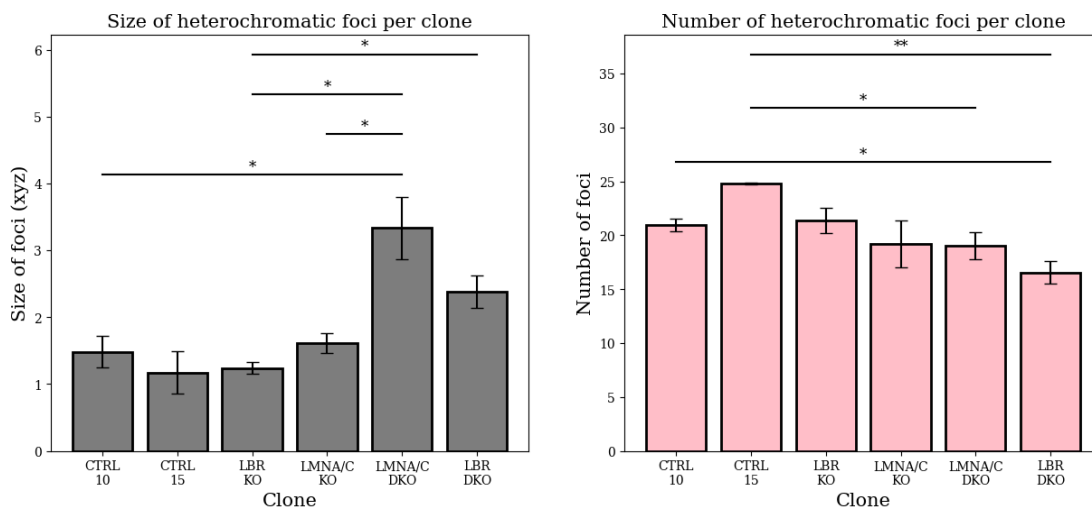


Figure 23: Left) Barplot representing differences in the size of heterochromatic foci between cells lacking the expression of either LMNA/C, LBR or both. Right) Barplot representing differences in the number of heterochromatic foci between cells lacking the expression of either LMNA/C, LBR or both. Horizontal bars are used to represent pairwise comparisons and stars represent significance levels. * for 0.05, ** for 0.01. Vertical bars represent standard error of the mean.

3.5 Chromatin dynamics remain unchanged upon LBR and LMNA/C loss.

Given the changes detected in the number and the size of heterochromatic foci in single and double KO clones we questioned whether these alterations reflect broader chromatin landscape

modifications following the deletion of LBR, LMNA/C or both. To test this hypothesis we assessed dynamics of heterochromatin in the KO clones using Fluorescence Recovery After Photobleaching (FRAP). This technique allowed us to examine potential changes in chromatin mobility. For FRAP analysis cells were transfected with a pPycagip-eGFP-huHP1 α plasmid which drives the expression of the human HP1 alpha isoform. HP1 α binds the H3K9me3-enriched heterochromatic foci primarily found in the pericentromeric and telomeric regions of mouse chromosomes. After 24 hours of incubation the exogenously expressed human HP1 α could be visualised in the heterochromatic foci of the NIH-3T3 cells, enabling the assessment of chromatin dynamics. For each clone, 50 different cells were assessed in order to acquire adequate statistical power for the subsequent statistical analysis while also ensuring that we capture as much variance of chromatin dynamics as possible (**Figure 24**).

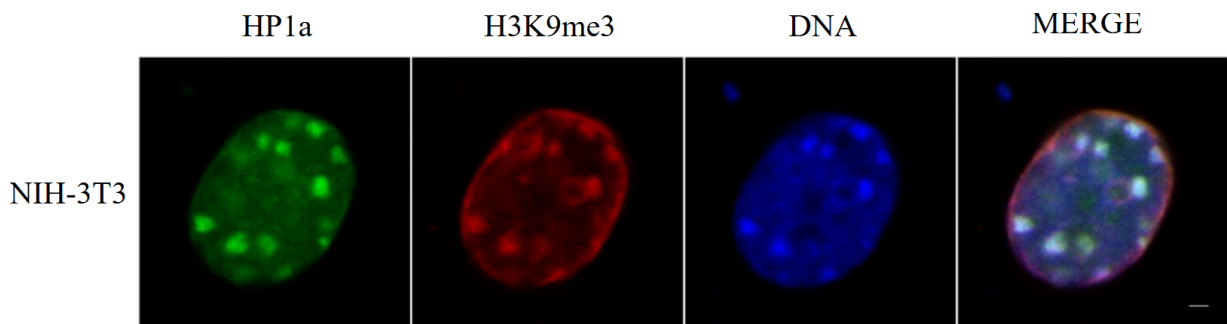


Figure 24: Immunofluorescence imaging of heterochromatin foci in NIH-3T3 cells. HP1 α is shown in green, H3K9me3 in red and DNA in blue. (adapted from E. Triantopoulou's M.Sc.thesis; scalebar 3 μ m)

To perform a FRAP experiment, a high intensity laser pulse was focused on a circular area with a 0.5 μ m diameter to bleach the fluorescence. The subsequent fluorescence recovery was then monitored. Measurements of fluorescence recovery over time were used to compute three different metrics describing the bleached heterochromatic foci (**Figure 25**). First, the recovery half-time, denoted as $t_{1/2}$ represents the time point at which the bleached foci regain half of the final fluorescent signal. Next, the Mobile Fraction, denoted as Mf , is the ratio of the fluorescent signal after recovery to the initial signal and represents the proportion of the signal that could be recovered. Mf is expected to range from 0 for static/immobile molecules to 1 for highly dynamic molecules. In our experiments, however, due to HP1 α 's high mobility and background noise, Mf in some cases exceeds 1. Finally, the diffusion coefficient, denoted as D_a , is a measure of molecular mobility and can be computed

from the recovery halftime, the diameter of the bleached region (here 0.5 μm) and the experimentally estimated diameter of the effective bleached region 0.57 μm (Kang et al., 2012).

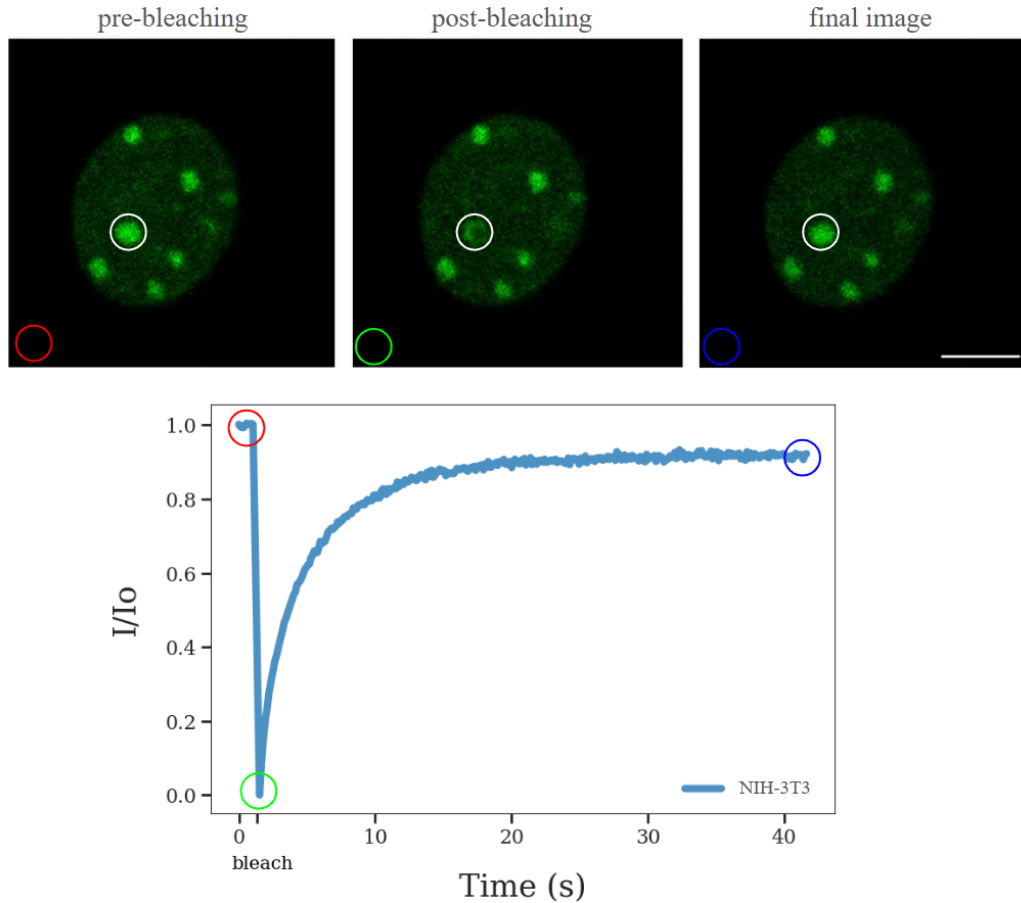


Figure 25: Live cell imaging of a representative NIH-3T3 cell expressing human HP1a (scalebar 10 μm). Line plot represents fluorescence recovery following photobleaching. Differently coloured circles indicate different timepoints of the experiment.

Evangelia Triantopoulou, a former MSc student in the lab examined chromatin dynamics by assessing and comparing the recovery halftime, the mobile fraction and the diffusion coefficient in cells lacking the expression of LBR or LMNA/C and in LMNA/C derived double KO cells. Significant changes in chromatin dynamics were observed between LMNA/C single KO clone 1 and wild type 10% NIH-3T3 cells as well as between LBR single KO clone 1 and wild type 15% NIH-3T3 cells, particularly when comparing the diffusion coefficients. In both cases the KO clones displayed an increased diffusion coefficient for heterochromatin protein 1 suggesting a less compact, more accessible chromatin state. To further assess whether changes in chromatin dynamics can be captured for the two LBR derived LMNA/C-LBR double KO clones we used the FRAP assay

following identical experimental procedure and analysis of the data with these two clones (**Figure 26**). No significant changes in chromatin dynamics were observed in any additional comparisons for either Da or Mf. These findings indicate that the depletion of LBR, LMNA/C, or both does not substantially impact chromatin dynamics in terms of HP1a kinetics in most cases. It is important to note, however, that these results do not exclude the possibility of more subtle changes in chromatin dynamics or alterations unrelated to HP1 α .

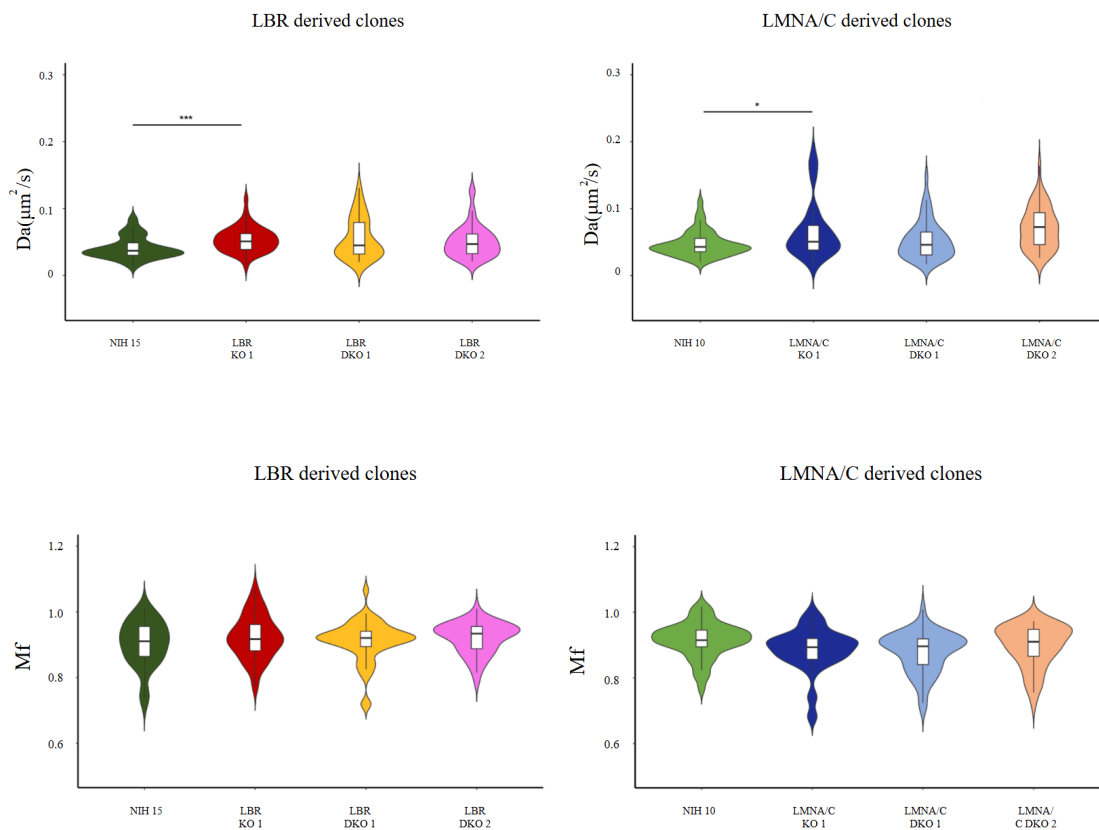


Figure 26: Pairwise comparisons of the Diffusion coefficient (Da) and Mobile fraction (Mf) of HP1 α in different KO clones. Significant differences are only observed when comparing Diffusion coefficients between LBR KO1 and NIH 15% cells and LMNA/C KO1 and NIH 10% cells. No significant changes were found in the mobile fractions across the samples (n=50 cells per clone). Experiments involving NIH 10, NIH 15, LMNA/C single KO, LBR single KO and LBR-LMNA/C double KO were conducted by E. Triantopoulou.

3.6 LBR and LMNA/C loss leads to transcriptional upsetting.

Monitoring the changes in the shape and the size of heterochromatic foci on single and double KO cells can only capture large/microscopically detectable alterations in chromatin organization.

Consequently, finer-scale chromatin changes remain undetectable through this approach. . Taking into account the intricate relationship between genome organization and gene expression we sought to explore finer changes in genome organization by analyzing and comparing transcriptome-wide expression profiles between single and double KO clones.

To achieve this, mRNA from all control, single and double KO cells was extracted, subsequently sequenced at the EMBL Genomics Facility and processed (K. Soupsana, unpublished results). We performed a bioinformatics analysis of the results. The first step in our analysis was to identify differentially expressed genes between control NIH cells and NIH cells null in LBR, LMNA/C or both. Loss of LBR in two biological replicates resulted in both shared and distinct transcriptional changes. In the first LBR single KO clone a set of 571 differentially expressed genes appear while in the second one there are 665 differentially expressed genes with 292 differentially expressed genes common between the two clones (**Figure 27**). Such diversity in the number of differentially expressed genes between two biological replicates of LBR KO could indicate that there is a subset of genes whose expression depends directly or indirectly on LBR-mediated chromatin tethering to the nuclear periphery and other genes are probably influenced by additional mechanisms. The presence of genes exclusive to each replicate indicates that gene expression regulation in the absence of LBR is not uniform across biological samples. Next we investigated whether the set of genes that appear in both replicates as differentially expressed exhibit statistically significant enrichment for any type of biological process. We used the Biological Process (BP) ontology from the Gene Ontology database to test the 292 common genes for significance. **Figure 27** depicts the twenty most significant terms found by the enrichment analysis. Two different but related biological processes seem to be mostly affected by loss of LBR. One regarding cell movement as terms like taxis and chemotaxis are represented among the significant terms and another one regarding cell adhesion properties, as terms related to integrin adhesion and extracellular matrix organization are also enriched. Although these terms appear significant in the differentially expressed gene list it is worth noting that apart from the suggested role of LBR in cholesterol biosynthesis, LBR is primarily recognized as a heterochromatin tether to the nuclear periphery. No prior studies have implicated LBR in specific biological pathways. Therefore, rather than expecting enrichment of particular biological processes, we anticipated a general transcriptional disruption due to the loss of a key heterochromatin tethering mechanism. The broad and overlapping nature of the enriched terms, along with the relatively small number of genes associated with a biological process (using a statistical cutoff of 0.01), further supports this notion.

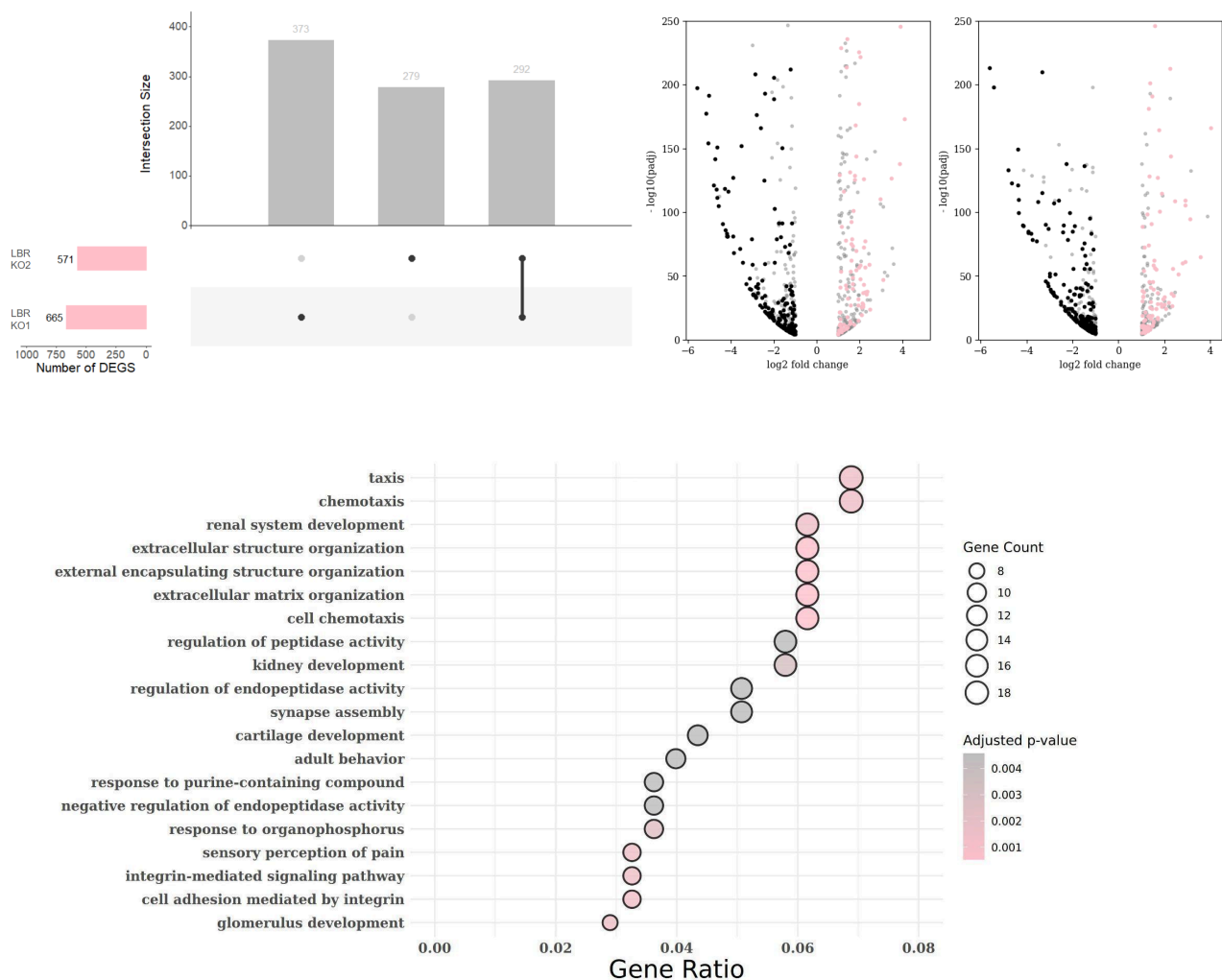
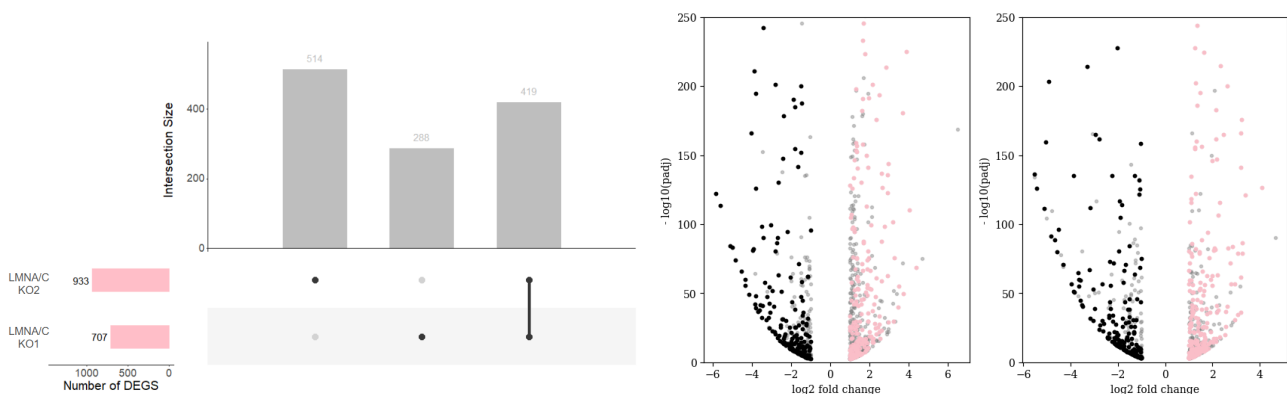


Figure 27: Differentially expressed genes of two biological replicates lacking the expression of LBR. Upset plot represents genes that are differentially expressed in both replicates, and genes that are differentially expressed in only one of the replicates. Common upregulated genes are represented with pink in the volcano plot, while common downregulated genes and genes that are not in common between the two replicates are represented with black and grey color respectively. Bubble plot represents significantly enriched biological processes arising from the common set of DEGs q value cutoff 0.05.

Regarding the LMNA/C KO clones, the two sequenced biological replicates show even more divergence when their expression profiles are compared. LMNA/C gene KO results in a total of 933 differentially expressed genes in the first biological replicate and 707 differentially expressed genes in the second one. The two replicates share 419 differentially expressed genes in common. (**Figure**

28). Similarly to the LBR KO experiments these differences in the number of DEGs between the two replicates can indicate the existence of genes whose expression is tightly related to the presence of A-type lamins in the nuclear periphery while the expression of others may rely on additional mechanisms. This higher divergence in gene expression could also potentially explain the different behavior that the two LMNA/C clones have in the cell growth experiment described above. Alternatively, the inherent heterogeneity that NIH-3T3 cells have could also contribute to the divergence in gene expression. Next we investigated whether the set of genes that appear in both replicates as differentially expressed exhibit statistically significant enrichment for any type of biological process. Interestingly, the loss of LMNA/C also affects genes related to cell motility and extracellular organization. Notably, the fact that LBR and LMNA/C depletion independently lead to overlapping gene expression changes aligns with the findings of Salovei et al., which suggest that LBR and LMNA/C serve the same function in tethering heterochromatin to the nuclear periphery but at different developmental stages. Finally, similar to LBR deletion, LMNA/C deletion results in only a small number of genes being associated with specific biological processes (p-value cutoff 0.01). This further supports the hypothesis that these proteins function as general-purpose heterochromatin tethers without direct involvement in specific biological pathways.



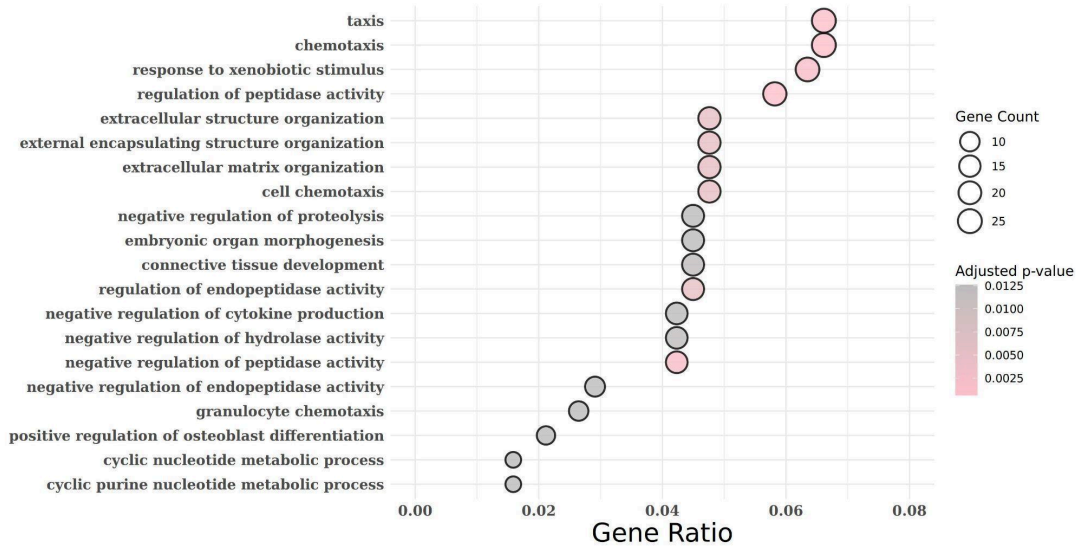


Figure 28: Differentially expressed genes of two biological replicates lacking the expression of LMNA/C. Upset plot represents genes that are differentially expressed in both replicates, and genes that are differentially expressed in only one of the replicates. Common upregulated genes are represented with pink in the volcano plot, while common downregulated genes and genes that are not in common between the two replicates are represented with black and grey color respectively. Bubble plot represents significantly enriched biological processes arising from the common set of DEGs q value cutoff 0.05.

As expected, additional deletion of LBR in LMNA/C or deletion of LBR in LMNA/C KO cells resulted in an even greater transcriptional upset on NIH-3T3 cells. Four biological replicates were used to assess differential expression, two for LBR-LMNA/C double KO cells and two for LMNA/C-LBR double KO cells. Further deletion of LMNA/C on LBR single KO cells resulted in 1409 and 1749 differentially expressed genes in the two replicates respectively. Reversely, further deletion of LBR in LMNA/C single KO cells resulted in 1859 and 2461 differentially expressed genes in the two replicates. Of great interest is the diversity in gene expression following the deletion of LBR in LMNA/C depleted cells as the one of the two LBR-LMNA/C replicates exhibits 1062 (out of 2461) unique differentially expressed genes that are absent from the other double KO clones, while the other replicate has 523 (out of 1859) unique differentially expressed genes. The corresponding numbers for LMNA/C-LBR double KO clones are 355 and 124 for the two replicates respectively. Our four double KO clones share 493 common differentially expressed genes in total that were subsequently used to investigate whether the set of genes that appear in all four double KO clones as differentially expressed exhibit statistically significant enrichment for any type of biological process (**Figure 29, Figure 30**). Cellular motility and cell adhesion terms are enriched in

the double KO cells as well, similarly to LBR single KO and LMNA/C single KO cells. Interestingly however, although absent from the terms enriched from the single KO cells the term “regulation of endothelial cell proliferation” is significantly enriched in double KO cells. The presence of such genes in the differential expression list of double KO cells could potentially capture and explain, at least partially, the reduced proliferation rate of double KO cells.

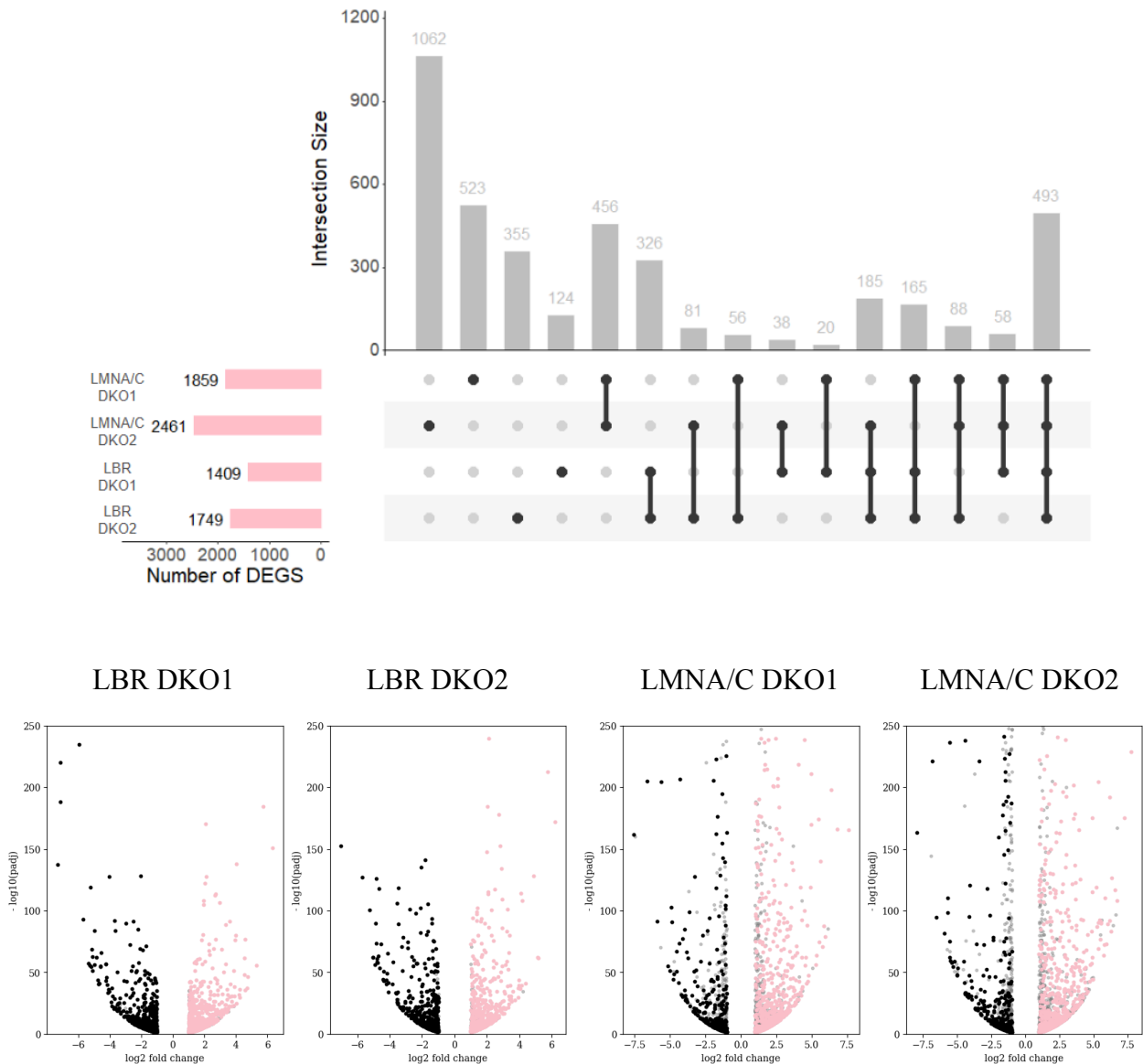


Figure 29: Differentially expressed genes of four biological replicates lacking the expression of both LBR and LMNA/C. Upset plot represents genes that are differentially expressed in all four double KO clones, genes that are differentially expressed in different combinations of the clones and genes that are differentially expressed specifically for a given clone. Common upregulated genes are represented with pink in the volcano plots, while common downregulated genes and genes that are not in common between the double KO clones are represented with black and grey color respectively.

Bubble plot represents significantly enriched biological processes arising from the common set of DEGs q value cutoff 0.05.

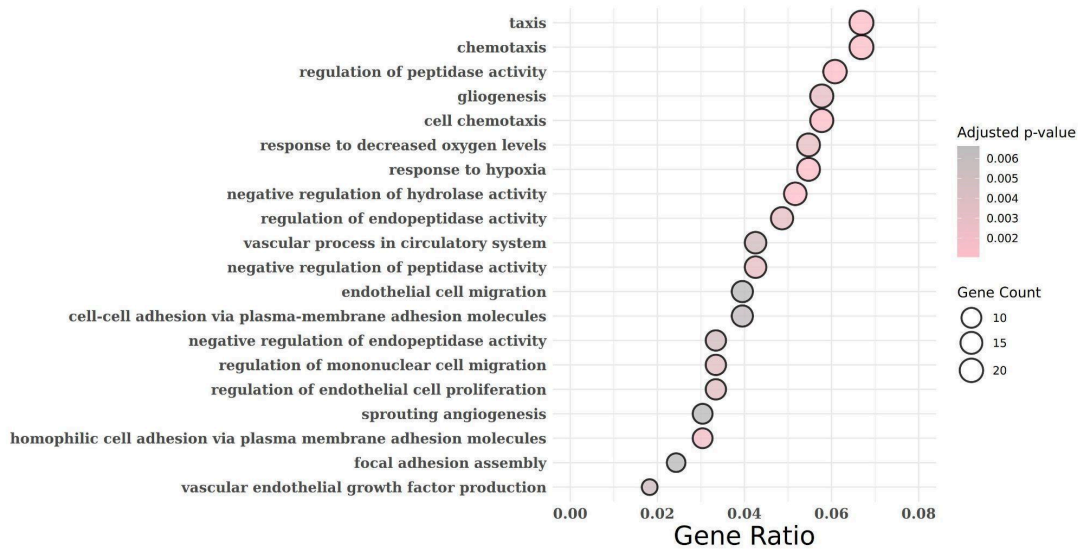


Figure 30: Bubble plot of the biological processes enriched by the differentially expressed genes of double KO clones (q value cutoff: 0.05).

Next, considering the sequential order that LBR and LMNA/C appear during normal development as described by Solovei et al., we sought to determine the differences that double KO cells exhibit due to the difference in the order of deletion of the genes expressing LBR and A-type lamins. To do so, we performed GO enrichment analysis but this time only for genes that are present in the LBR-LMNA/C DEG list but not in the LMNA/C-LBR DEG list and vice versa (**Figure 31**). Results show that genes that are present in LMNA/C-LBR KO cells and not in LBR-LMNA/C KO cells are involved in immune system response, as interleukin related and complement processes are enriched. Regarding the gene set that is present in LBR-LMNA/C double KO cells but not in LMNA/C-LBR double KO cells, results show that there are enriched processes related to cell proliferation and cell movement. Collectively, these data demonstrate that the sequential loss of LBR and LMNA/C results in differential expression of both shared and different genes.

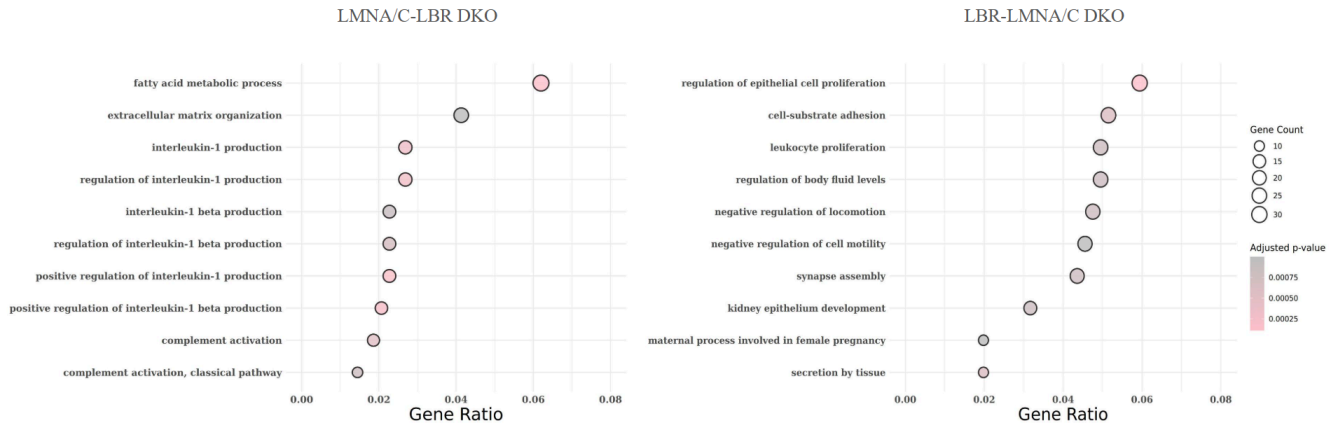


Figure 31: Bubble plots of the biological processes enriched in double KO clones. (Left) bubble plot represents the biological processes enriched by genes that are differentially expressed in LMNA/C-LBR double KO clones but not in the LBR-LMNA/C double KO clones. (Right) the plot represents the biological processes enriched by genes that are differentially expressed in LBR-LMNA/C double KO clones but not in the LMNA/C-LBR double KO clones. (q value cutoff: 0.05).

Considering the changes in gene expression that occur in all clones upon KO, a set of 47 genes is found to be consistently differentially expressed in both single and double KO clones (**Figure 32**). Interestingly, not only do these genes overlap between clones, but their expression is also affected in the same direction upon deletion. **Figure 18** presents a heatmap illustrating the expression patterns of the common differentially expressed genes across all clones. Dendrograms are used to represent clustering of genes (rows of the heatmap) and clustering of clones (columns of the heatmap). From the dendrogram of the gene clustering two main clusters arise, the one representing mostly upregulated genes and the one representing mostly down regulated genes. When clones are clustered based on the expression of common genes, their grouping closely follows the sequence in which the knockout (KO) experiments were conducted. Regarding LBR clones, LBR KO1 and LBR KO2 are close in the dendrogram, as do LBR DKO1 and LBR DKO2. Additionally, LBR DKO1 is the next closest clone, which aligns with its role as the precursor for both LBR DKO1 and LBR DKO2. Finally, the same holds true for the LMNA/C DKO clones. The LMNA/C KO1 clone closely resembles the two LMNA/C DKO clones reflecting the order in which the KO experiments were performed. However, the expression of this gene set separates the LMNA/C KO2 clone from all others.

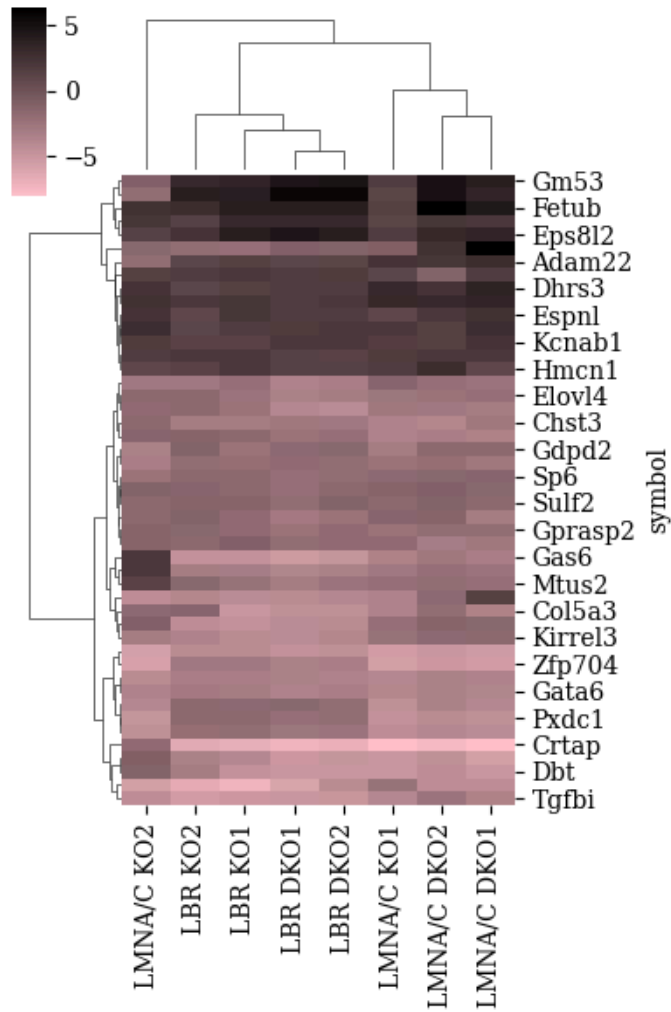


Figure 32: Heatmap representing the expression of all genes that are differentially expressed in all KO clones. Ward’s hierarchical clustering algorithm is used to cluster genes and clones separately.

Finally, in order to assess if any trends regarding the direction of differential expression appear in all studied clones, we compared the number of upregulated and downregulated genes in all KO clones (**Figure 33**). In cells lacking only the expression of LBR, a greater number of downregulated genes is observed compared to the number of upregulated genes. On the other hand, in cells lacking the expression of only LMNA/C as well as in cells lacking the expression of both LBR and LMNA/C the number of upregulated genes exceeds the number of downregulated genes..

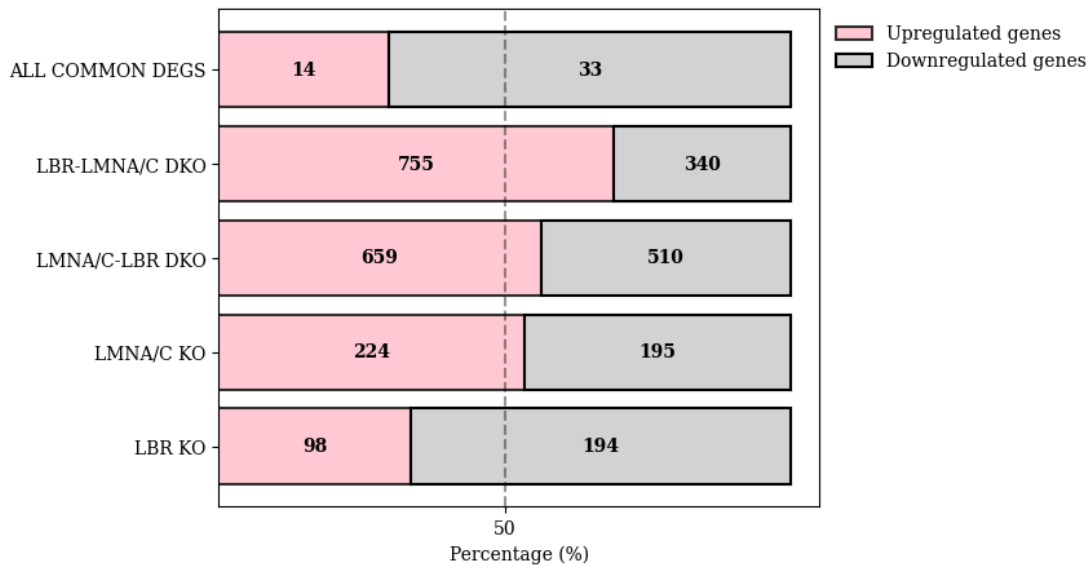


Figure 33: Barplot representing the ratio between the number of upregulated and downregulated genes in each KO clone and in the set of genes differentially expressed in all clones.

3.7 Generation of stable cell lines expressing LBR or PRR14 fused with a biotin ligase.

Following the deletion of LBR, LMNA/C or even both genes we observed subtle, though not profound changes in genome organization, suggesting that additional mechanisms might be responsible for heterochromatin tethering to the nuclear periphery that are capable of maintaining the conventional genome organization even in the absence of LBR and A-type lamins. These mechanisms should involve proteins in the vicinity of LBR, which act in cooperation with it and play a compensatory role in its absence. While several such proteins, such as Lap2 β , emerin and others have been extensively studied, no such role has been identified to date. On the other hand, there is another nuclear peripheral protein, PRR14, found in the vicinity of LBR, that has recently been recognized as a heterochromatin tether to the nuclear periphery. PRR14 has no INM integrated regions and its heterochromatin tethering function is mediated through A-type lamin binding, yet its exact role remains unclear to date with only a few studies investigating it (see Introduction). For these reasons, PRR14 was sorted out of the list of the potential proteins that might compensate for the loss of LBR and LMNA/C in maintaining conventional genome architecture (loss of LMNA/C depletes PRR14 tethering capabilities). To probe the interaction of LBR with PRR14 and identify

additional potential interactors of both proteins we set-up a strategy based on the implementation of BioID2 protocol established by Kyle Roux's lab (Kim et al., 2016).

The protocol is based on the idea of generating a chimeric protein carrying at its one end a protein of interest and at the other end a biotin ligase. The chimeric protein is estimated to add biotin molecules to the proteins in a radius of 10-15 nm around the chimeric protein when the culturing medium is supplemented with biotin. Biotinylation events are rare in mammalian cells, thus allowing for considering the biotin labeled proteins as potential interactors of the protein of interest.

As a first step, we generated plasmid constructs where either the LBR or PRR14 gene was cloned in frame with the birA biotin ligase and an HA tag. Aiming to construct cells that stably express the chimeric proteins we initiated our study by transfecting NIH-3T3 cell line with birA only, LBR-birA or PRR14-birA constructs to assess proper localization and proper biotinylation of the chimeric proteins (**Figure 34**). As expected, in immunofluorescence experiments with birA-HA transfected cells, birA alone is distributed throughout the entire cell, while LBR-birA-HA localizes at the nuclear envelope and the ER. Finally, PRR14 shows strong enrichment at the nuclear rim. Western blot analysis was conducted to further confirm the expression of the chimeric proteins. Using an a-HA antibody we confirmed that all chimeric proteins are properly expressed in the presence and absence of biotin, with an exception of PRR14-BirA-HA where only a faint signal could be obtained in the biotin sample. However, since we were able to obtain a proper signal in the IF experiment for that sample, we attributed the lack of signal in the WB to a technical issue in the experimental procedure rather than an absence of expression in the presence of biotin, and proceeded accordingly. Lastly, birA's ability to biotinylate was confirmed by supplementing the medium with biotin and performing IF and western blot analysis using streptavidin conjugated HRP.

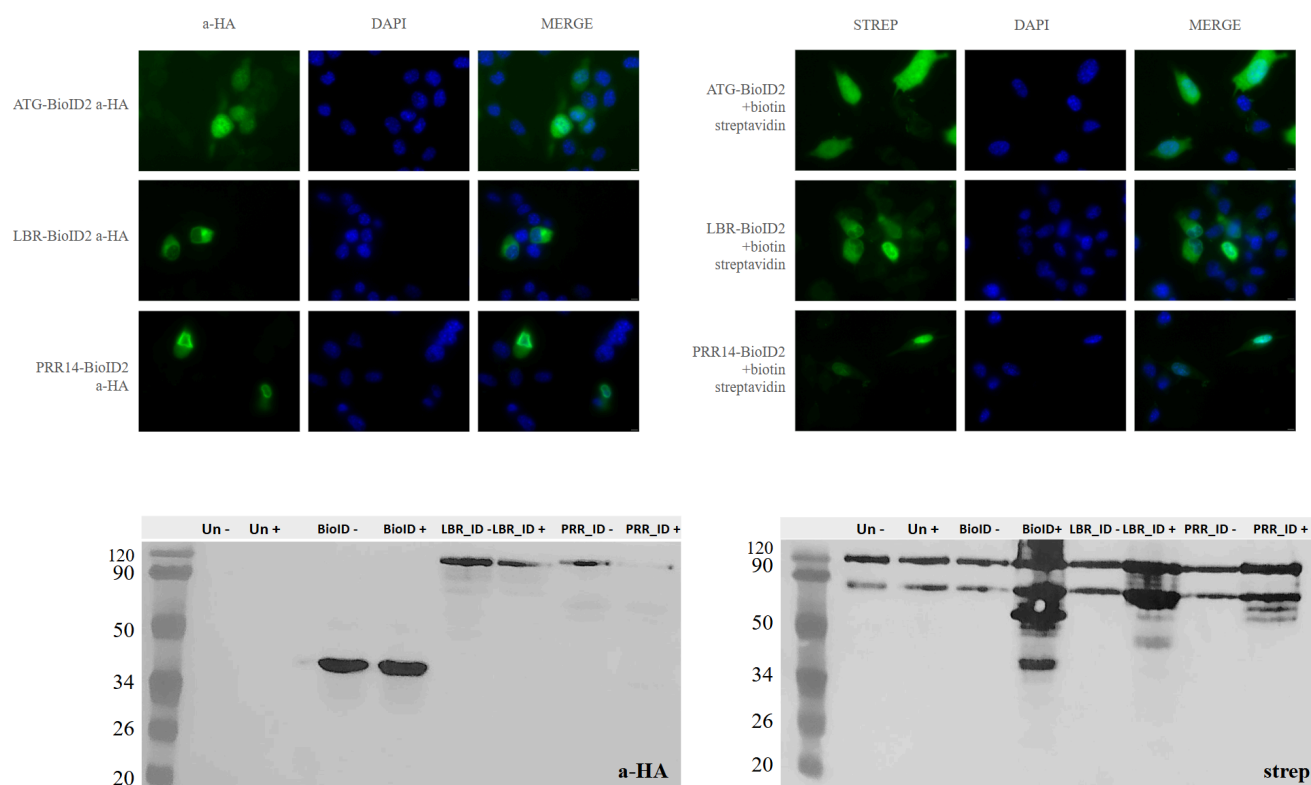


Figure 34: Transfection of NIH-3T3 cells with a construct containing either birA-HA, LBR-BirA-HA or PRR14-BirA-HA. Immunofluorescence panels represent localization of the expressed chimeric protein (left) and biotinylation of the chimeric protein (right). Similarly western blots represent relative abundance of the chimeric proteins (right) and relative abundance of the biotinylated proteins (right)

Following the transfection we cultured cells with addition of puromycin. pPycagip, the plasmid used to insert the constructs carries an internal ribosome entry site (IRES) followed by a puromycin resistance gene allowing for selection of cells only carrying the plasmid and, therefore, only cells expressing the biotin ligase along with the protein of interest. We cultured cells after full recovery following puromycin addition and monitored again the localization of the chimeric protein to ensure that selection was done efficiently and that the chimeric proteins maintain correct localization in the cells (**Figure 35**).

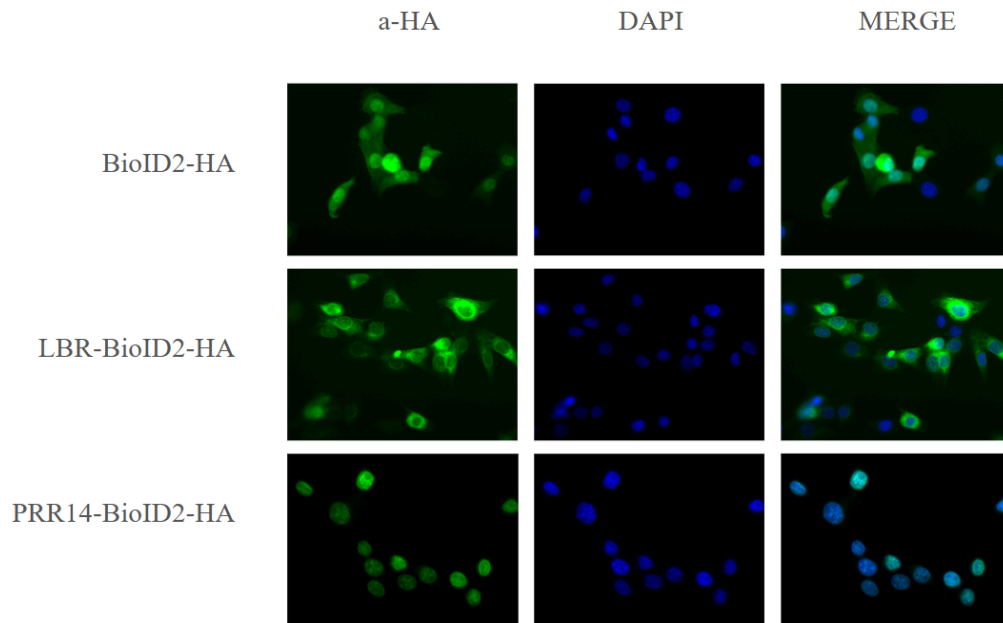
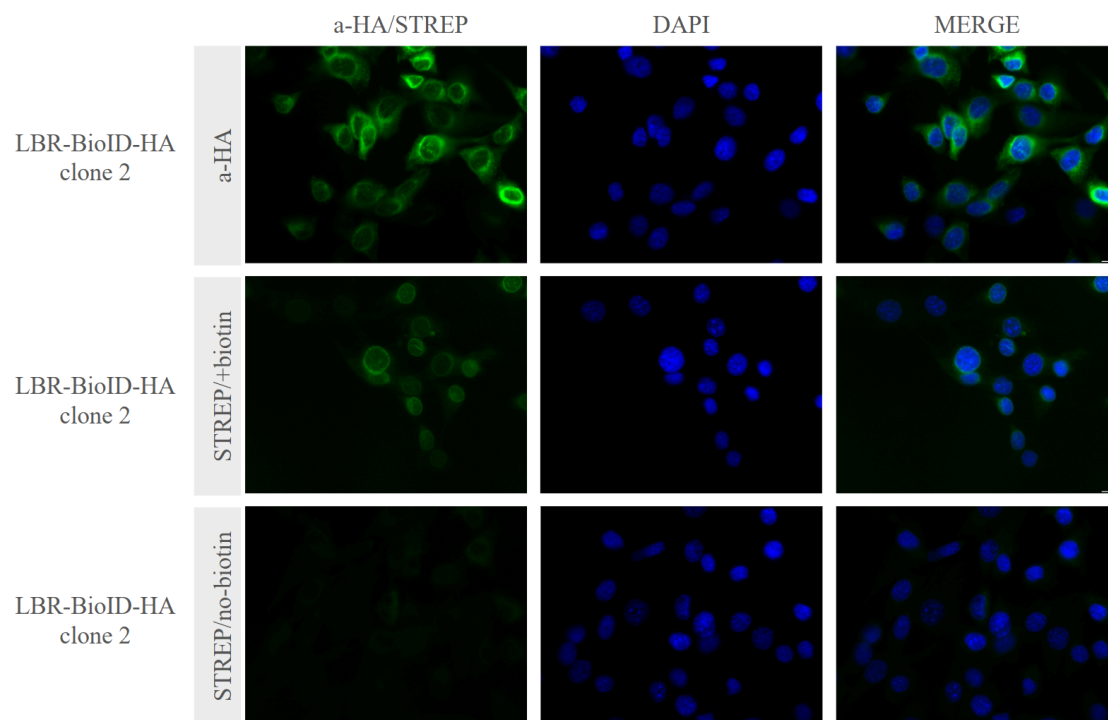
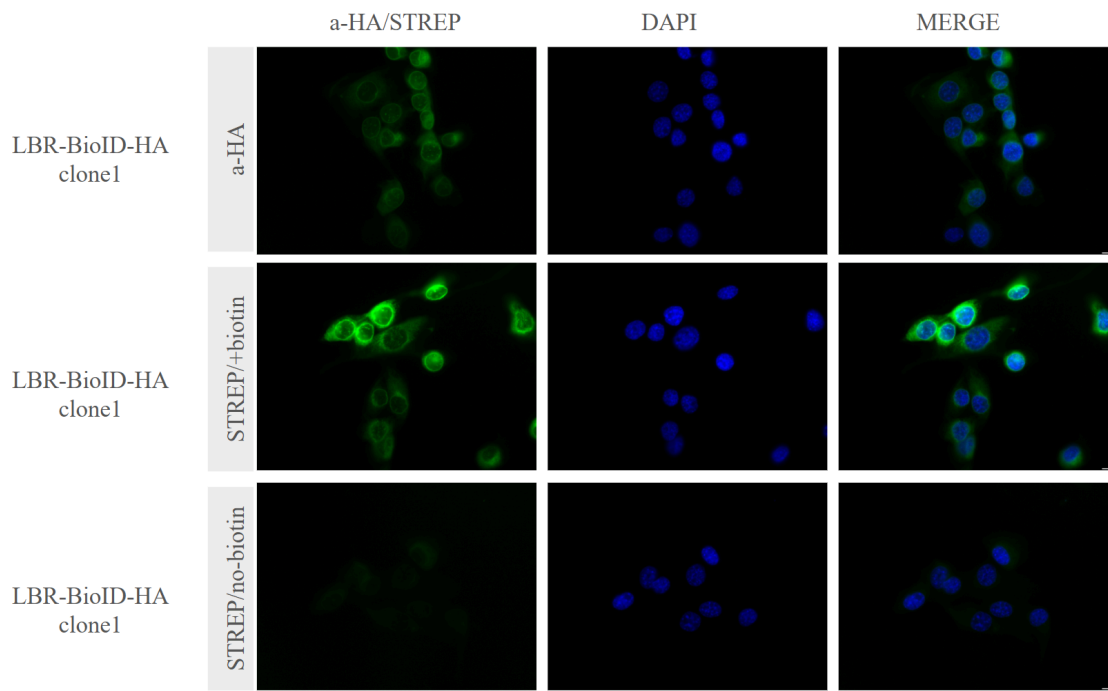
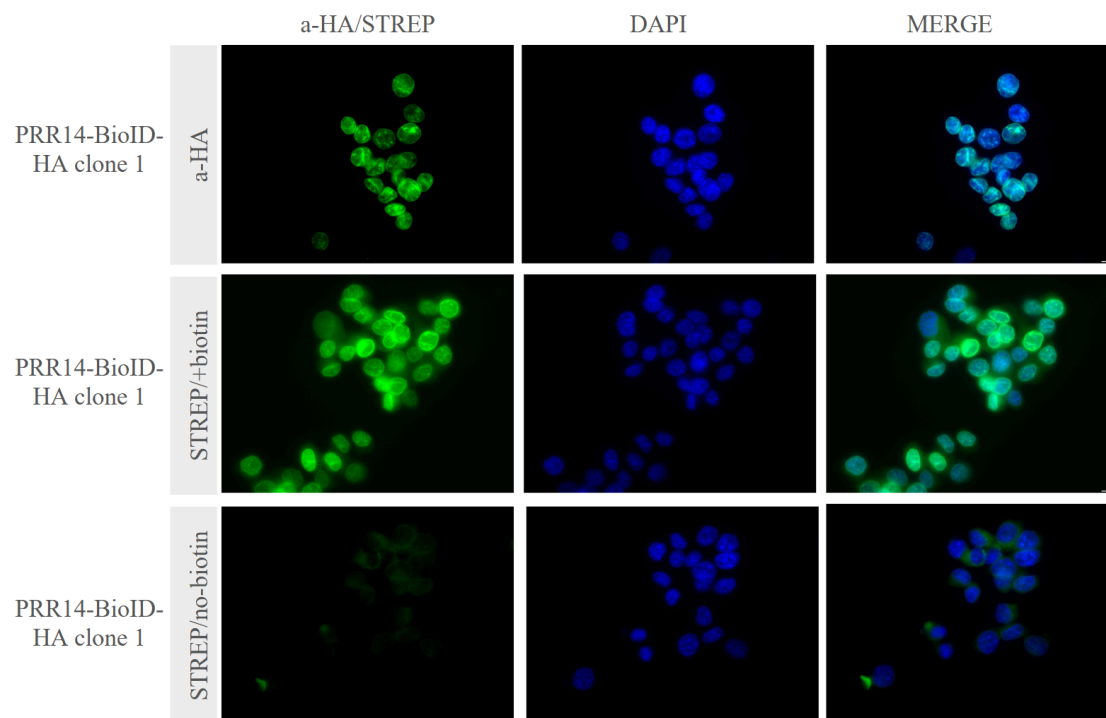
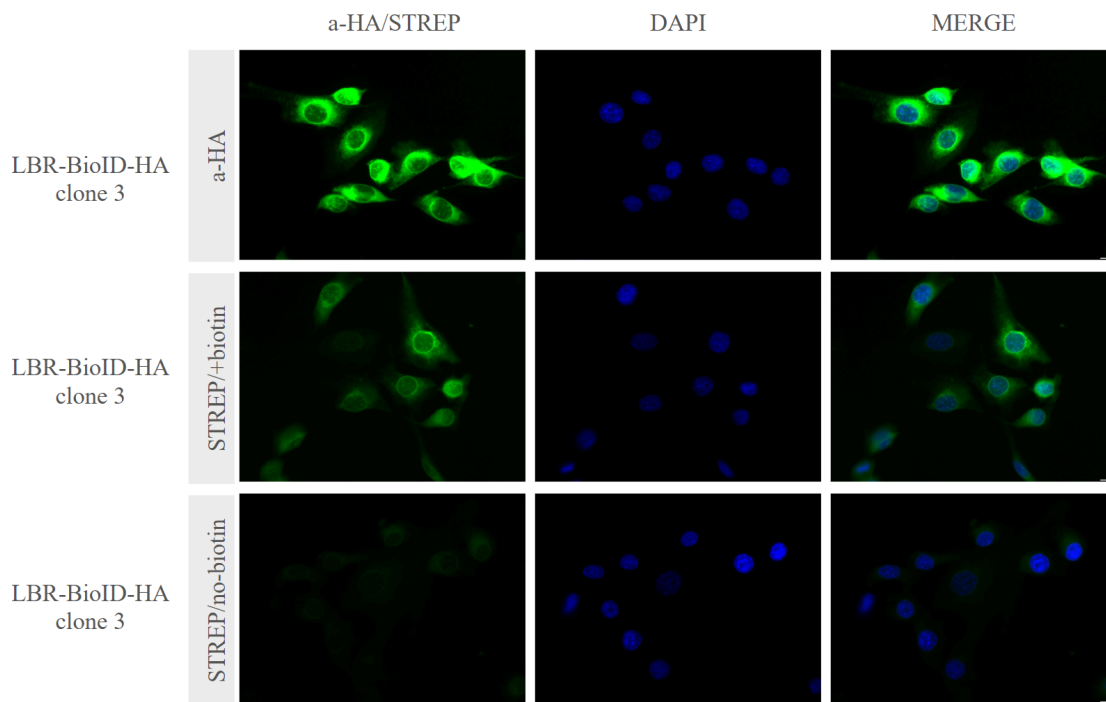
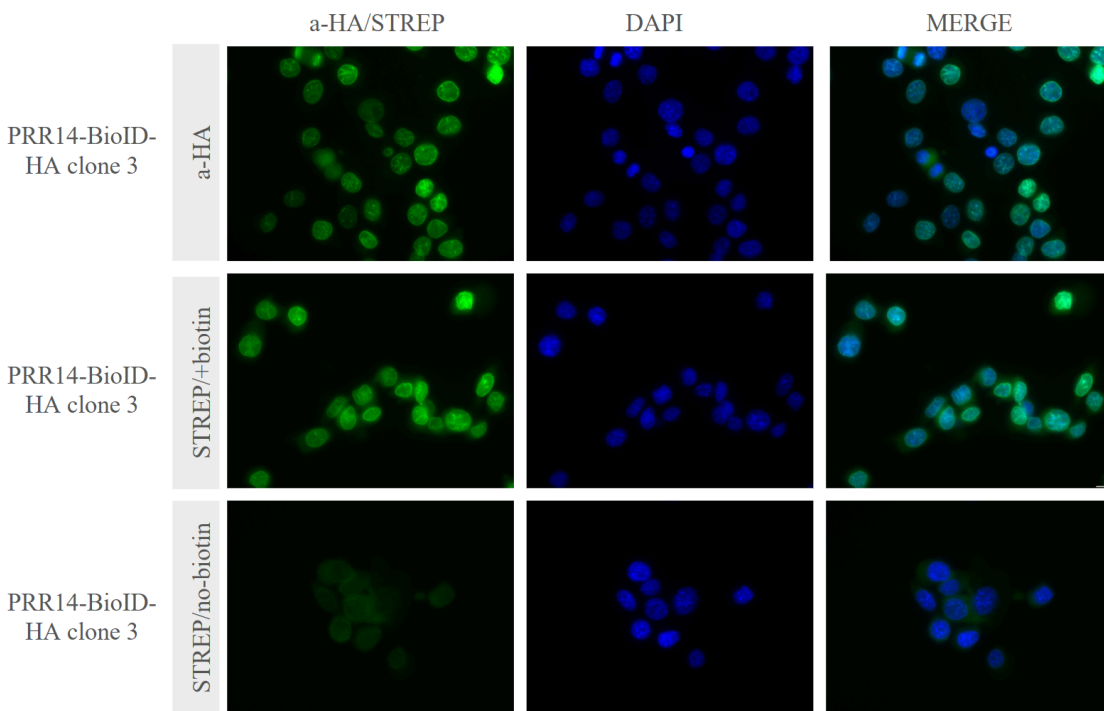
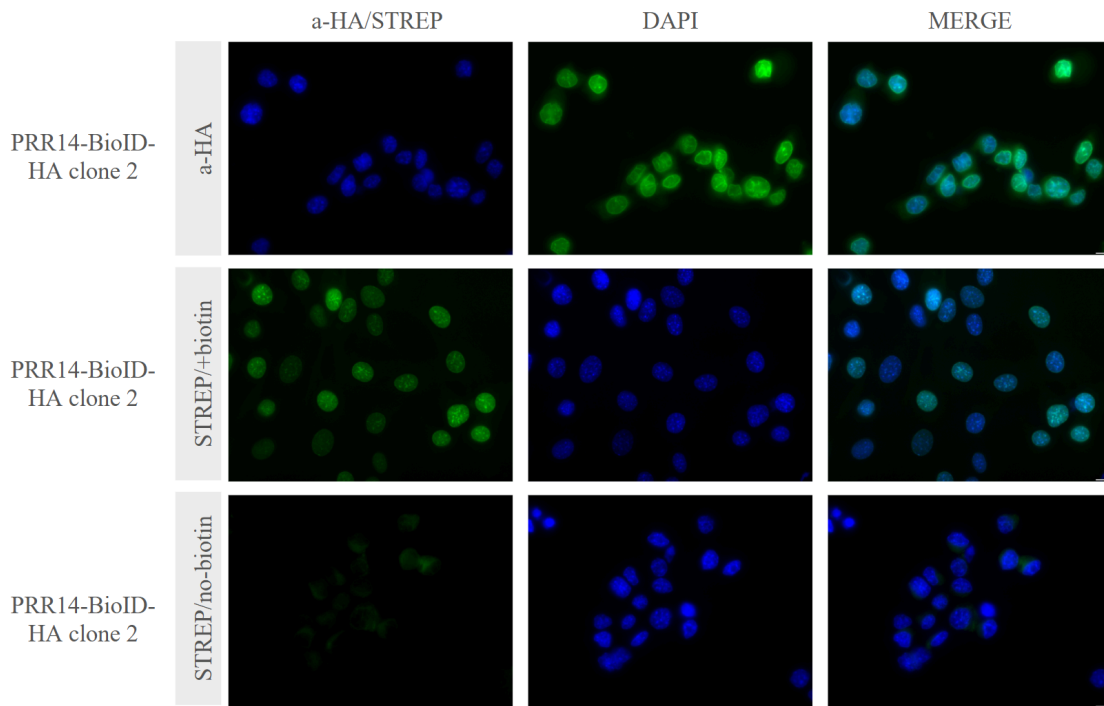


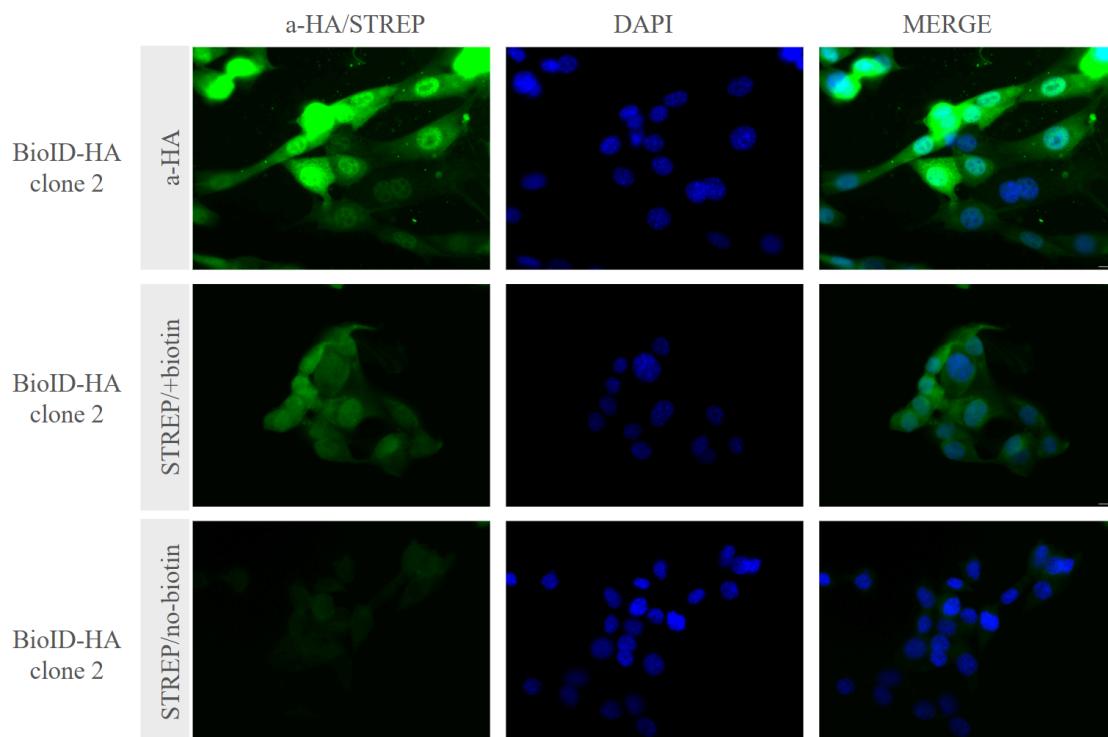
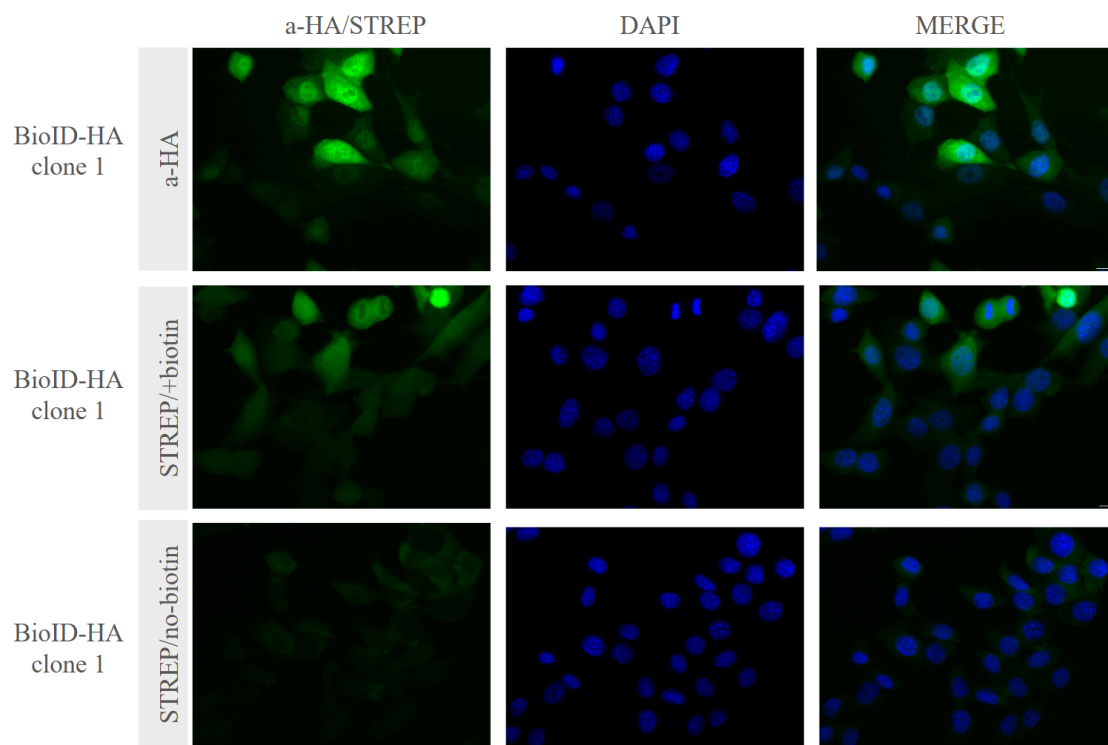
Figure 35: Localization of the chimeric proteins after puromycin selection.

To obtain pure clones we next subcloned the above cultures in 96 well plates after seeding 1 cell per well. Following this strategy we could ensure that all cells in the final clones are derived from the same initial cell. After the subcloning process was completed and subclones could be cultured separately, we tested all the derived clones for proper protein localization and signal intensity. We filtered out clones that produced high intensity signals in immunofluorescence imaging in order to avoid biotinylation of proteins that are outside the desired biotinylation range. We ended up with nine clones in total, three for birA-HA only, three for LBR-birA-HA and three for PRR14-birA-HA (**Figure 36**).









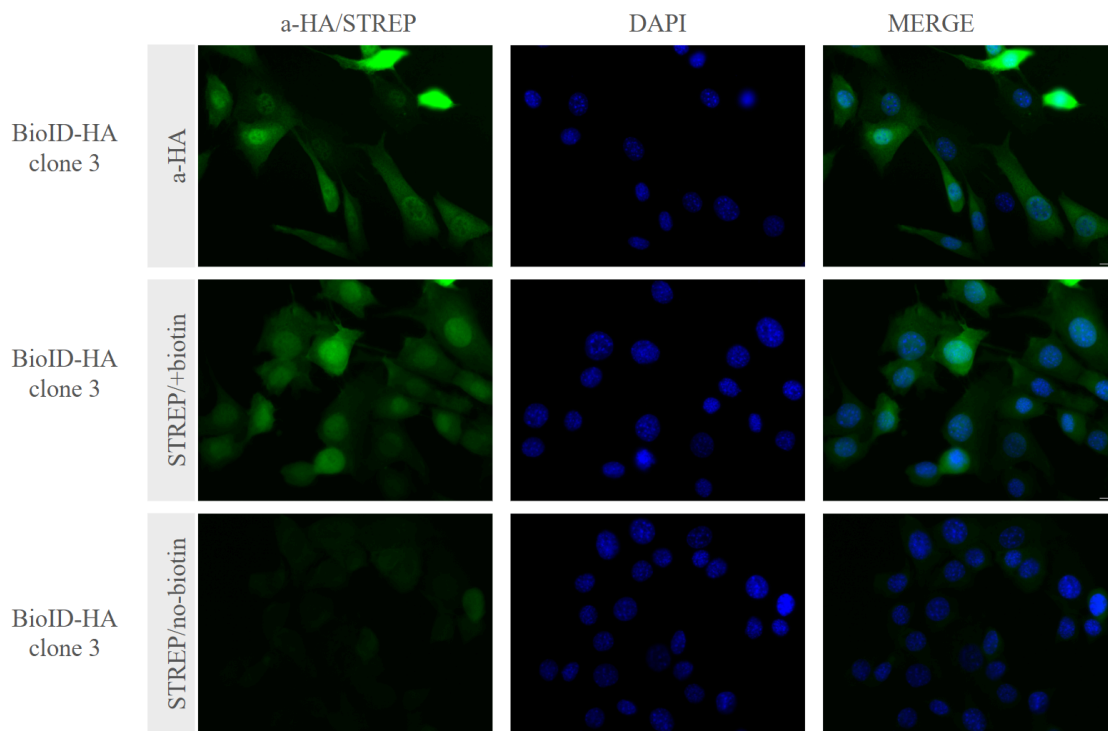


Figure 36: Final clones expressing either the birA biotin ligase alone or the biotin ligase along with LBR or PRR14. Three clones were generated for each one of the three conditions and tested for proper protein localization and proper biotinylation. Each one of the nine panels depicts IF signal for a-HA antibody, streptavidin in presence of biotin and streptavidin in absence of biotin.

Finally, we further tested biotinylation efficacy of the produced clones using western blot analysis (**Figure 37**).

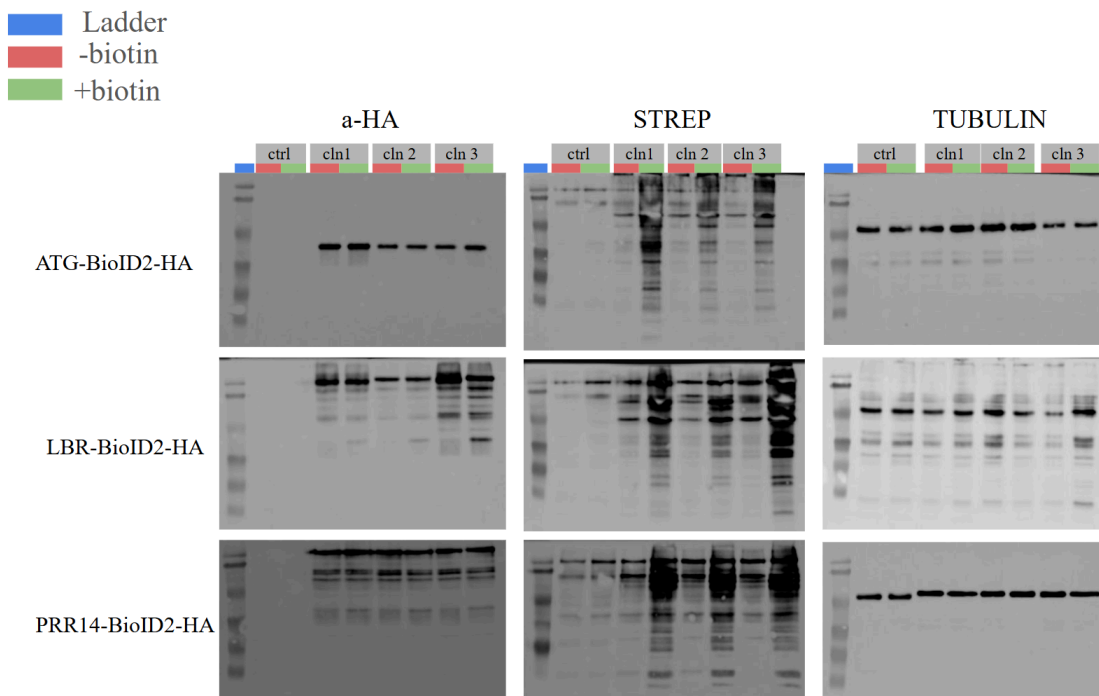


Figure 37: Western blots of the nine selected clones. Each generated clone was subjected to WB. a-HA antibody was used in order to confirm that chimeric proteins are represented in the expected molecular weights, while streptavidin was used to provide semi-quantitative measurements of the biotinylation ability of the clones.

3.8 Pulldown of biotinylated proteins of the generated cell lines.

After generating the cell lines described in section 3.7 we should identify the proteins that get biotinylated after administration of biotin in the cell culture media. In collaboration with Dr K.Soupsana we followed the same protocol described in Roux et al. 2020 paper. Briefly, after cells reached a confluence level of approximately 80% in 100 mm diameter culture dishes (2 dishes per clone) 50 μ M biotin was added and left overnight to ensure that the expressed chimeric protein biotinylates proteins of close proximity. Subsequently cells were washed, lysed and biotinylated proteins were pulled down using streptavidin conjugated sepharose beads. A pre-clearing step with gelatin sepharose beads precedes the streptavidin pulldown to eliminate as effectively as possible non specific biotinylation events that would lead to false positive interactors. During this experimental procedure samples were collected after lysis, after gelatin clearance and after streptavidin pull-down

to validate the effectiveness of each step of the protocol via western blotting as schematically represented in **Figure 38**.

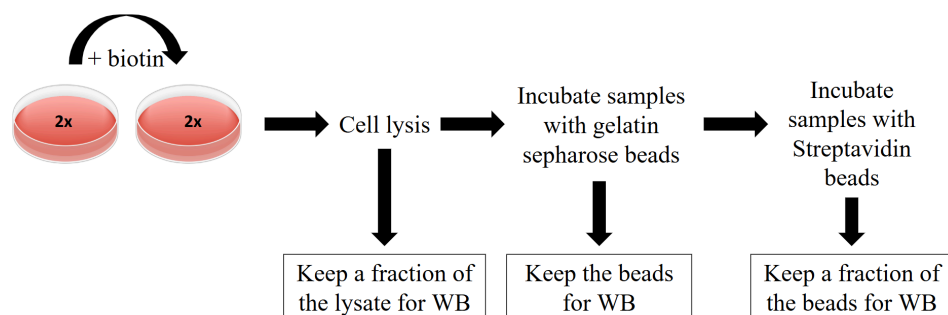


Figure 38: Schematic representation of the experimental procedure followed for the validation of the protocol. Samples were collected after cell lysis, after pre-clearing with gelatin beads as well as after the final step of streptavidin bead pulldown.

Figure 39 demonstrates the abundance of the chimeric protein and the abundance of biotinylated proteins across the three samples. As expected the greatest signal intensity acquired through immunoblotting is observed on the sample collected after cell lysis, where all the cellular content is present. The presence of low intensity bands on all three cell lines on the sample drawn after the clearance step with gelatin-sepharose beads validates that indeed a set of non-specific proteins were excluded from the final selection. Interestingly, bands also appear on the a-HA blot of the pre-clearance sample indicating that some of the chimeric protein is also filtered out. However, considering that strong bands are observed after the streptavidin pulldown this was considered expected and probably the result of clearing excess chimeric protein resulted from overexpression.

The final step of the whole experimental procedure that started from the generation of cell lines expressing the protein of interest fused with the protein ligase was to identify the biotinylated proteins through mass spectrometry. Since our university lacked a mass spectrometry facility we decided to send them over to the mass spectrometry facility of the Biomedical Research Foundation Academy of Athens. We considered obtaining three technical replicates from each cell line to ensure statistical confidence. Prior to that however we decided to only send one sample from each cell line, (the sample collected from the above experiments) to ensure that all prior experimental procedures yielded expected results. Unfortunately, due to technical issues on the HPLC unit of the mass

spectrometer these preliminary samples never got subjected to mass spectrometry analysis and we couldn't proceed to the analysis of the actual replicates.

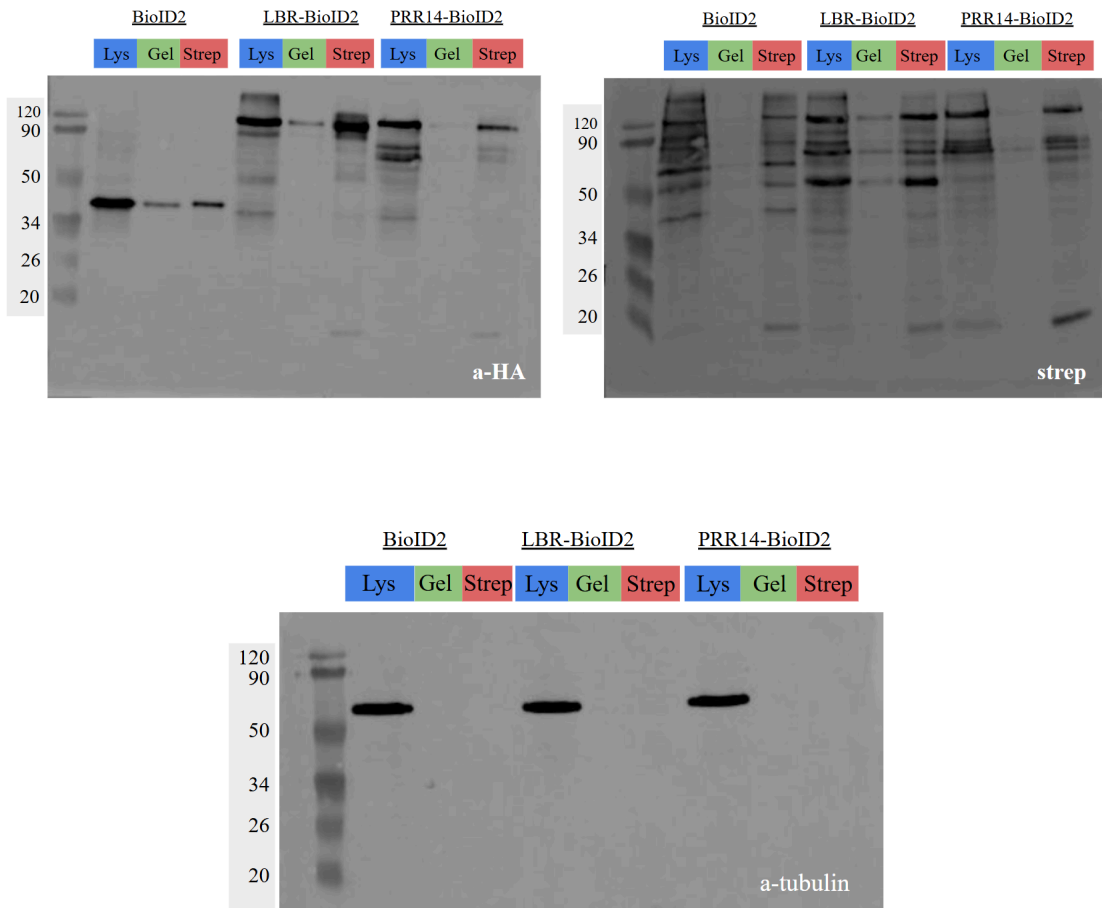


Figure 39: Western blot analysis of samples collected throughout the pulldown experiments. Each cell line is represented by three different samples/lanes in the blot. The first one represents the cell lysate, the second one the protein content retrieved from pre-clearing of the cell lysate with gelatin-sepharose beads and the last one represents the actual biotinylated content collected after pull down with streptavidin conjugated sepharose beads. On the top left blot the abundance of the chimeric proteins is monitored through a-HA antibody. On the top right blot the abundance of biotinylated proteins is monitored through streptavidin-HRP conjugate. On the bottom blot the reference abundance of a-tubulin is monitored through anti tubulin antibody.

4. Discussion

In this study we investigated the effects of LBR and LMNA/C deletion on the chromatin landscape and the transcriptional profiles of mouse NIH-3T3 cells. Cells subjected to LBR and LMNA/C deletion were also assayed for changes in their ability to proliferate. Previous studies have linked the loss of LBR to reduced cell proliferation. In more detail, Gaines et al., used EML (erythroid, myeloid and lymphocyte cells) derived promyelocytes (EPRO cells) from bone marrow of ichthyosis mice harboring either one functional copy of the LBR gene or none (Gaines et al., 2008). In agreement with our findings, cells harboring no functional copies of the LBR gene exhibited decreased proliferation when compared to cells with at least one functional copy of the LBR gene. Interestingly in our experimental set up we were able to compensate for this proliferation lag by supplying cells with extra serum. However, this was possible only for cells that were lacking LBR expression while maintaining proper LMNA/C expression. In the case of cells where both LMNA/C and LBR expression were prevented the proliferation lag was prominent, even after serum supplementation indicating a potential interaction effect of loss of LBR and loss of LMNA/C. Additionally, recent studies link reduced LBR expression to cellular senescence, a phenotype described by cell cycle arrest induced by various factors ranging from exposure to chemicals to aging and oncogene activation. On the other hand, regarding A-type lamins, a recent study by Onoue et al., revealed that lack of LMNA/C expression in LMNA/C null mice resulted in reduced cell cycle activity and retarded cell maturation of cardiomyocytes (Onoue et al., 2021). Overall recent literature supports the implication of LBR and LMNA/C in cell proliferation in agreement with findings of the current study. Collectively, we speculate a synergistic role of LBR and LMNA/C in regulating cell cycle progression in NIH-3T3 cells due to the prominent proliferation lag observed in all tested double KO clones.

Furthermore, contrary to existing literature supporting increased cell proliferation, cell cycle progression and reduced apoptosis of cancer cells when supplemented with cholesterol, our double KO clones fail to regain proliferation rates comparable to wild type NIH-3T3 cells when supplemented with cholesterol (Wang et al., 2019). Adding to that, the possibility that the reduced proliferation rate of double KO clones is due to their demolished LBR mediated lanosterol reduction is shorted out. Collectively, we can expand our hypothesis of synergy between LBR and LMNA/C to slow down cell proliferation and hypothesize that this synergy at least in part is not due to LBR's implication in cholesterol biosynthesis. However, ethanol, used as a solvent for cholesterol, significantly affects cell proliferation, making the conclusions from this series of experiments uncertain.

Regarding the architectural properties of the cells lacking LBR, LMNA/C or both it has been already demonstrated both by our lab and others that deletion or just specific mutations on the gene encoding A-type lamins result in subpopulations of cells where the distribution of several members of the nuclear periphery proteome deviates from the usual distribution (Sullivan et al., 1999, Vigoroux et al., 2001; Martzios et al., unpublished results). Additionally, loss of LMNA/C has been associated with altered nuclear shape as the lamin meshwork underlying the nuclear envelope provides mechanical support and stiffness to the cell nucleus (Sullivan et al., 1999, Goelzer et al., 2021). In more detail, a recent study by Goelzer et al., demonstrated that in differentiating Mesenchymal Stem Cells (MSCs) siRNA targeting LMNA/C gene resulted in expanded nuclei that exhibited decreased circularity and stiffness (Goelzer et al., 2021). Although our KO clones were not tested for circularity nor for stiffness, we evaluated nuclear envelope integrity by investigating whether the asymmetrical distributions of the peripheral proteins represent holes in the nuclear envelope thus pointing to malformations at the nuclear envelope. Our results for the overexpressed H1 clearly demonstrate that these asymmetrical regions of the envelope do not correspond to nuclear ruptures. Finally, of particular interest is the mechanical aspect of these asymmetries. Literature regarding this phenotype is limited and the experimental approach to further characterize them seems very challenging. We speculate several mechanisms that possibly give rise to such asymmetries all directly related to cell division. One such mechanism could be that cells lacking A-type lamins fail to properly undergo the mitotic phases due to the importance of lamin meshwork breakdown during NE disassembly. Here we hypothesize that peripheral proteins are not properly arranged prior to cell division. Another explanatory cause could be an impaired localization of the NE proteins this time during NE formation on the daughter cells given that lamin contacts with chromatin proceed nuclear envelope formation on the daughter cells (Lopez-Soler et al., 2001). Taking these into account, along with the reduced proliferation that double KO clones exhibit it would be interesting to investigate the viability and the proliferative capacity of this subpopulation of cells as they can be the explanatory cause of the reduced proliferation assessed in bulk for the double KO cells. In any case, further studies, potentially to single cell resolution, need to be conducted in order to confer valid conclusions regarding the source of these asymmetries.

Our results regarding large scale chromatin changes only partially overlap with existing data supporting that loss of LBR along with LMNA/C leads to complete reverse of genome organization and localization of heterochromatin to the nuclear interior and euchromatin at the nuclear periphery (Salovei et al., 2012). In our NIH-3T3 cells loss of either LBR, LMNA/C or both could not yield full inversion of heterochromatin and euchromatin spanned nuclear regions. However, measurements

regarding the size and the number of heterochromatic foci indicated only a tendency towards chromatin inversion inferred from a statistically significant increase in the number and decrease in the size of heterochromatic foci in cells lacking the expression of both LMNA/C and LBR. No significant changes were observed in the size and the shape of heterochromatic foci for cells depleted for only LMNA/C or LBR. Regarding the cells lacking the expression of only LMNA/C the fact that no changes were observed in the heterochromatic foci come with agreement with experiments conducted by Amendola and van Steensel who demonstrated on mouse embryonic stem cells that depletion of all lamins is not sufficient to induce changes in genome-wide interaction patterns of chromatin (Amendola and van Steensel, 2015). On the other hand, regarding the relationship of LBR expression and heterochromatic foci formation experiments by En et al., demonstrated correlation of LBR expression with reduced formation of a specific type of heterochromatic foci related to the senescent phenotype named Senescence Associated Heterochromatic Foci (SASP) (En et al 2020). En et al chemically induced senescence in HeLa and TIG-7 human cells and after ensuring LBR downregulation inspected the formation of SAHF. Senescent cells lacking LBR exhibited SAHF that were suppressed when cells were transfected with plasmids carrying the LBR gene thus forcing LBR overexpression. These results demonstrate negative correlation between LBR expression and SAHF formation (En et al 2019). Based on our data however no relationship could be exerted between deletion of LBR and neither the size nor the number of heterochromatic foci. Interestingly however, when the heterochromatic foci were tested for changes in their dynamics in the course of the FRAP experiments the only comparisons that yielded statistically significant, but subtle changes in HP1a dynamics were between one of the two LBR single KO clones and the corresponding control as well as one of the LMNA/C single KO clones and their controls. Changes in HP1a dynamics of cells lacking the expression of both LMNA/C and LBR were not statistically significant when compared with their controls. In this context an interesting study conducted by Schmiedeberg et al. utilized Fluorescence Correlation Spectroscopy along with FRAP to perform an in depth analysis of the HP1 kinetics in human epithelial cells. Two different HP1 populations were recognized from the experiments, one with high mobility attributed to euchromatin and one with very low mobility attributed to heterochromatin (Schmiedeberg et al., 2004). Taking these into account along with findings suggesting that heterochromatin to euchromatin transition moving from the nuclear periphery to the nuclear interior follows a gradient rather than an abrupt transition it would be interesting to test chromatin dynamics between our KO clones along with their spatial information with regard to the nuclear envelope (Fišerová et al., 2017).

As expected deletion of LBR and LMNA/C genes resulted in changes in gene expression of all clones. Affected genes were characteristic of the fibroblast cell line used, as biological processes regarding extracellular matrix organization and cellular mobility were affected. However, when clones were tested for their migration ability no changes were observed between KO clones and wild type cells (Evangelia Triantopoulou thesis work). Interestingly, all knockouts resulted in significant changes in expression of genes related to chemotaxis. These results come in agreement with findings from Gaines et al., that showcase that neutrophils lacking the expression of LBR exhibit deficient response to cytokine stimulation (Gaines et al., 2008). If we generalize this to our clones we can expand this notion and hypothesize that cells lacking either LBR, LMNA/C or both may exhibit deficiencies in cytokine response. However, further experimental validation of this hypothesis is needed to confirm such hypothesis.

Regarding the transcriptional changes observed upon LBR and LMNA/C loss, it is worth noting that apart from taxis and chemotaxis that appeared as the most statistically significant and most enriched biological processes following every knockout, the rest of the enriched biological processes represent general terms highly associated with fibroblasts, highlighting the already accepted notion that LBR and LMNA/C are not directly related to any specific biological process and their primary function is structural, ensuring heterochromatin remains at the nuclear periphery and maintaining nuclear stiffness.

Finally, contrary to the findings of Salovei et al. we conclude that LBR and LMNA/C are not sufficient to completely shift chromatin architecture to a reversed state, at least in the cell type we studied. Thus we speculate the presence of one or more proteins responsible for maintaining conventional genome organization in the absence of A-type lamins and LBR. Our attention was drawn to PRR14, another nuclear peripheral protein located near LBR, which has recently been identified as a heterochromatin tether to the nuclear periphery. Unlike LBR, PRR14 lacks INM-integrated regions, and its tethering function is mediated through A-type lamin binding. However, its exact role remains unclear, with only a few studies investigating it to date. In the context of this thesis stable cell lines have been completed and successfully validated for the identification of such proteins.

More specifically, to probe the interaction of LBR with PRR14 and identify additional potential interactors of both proteins we set-up a strategy based on the implementation of the BioID2 protocol established by Kyle Roux's lab (Kim et al., 2016). We generated and validated stable cell lines expressing LBR or PRR14 fused with a biotin ligase. We then proceeded to pulldown experiments that resulted in samples enriched for biotinylated proteins each time specific to the studied protein.

Finally, we submitted the corresponding gel bands to the Proteomics Facility of the Biomedical Research Foundation of the Academy of Athens (BRFAA) for proteomic analysis. However due to technical issues, the results were not available within the timeframe of this thesis.

Future Perspectives

Our experimental data raise new questions about the intricate organization of chromatin. Results from the work described in this thesis as well as work conducted by former lab members highlight the importance of LMNA/C and LBR in proper protein distribution at the nuclear periphery, efficient cell proliferation and overall genome organization. However, the exact mechanisms underlying these processes are not yet clearly understood and require further investigation.

First, the identification of interaction partners of LBR and PRR14 needs to be completed. Due to technical issues with the mass spectrometer these experiments could not be completed under the scope of the current thesis.

Additionally, electron microscopy can be used in order to monitor in the finest detail possible the peripheral nuclear regions that exhibit asymmetrical protein distribution. Such experiments would allow us to visualize the protein and lipid content in these regions, potentially uncovering causal mechanisms of the asymmetries. Complementing such experiments, a very interesting expansion of imaging experiments would be the combination of microscopy with chemicals that arrest the mitotic process at different time points. Introducing time as a variable in the experimental design could help determine when, if at all, these asymmetries occur during the cell cycle.

Finally, given the significance of these two proteins in genome organization, a thorough genomic analysis of the clones could prove highly insightful. Starting with ATAC-seq and CHIP-seq we could get a precise comparison of accessible genomic regions and differences in distributions of desired histone marks. For example we could address chromatin regions that exhibit differences in H3K9me2 between control and KO clones. These genomic regions can be considered as regions that lost their peripheral tethering upon LBR or LMNA/C loss. Furthermore, regarding the clones that exhibit subpopulation with asymmetrical protein distribution, single cell sequencing approaches could be implemented in order to test whether expression profiles of different cells can be used to identify subclones with distinct expression profiles inside the bulk population. Finally, a more comprehensive understanding of chromatin organization changes could be achieved through chromatin conformation capture assays that map long range chromatin contacts across the whole genome.

References

Mereschkowsky C. 1905. Über Natur und Ursprung der Chromatophoren im Pflanzenreiche. Biol. Zentrablatt. 25, 593–604.

- Cavalier-Smith T. 2002. The phagotrophic origin of eukaryotes and phylogenetic classification on Protozoa. *Int. J. Syst. Evol. Microbiol.* 52, 297–354.
- Lisitsyna, O. M., & Sheval, E. V. (2016). Origin and early evolution of the nuclear envelope. *Biochemistry (Moscow) Supplement Series A: Membrane and Cell Biology*, 10(4), 251–258.
- Gould G.W., Dring G.J. 1979. On a possible relationship between bacterial endospore formation and the origin of eukaryotic cells. *J. Theor. Biol.* 81, 47–53.
- WATSON, M L. “The nuclear envelope; its structure and relation to cytoplasmic membranes.” *The Journal of biophysical and biochemical cytology* vol. 1,3 (1955): 257-70. doi:10.1083/jcb.1.3.257
- Callan, H. G., and Tomlin, S. G., *Proc. Roy. Soc. London, Series B*, 1950, 137, 367.
- HARTMANN, J F. “An electron optical study of sections of central nervous system.” *The Journal of comparative neurology* vol. 99,1 (1953): 201-49. doi:10.1002/cne.900990111
- D'Angelo, Maximiliano A, and Martin W Hetzer. “Structure, dynamics and function of nuclear pore complexes.” *Trends in cell biology* vol. 18,10 (2008): 456-66.
- Calero-Cuenca FJ, Janota CS, Gomes ER. Dealing with the nucleus during cell migration. *Curr Opin Cell Biol.* 2018 Feb;50:35-41. doi: 10.1016/j.ceb.2018.01.014. Epub 2018 Feb 20. PMID: 29454272.
- Gomes ER, Jani S, Gundersen GG. Nuclear movement regulated by Cdc42, MRCK, myosin, and actin flow establishes MTOC polarization in migrating cells. *Cell.* 2005 May 6;121(3):451-63. doi: 10.1016/j.cell.2005.02.022. PMID: 15882626.
- Zhen Y. Y., Libotte T., Munck M., Noegel A. A. and Korenbaum E. (2002) NUANCE, a giant protein connecting the nucleus and actin cytoskeleton. *J. Cell. Sci.* 115: 3207–3222
- Padmakumar V. C., Abraham S., Braune S., Noegel A. A., Tunggal B., Karakesisoglou I. et al. (2004) Enaptin, a giant actin-binding protein, is an element of the nuclear membrane and the actin cytoskeleton. *Exp. Cell Res.* 295: 330–339
- Solovei, Irina et al. “LBR and lamin A/C sequentially tether peripheral heterochromatin and inversely regulate differentiation.” *Cell* vol. 152,3 (2013): 584-98. doi:10.1016/j.cell.2013.01.009
- Grossman, Einat et al. “Functional architecture of the nuclear pore complex.” *Annual review of biophysics* vol. 41 (2012): 557-84. doi:10.1146/annurev-biophys-050511-102328

- Raices, Marcela, and Maximiliano A D'Angelo. "Nuclear pore complex composition: a new regulator of tissue-specific and developmental functions." *Nature reviews. Molecular cell biology* vol. 13,11 (2012): 687-99. doi:10.1038/nrm3461
- Henikoff, Steven, and M Mitchell Smith. "Histone variants and epigenetics." *Cold Spring Harbor perspectives in biology* vol. 7,1 a019364. 5 Jan. 2015, doi:10.1101/cshperspect.a019364
- Wong X, Loo TH, Stewart CL. LINC complex regulation of genome organization and function. *Curr Opin Genet Dev.* 2021 Apr;67:130-141. doi: 10.1016/j.gde.2020.12.007. Epub 2021 Jan 30. PMID: 33524904.
- Lamis A, Siddiqui SW, Ashok T, Patni N, Fatima M, Aneef AN. Hutchinson-Gilford Progeria Syndrome: A Literature Review. *Cureus.* 2022 Aug 31;14(8):e28629. doi: 10.7759/cureus.28629. PMID: 36196312; PMCID: PMC9524302.
- López-Otín, Carlos et al. "Hallmarks of aging: An expanding universe." *Cell* vol. 186,2 (2023): 243-278. doi:10.1016/j.cell.2022.11.001
- Martins, Filipa et al. "Nuclear envelope dysfunction and its contribution to the aging process." *Aging cell* vol. 19,5 (2020): e13143. doi:10.1111/accel.13143
- Vargas, Jesse D et al. "Transient nuclear envelope rupturing during interphase in human cancer cells." *Nucleus (Austin, Tex.)* vol. 3,1 (2012): 88-100. doi:10.4161/nucl.18954
- Denais, Celine M et al. "Nuclear envelope rupture and repair during cancer cell migration." *Science (New York, N.Y.)* vol. 352,6283 (2016): 353-8. doi:10.1126/science.aad7297
- Arai R, En A, Takauji Y, Maki K, Miki K, Fujii M, Ayusawa D. Lamin B receptor (LBR) is involved in the induction of cellular senescence in human cells. *Mech Ageing Dev.* 2019 Mar;178:25-32. doi: 10.1016/j.mad.2019.01.001. Epub 2019 Jan 4. PMID: 30615890.
- Hennen J, Kohler J, Karuka SR, Saunders CA, Luxton GWG, Mueller JD. Differentiating Luminal and Membrane-Associated Nuclear Envelope Proteins. *Biophys J.* 2020 May 19;118(10):2385-2399. doi: 10.1016/j.bpj.2020.03.025. Epub 2020 Apr 8. PMID: 32304637; PMCID: PMC7231917.
- Bahmanyar, Shirin, and Christian Schlieker. "Lipid and protein dynamics that shape nuclear envelope identity." *Molecular biology of the cell* vol. 31,13 (2020): 1315-1323. doi:10.1091/mbc.E18-10-0636

Bahmanyar, Shirin, and Christian Schlieker. "Lipid and protein dynamics that shape nuclear envelope identity." *Molecular biology of the cell* vol. 31,13 (2020): 1315-1323.
doi:10.1091/mbc.E18-10-0636

De Magistris, Paola, and Wolfram Antonin. "The Dynamic Nature of the Nuclear Envelope." *Current biology : CB* vol. 28,8 (2018): R487-R497. doi:10.1016/j.cub.2018.01.073

Marschall, Manfred et al. "Regulatory roles of protein kinases in cytomegalovirus replication." *Advances in virus research* vol. 80 (2011): 69-101. doi:10.1016/B978-0-12-385987-7.00004-X

Hatch, Emily, and Martin Hetzer. "Breaching the nuclear envelope in development and disease." *The Journal of cell biology* vol. 205,2 (2014): 133-41. doi:10.1083/jcb.201402003

Berg JM, Tymoczko JL, Stryer L (2002). Section 12.6, lipids and many membrane proteins diffuse rapidly in the plane of the membrane. In: *Biochemistry*, 5th ed., New York: WH Freeman.

Drin, Guillaume et al. "A general amphipathic alpha-helical motif for sensing membrane curvature." *Nature structural & molecular biology* vol. 14,2 (2007): 138-46. doi:10.1038/nsmb1194

van Meer, Gerrit et al. "Membrane lipids: where they are and how they behave." *Nature reviews. Molecular cell biology* vol. 9,2 (2008): 112-24. doi:10.1038/nrm2330

Tsai, Pei-Ling et al. "The Lamin B receptor is essential for cholesterol synthesis and perturbed by disease-causing mutations." *eLife* vol. 5 e16011. 23 Jun. 2016, doi:10.7554/eLife.16011

Kinugasa, Yasuha et al. "The very-long-chain fatty acid elongase Elo2 rescues lethal defects associated with loss of the nuclear barrier function in fission yeast cells." *Journal of cell science* vol. 132,10 jcs229021. 15 May. 2019, doi:10.1242/jcs.229021

Hwang, Sunyoung et al. "Suppressing Aneuploidy-Associated Phenotypes Improves the Fitness of Trisomy 21 Cells." *Cell reports* vol. 29,8 (2019): 2473-2488.e5. doi:10.1016/j.celrep.2019.10.059

Romanauska, Anete, and Alwin Köhler. "The Inner Nuclear Membrane Is a Metabolically Active Territory that Generates Nuclear Lipid Droplets." *Cell* vol. 174,3 (2018): 700-715.e18.
doi:10.1016/j.cell.2018.05.047

Peter, Annette, and Reimer Stick. "Evolutionary aspects in intermediate filament proteins." *Current opinion in cell biology* vol. 32 (2015): 48-55. doi:10.1016/j.ceb.2014.12.009

Bahmanyar, Shirin, and Christian Schlieker. "Lipid and protein dynamics that shape nuclear envelope identity." *Molecular biology of the cell* vol. 31,13 (2020): 1315-1323.
doi:10.1091/mbc.E18-10-0636

Barger, Sarah R et al. “Coupling lipid synthesis with nuclear envelope remodeling.” *Trends in biochemical sciences* vol. 47,1 (2022): 52-65. doi:10.1016/j.tibs.2021.08.009

Doucet CM, Talamas JA, Hetzer MW (2010). Cell cycle-dependent differences in nuclear pore complex assembly in metazoa. *Cell* 141, 1030–1041.

Maul, G G et al. “Time sequence of nuclear pore formation in phytohemagglutinin-stimulated lymphocytes and in HeLa cells during the cell cycle.” *The Journal of cell biology* vol. 55,2 (1972): 433-47. doi:10.1083/jcb.55.2.433

Otsuka, Shotaro, and Jan Ellenberg. “Mechanisms of nuclear pore complex assembly - two different ways of building one molecular machine.” *FEBS letters* vol. 592,4 (2018): 475-488. doi:10.1002/1873-3468.12905

Otsuka, Shotaro et al. “Nuclear pore assembly proceeds by an inside-out extrusion of the nuclear envelope.” *eLife* vol. 5 e19071. 15 Sep. 2016, doi:10.7554/eLife.19071

Otsuka, Atsushi et al. “The interplay between genetic and environmental factors in the pathogenesis of atopic dermatitis.” *Immunological reviews* vol. 278,1 (2017): 246-262. doi:10.1111/imr.12545

Rasala, Beth A et al. “Capture of AT-rich chromatin by ELYS recruits POM121 and NDC1 to initiate nuclear pore assembly.” *Molecular biology of the cell* vol. 19,9 (2008): 3982-96. doi:10.1091/mbc.e08-01-0012

Mansfeld, Jörg et al. “The conserved transmembrane nucleoporin NDC1 is required for nuclear pore complex assembly in vertebrate cells.” *Molecular cell* vol. 22,1 (2006): 93-103. doi:10.1016/j.molcel.2006.02.015

Vollmer, Benjamin et al. “Dimerization and direct membrane interaction of Nup53 contribute to nuclear pore complex assembly.” *The EMBO journal* vol. 31,20 (2012): 4072-84. doi:10.1038/emboj.2012.256

Eisenhardt, Nathalie et al. “Interaction of Nup53 with Ndc1 and Nup155 is required for nuclear pore complex assembly.” *Journal of cell science* vol. 127,Pt 4 (2014): 908-21. doi:10.1242/jcs.141739

Goldberg, M W et al. “Dimples, pores, star-rings, and thin rings on growing nuclear envelopes: evidence for structural intermediates in nuclear pore complex assembly.” *Journal of cell science* vol. 110 (Pt 4) (1997): 409-20. doi:10.1242/jcs.110.4.409

Kiseleva, E et al. “Steps of nuclear pore complex disassembly and reassembly during mitosis in early *Drosophila* embryos.” *Journal of cell science* vol. 114,Pt 20 (2001): 3607-18. doi:10.1242/jcs.114.20.3607

- Dultz, Elisa et al. "Systematic kinetic analysis of mitotic dis- and reassembly of the nuclear pore in living cells." *The Journal of cell biology* vol. 180,5 (2008): 857-65. doi:10.1083/jcb.200707026
- Bodoor, K et al. "Sequential recruitment of NPC proteins to the nuclear periphery at the end of mitosis." *Journal of cell science* vol. 112 (Pt 13) (1999): 2253-64. doi:10.1242/jcs.112.13.2253
- Dawson, T Renee et al. "ER membrane-bending proteins are necessary for de novo nuclear pore formation." *The Journal of cell biology* vol. 184,5 (2009): 659-75. doi:10.1083/jcb.200806174
- Doucet, Christine M et al. "Cell cycle-dependent differences in nuclear pore complex assembly in metazoa." *Cell* vol. 141,6 (2010): 1030-41. doi:10.1016/j.cell.2010.04.036
- Talamas, Jessica A, and Martin W Hetzer. "POM121 and Sun1 play a role in early steps of interphase NPC assembly." *The Journal of cell biology* vol. 194,1 (2011): 27-37. doi:10.1083/jcb.201012154
- Funakoshi, Tomoko et al. "Localization of Pom121 to the inner nuclear membrane is required for an early step of interphase nuclear pore complex assembly." *Molecular biology of the cell* vol. 22,7 (2011): 1058-69. doi:10.1091/mbc.E10-07-0641
- Laurell, Eva et al. "Phosphorylation of Nup98 by multiple kinases is crucial for NPC disassembly during mitotic entry." *Cell* vol. 144,4 (2011): 539-50. doi:10.1016/j.cell.2011.01.012
- Lénárt, Péter et al. "Nuclear envelope breakdown in starfish oocytes proceeds by partial NPC disassembly followed by a rapidly spreading fenestration of nuclear membranes." *The Journal of cell biology* vol. 160,7 (2003): 1055-68. doi:10.1083/jcb.200211076
- Ellenberg J, Siggia ED, Moreira JE, Smith CL, Presley JF, Worman HJ, Lippincott-Schwartz J: Nuclear membrane dynamics and reassembly in living cells: targeting of an inner nuclear membrane protein in interphase and mitosis. *J Cell Biol* 1997, 138:1193–1206.
- Linder MI, Köhler M, Boersema P, Weberruss M, Wandke C, Marino J, Ashiono C, Picotti P, Antonin W, Kutay U: Mitotic disassembly of nuclear pore complexes involves CDK1- and PLK1-mediated phosphorylation of key interconnecting nucleoporins. *Dev Cell* 2017, 43:141–156. e7.
- Okada N, Sato M: Spatiotemporal regulation of nuclear transport machinery and microtubule organization. *Cells* 2015, 4:406–426
- Guttinger S, Laurell E, Kutay U: Orchestrating nuclear envelope disassembly and reassembly during mitosis. *Nat Rev Mol Cell Biol* 2009, 10:178-191.

Ungricht, R., Klann, M., Horvath, P. & Kutay, U. Diffusion and retention are major determinants of protein targeting to the inner nuclear membrane. *J. Cell Biol.* 209, 687–703 (2015)

Ungricht, Rosemarie, and Ulrike Kutay. “Mechanisms and functions of nuclear envelope remodelling.” *Nature reviews. Molecular cell biology* vol. 18,4 (2017): 229-245.
doi:10.1038/nrm.2016.153

Schooley, Allana et al. “The lysine demethylase LSD1 is required for nuclear envelope formation at the end of mitosis.” *Journal of cell science* vol. 128,18 (2015): 3466-77. doi:10.1242/jcs.173013

Afonso, O. et al. Feedback control of chromosome separation by a midzone Aurora B gradient. *Science* 345, 332–336 (2014).

Vagnarelli, Paola et al. “Repo-Man coordinates chromosomal reorganization with nuclear envelope reassembly during mitotic exit.” *Developmental cell* vol. 21,2 (2011): 328-42.
doi:10.1016/j.devcel.2011.06.020

Wandke, Cornelia, and Ulrike Kutay. “Enclosing chromatin: reassembly of the nucleus after open mitosis.” *Cell* vol. 152,6 (2013): 1222-5. doi:10.1016/j.cell.2013.02.046

Anderson, Daniel J, and Martin W Hetzer. “Nuclear envelope formation by chromatin-mediated reorganization of the endoplasmic reticulum.” *Nature cell biology* vol. 9,10 (2007): 1160-6.
doi:10.1038/ncb1636

Anderson, Daniel J, and Martin W Hetzer. “Reshaping of the endoplasmic reticulum limits the rate for nuclear envelope formation.” *The Journal of cell biology* vol. 182,5 (2008): 911-24.
doi:10.1083/jcb.200805140

Guttinger S, Laurell E, Kutay U: Orchestrating nuclear envelope disassembly and reassembly during mitosis. *Nat Rev Mol Cell Biol* 2009, 10:178-191

Gorjanacz, M. et al. *Caenorhabditis elegans* BAF-1 and its kinase VRK-1 participate directly in post-mitotic nuclear envelope assembly. *EMBO J.* 26, 132–143 (2007).

Dechat, T. et al. LAP2 α and BAF transiently localize to telomeres and specific regions on chromatin during nuclear assembly. *J. Cell Sci.* 117, 6117–6128 (2004)

Haraguchi, Tokuko et al. “Live cell imaging and electron microscopy reveal dynamic processes of BAF-directed nuclear envelope assembly.” *Journal of cell science* vol. 121,Pt 15 (2008): 2540-54.
doi:10.1242/jcs.033597

Newport, J. W., Wilson, K. L. & Dunphy, W. G. A lamin- independent pathway for nuclear envelope assembly.

Krietenstein, Nils et al. “Ultrastructural Details of Mammalian Chromosome Architecture.” *Molecular cell* vol. 78,3 (2020): 554-565.e7. doi:10.1016/j.molcel.2020.03.003

Hughes, Amanda L, and Oliver J Rando. “Comparative Genomics Reveals Chd1 as a Determinant of Nucleosome Spacing in Vivo.” *G3 (Bethesda, Md.)* vol. 5,9 1889-97. 14 Jul. 2015, doi:10.1534/g3.115.020271

Hsieh, Tsung-Han S et al. “Resolving the 3D Landscape of Transcription-Linked Mammalian Chromatin Folding.” *Molecular cell* vol. 78,3 (2020): 539-553.e8. doi:10.1016/j.molcel.2020.03.002

Dekker, Job, and Tom Misteli. “Long-Range Chromatin Interactions.” *Cold Spring Harbor perspectives in biology* vol. 7,10 a019356. 1 Oct. 2015, doi:10.1101/cshperspect.a019356

Vermunt, Marit W et al. “The interdependence of gene-regulatory elements and the 3D genome.” *The Journal of cell biology* vol. 218,1 (2019): 12-26. doi:10.1083/jcb.201809040

Cremer, Thomas, and Marion Cremer. “Chromosome territories.” *Cold Spring Harbor perspectives in biology* vol. 2,3 (2010): a003889. doi:10.1101/cshperspect.a003889

Lieberman-Aiden, Erez et al. “Comprehensive mapping of long-range interactions reveals folding principles of the human genome.” *Science (New York, N.Y.)* vol. 326,5950 (2009): 289-93. doi:10.1126/science.1181369

Kim, Yoori, and Hongtao Yu. “Shaping of the 3D genome by the ATPase machine cohesin.” *Experimental & molecular medicine* vol. 52,12 (2020): 1891-1897. doi:10.1038/s12276-020-00526-2

van Schaik, Tom et al. “Dynamic chromosomal interactions and control of heterochromatin positioning by Ki-67.” *EMBO reports* vol. 23,12 (2022): e55782. doi:10.15252/embr.202255782

de Wit, Elzo et al. “CTCF Binding Polarity Determines Chromatin Looping.” *Molecular cell* vol. 60,4 (2015): 676-84. doi:10.1016/j.molcel.2015.09.023

Dixon, Jesse R et al. “Topological domains in mammalian genomes identified by analysis of chromatin interactions.” *Nature* vol. 485,7398 376-80. 11 Apr. 2012, doi:10.1038/nature11082

Nora, Elphège P et al. “Spatial partitioning of the regulatory landscape of the X-inactivation centre.” *Nature* vol. 485,7398 381-5. 11 Apr. 2012, doi:10.1038/nature11049

- Mariño-Ramírez, Leonardo et al. "Histone structure and nucleosome stability." *Expert review of proteomics* vol. 2,5 (2005): 719-29. doi:10.1586/14789450.2.5.719
- Rossetto, Dorine et al. "Histone phosphorylation: a chromatin modification involved in diverse nuclear events." *Epigenetics* vol. 7,10 (2012): 1098-108. doi:10.4161/epi.21975
- Kumar, Amarjeet, and Hidetoshi Kono. "Heterochromatin protein 1 (HP1): interactions with itself and chromatin components." *Biophysical reviews* vol. 12,2 (2020): 387-400. doi:10.1007/s12551-020-00663-y
- Deaton, Aimée M, and Adrian Bird. "CpG islands and the regulation of transcription." *Genes & development* vol. 25,10 (2011): 1010-22. doi:10.1101/gad.2037511
- Piccolo, Francesco M, and Amanda G Fisher. "Getting rid of DNA methylation." *Trends in cell biology* vol. 24,2 (2014): 136-43. doi:10.1016/j.tcb.2013.09.001
- van Steensel, Bas, and Andrew S Belmont. "Lamina-Associated Domains: Links with Chromosome Architecture, Heterochromatin, and Gene Repression." *Cell* vol. 169,5 (2017): 780-791. doi:10.1016/j.cell.2017.04.022
- Briand, Nolwenn, and Philippe Collas. "Lamina-associated domains: peripheral matters and internal affairs." *Genome biology* vol. 21,1 85. 2 Apr. 2020, doi:10.1186/s13059-020-02003-5
- Kind, Jop et al. "Genome-wide maps of nuclear lamina interactions in single human cells." *Cell* vol. 163,1 (2015): 134-47. doi:10.1016/j.cell.2015.08.040
- Guelen, Lars et al. "Domain organization of human chromosomes revealed by mapping of nuclear lamina interactions." *Nature* vol. 453,7197 (2008): 948-51. doi:10.1038/nature06947
- Kind, Jop et al. "Single-cell dynamics of genome-nuclear lamina interactions." *Cell* vol. 153,1 (2013): 178-92. doi:10.1016/j.cell.2013.02.028
- Kind, Jop, and Bas van Steensel. "Genome-nuclear lamina interactions and gene regulation." *Current opinion in cell biology* vol. 22,3 (2010): 320-5. doi:10.1016/j.ceb.2010.04.002
- Padeken, Jan et al. "Establishment of H3K9-methylated heterochromatin and its functions in tissue differentiation and maintenance." *Nature reviews. Molecular cell biology* vol. 23,9 (2022): 623-640. doi:10.1038/s41580-022-00483-w
- Shokrollahi, Mitra et al. "DNA double-strand break-capturing nuclear envelope tubules drive DNA repair." *Nature structural & molecular biology* vol. 31,9 (2024): 1319-1330. doi:10.1038/s41594-024-01286-7

- Tenga, Rafael, and Ohad Medalia. "Structure and unique mechanical aspects of nuclear lamin filaments." *Current opinion in structural biology* vol. 64 (2020): 152-159. doi:10.1016/j.sbi.2020.06.017
- Shimi, Takeshi et al. "Structural organization of nuclear lamins A, C, B1, and B2 revealed by superresolution microscopy." *Molecular biology of the cell* vol. 26,22 (2015): 4075-86. doi:10.1091/mbc.E15-07-0461
- Harhour, Karim et al. "An overview of treatment strategies for Hutchinson-Gilford Progeria syndrome." *Nucleus (Austin, Tex.)* vol. 9,1 (2018): 246-257. doi:10.1080/19491034.2018.1460045
- Briand, Nolwenn, and Philippe Collas. "Lamina-associated domains: peripheral matters and internal affairs." *Genome biology* vol. 21,1 85. 2 Apr. 2020, doi:10.1186/s13059-020-02003-5
- Meaburn, Karen J et al. "Disease-specific gene repositioning in breast cancer." *The Journal of cell biology* vol. 187,6 (2009): 801-12. doi:10.1083/jcb.200909127
- Williams, Ruth R E et al. "Neural induction promotes large-scale chromatin reorganisation of the Mash1 locus." *Journal of cell science* vol. 119,Pt 1 (2006): 132-40. doi:10.1242/jcs.02727
- Branco, Miguel R, and Ana Pombo. "Intermingling of chromosome territories in interphase suggests role in translocations and transcription-dependent associations." *PLoS biology* vol. 4,5 (2006): e138. doi:10.1371/journal.pbio.0040138
- McStay, Brian. "Nucleolar organizer regions: genomic 'dark matter' requiring illumination." *Genes & development* vol. 30,14 (2016): 1598-610. doi:10.1101/gad.283838.116
- Lomvardas, Stavros et al. "Interchromosomal interactions and olfactory receptor choice." *Cell* vol. 126,2 (2006): 403-13. doi:10.1016/j.cell.2006.06.035
- Monahan, Kevin et al. "Cooperative interactions enable singular olfactory receptor expression in mouse olfactory neurons." *eLife* vol. 6 e28620. 21 Sep. 2017, doi:10.7554/eLife.28620
- Barutcu, A Rasim et al. "Systematic mapping of nuclear domain-associated transcripts reveals speckles and lamina as hubs of functionally distinct retained introns." *Molecular cell* vol. 82,5 (2022): 1035-1052.e9. doi:10.1016/j.molcel.2021.12.010
- Misteli, Tom. "The Self-Organizing Genome: Principles of Genome Architecture and Function." *Cell* vol. 183,1 (2020): 28-45. doi:10.1016/j.cell.2020.09.014
- Rao, Suhas S P et al. "A 3D map of the human genome at kilobase resolution reveals principles of chromatin looping." *Cell* vol. 159,7 (2014): 1665-80. doi:10.1016/j.cell.2014.11.021

- Mao, Yuntao S et al. "Biogenesis and function of nuclear bodies." *Trends in genetics : TIG* vol. 27,8 (2011): 295-306. doi:10.1016/j.tig.2011.05.006
- Hetzer, Martin W, and Susan R Wente. "Border control at the nucleus: biogenesis and organization of the nuclear membrane and pore complexes." *Developmental cell* vol. 17,5 (2009): 606-16. doi:10.1016/j.devcel.2009.10.007
- Cheng, Li-Chun et al. "Comparative membrane proteomics reveals diverse cell regulators concentrated at the nuclear envelope." *Life science alliance* vol. 6,9 e202301998. 11 Jul. 2023, doi:10.26508/lsa.202301998
- Berk, Jason M et al. "The nuclear envelope LEM-domain protein emerin." *Nucleus (Austin, Tex.)* vol. 4,4 (2013): 298-314. doi:10.4161/nucl.25751
- Wong, Xianrong et al. "The Nuclear Lamina." *Cold Spring Harbor perspectives in biology* vol. 14,2 a040113. 1 Feb. 2022, doi:10.1101/cshperspect.a040113
- Haraguchi, Tokuko et al. "Live cell imaging and electron microscopy reveal dynamic processes of BAF-directed nuclear envelope assembly." *Journal of cell science* vol. 121,Pt 15 (2008): 2540-54. doi:10.1242/jcs.033597
- Knockenbauer, Kevin E, and Thomas U Schwartz. "The Nuclear Pore Complex as a Flexible and Dynamic Gate." *Cell* vol. 164,6 (2016): 1162-1171. doi:10.1016/j.cell.2016.01.034
- Wente, Susan R, and Michael P Rout. "The nuclear pore complex and nuclear transport." *Cold Spring Harbor perspectives in biology* vol. 2,10 (2010): a000562. doi:10.1101/cshperspect.a000562
- Hoelz, André et al. "Toward the atomic structure of the nuclear pore complex: when top down meets bottom up." *Nature structural & molecular biology* vol. 23,7 (2016): 624-30. doi:10.1038/nsmb.3244
- Beck, Martin, and Ed Hurt. "The nuclear pore complex: understanding its function through structural insight." *Nature reviews. Molecular cell biology* vol. 18,2 (2017): 73-89. doi:10.1038/nrm.2016.147
- Kim, Seung Joong et al. "Integrative structure and functional anatomy of a nuclear pore complex." *Nature* vol. 555,7697 (2018): 475-482. doi:10.1038/nature26003
- Capelson, Maya et al. "Chromatin-bound nuclear pore components regulate gene expression in higher eukaryotes." *Cell* vol. 140,3 (2010): 372-83. doi:10.1016/j.cell.2009.12.054
- Sood, Varun, and Jason H Brickner. "Nuclear pore interactions with the genome." *Current opinion in genetics & development* vol. 25 (2014): 43-9. doi:10.1016/j.gde.2013.11.018

- Luthra, Roopa et al. "Actively transcribed GAL genes can be physically linked to the nuclear pore by the SAGA chromatin modifying complex." *The Journal of biological chemistry* vol. 282,5 (2007): 3042-9. doi:10.1074/jbc.M608741200
- Franks, Tobias M et al. "Evolution of a transcriptional regulator from a transmembrane nucleoporin." *Genes & development* vol. 30,10 (2016): 1155-71. doi:10.1101/gad.280941.116
- Gozalo, Alejandro et al. "Core Components of the Nuclear Pore Bind Distinct States of Chromatin and Contribute to Polycomb Repression." *Molecular cell* vol. 77,1 (2020): 67-81.e7. doi:10.1016/j.molcel.2019.10.017
- Lombardi, Maria L, and Jan Lammerding. "Keeping the LINC: the importance of nucleocytoskeletal coupling in intracellular force transmission and cellular function." *Biochemical Society transactions* vol. 39,6 (2011): 1729-34. doi:10.1042/BST20110686
- Kirby, Tyler J, and Jan Lammerding. "Emerging views of the nucleus as a cellular mechanosensor." *Nature cell biology* vol. 20,4 (2018): 373-381. doi:10.1038/s41556-018-0038-y
- Villeneuve, Clémentine et al. "Mechanical forces across compartments coordinate cell shape and fate transitions to generate tissue architecture." *Nature cell biology* vol. 26,2 (2024): 207-218. doi:10.1038/s41556-023-01332-4
- Gruenbaum, Yosef et al. "The nuclear lamina comes of age." *Nature reviews. Molecular cell biology* vol. 6,1 (2005): 21-31. doi:10.1038/nrm1550
- Nazer, Ezequiel. "To be or not be (in the LAD): emerging roles of lamin proteins in transcriptional regulation." *Biochemical Society transactions* vol. 50,2 (2022): 1035-1044. doi:10.1042/BST20210858
- Tenga, Rafael, and Ohad Medalia. "Structure and unique mechanical aspects of nuclear lamin filaments." *Current opinion in structural biology* vol. 64 (2020): 152-159. doi:10.1016/j.sbi.2020.06.017
- Balaji AK, Saha S, Deshpande S, Poola D, Sengupta K. Nuclear envelope, chromatin organizers, histones, and DNA: The many achilles heels exploited across cancers. *Front Cell Dev Biol.* 2022 Dec 16;10:1068347. doi: 10.3389/fcell.2022.1068347. PMID: 36589746; PMCID: PMC9800887
- Worman, H J et al. "A lamin B receptor in the nuclear envelope." *Proceedings of the National Academy of Sciences of the United States of America* vol. 85,22 (1988): 8531-4. doi:10.1073/pnas.85.22.8531
- Olins, Ada L et al. "Lamin B receptor: multi-tasking at the nuclear envelope." *Nucleus (Austin, Tex.)* vol. 1,1 (2010): 53-70. doi:10.4161/nucl.1.1.10515

Hirano, Yasuhiro et al. "Lamin B receptor recognizes specific modifications of histone H4 in heterochromatin formation." *The Journal of biological chemistry* vol. 287,51 (2012): 42654-63. doi:10.1074/jbc.M112.397950

Nikolakaki, Eleni et al. "Lamin B Receptor: Interplay between Structure, Function and Localization." *Cells* vol. 6,3 28. 31 Aug. 2017, doi:10.3390/cells6030028

Liokatis, Stamatios et al. "Phosphorylation of histone H3 Ser10 establishes a hierarchy for subsequent intramolecular modification events." *Nature structural & molecular biology* vol. 19,8 (2012): 819-23. doi:10.1038/nsmb.2310

Soullam, B, and H J Worman. "The amino-terminal domain of the lamin B receptor is a nuclear envelope targeting signal." *The Journal of cell biology* vol. 120,5 (1993): 1093-100. doi:10.1083/jcb.120.5.1093

Smith, S, and G Blobel. "The first membrane spanning region of the lamin B receptor is sufficient for sorting to the inner nuclear membrane." *The Journal of cell biology* vol. 120,3 (1993): 631-7. doi:10.1083/jcb.120.3.631

Smith, S, and G Blobel. "The first membrane spanning region of the lamin B receptor is sufficient for sorting to the inner nuclear membrane." *The Journal of cell biology* vol. 120,3 (1993): 631-7. doi:10.1083/jcb.120.3.631

Makatsori, Dimitra et al. "The inner nuclear membrane protein lamin B receptor forms distinct microdomains and links epigenetically marked chromatin to the nuclear envelope." *The Journal of biological chemistry* vol. 279,24 (2004): 25567-73. doi:10.1074/jbc.M313606200

Nikolakaki, E et al. "A nuclear envelope-associated kinase phosphorylates arginine-serine motifs and modulates interactions between the lamin B receptor and other nuclear proteins." *The Journal of biological chemistry* vol. 271,14 (1996): 8365-72. doi:10.1074/jbc.271.14.8365

Olins, Ada L et al. "Lamin B receptor: multi-tasking at the nuclear envelope." *Nucleus (Austin, Tex.)* vol. 1,1 (2010): 53-70. doi:10.4161/nucl.1.1.10515

Lukášová, Emilie et al. "Loss of lamin B receptor is necessary to induce cellular senescence." *The Biochemical journal* vol. 474,2 (2017): 281-300. doi:10.1042/BCJ20160459

Poleshko, Andrey et al. "Genome-Nuclear Lamina Interactions Regulate Cardiac Stem Cell Lineage Restriction." *Cell* vol. 171,3 (2017): 573-587.e14. doi:10.1016/j.cell.2017.09.018

- Kiseleva, Anna A et al. "PRR14 organizes H3K9me3-modified heterochromatin at the nuclear lamina." *Nucleus (Austin, Tex.)* vol. 14,1 (2023): 2165602. doi:10.1080/19491034.2023.2165602
- Poleshko, Andrey et al. "Identification of a functional network of human epigenetic silencing factors." *The Journal of biological chemistry* vol. 285,1 (2010): 422-33. doi:10.1074/jbc.M109.064667
- Poleshko, Andrey et al. "Human factors and pathways essential for mediating epigenetic gene silencing." *Epigenetics* vol. 9,9 (2014): 1280-9. doi:10.4161/epi.32088
- Poleshko, Andrey et al. "The human protein PRR14 tethers heterochromatin to the nuclear lamina during interphase and mitotic exit." *Cell reports* vol. 5,2 (2013): 292-301. doi:10.1016/j.celrep.2013.09.024
- Nozawa, Ryu-Suke et al. "Human POGZ modulates dissociation of HP1alpha from mitotic chromosome arms through Aurora B activation." *Nature cell biology* vol. 12,7 (2010): 719-27. doi:10.1038/ncb2075
- Guruharsha, K G et al. "A protein complex network of *Drosophila melanogaster*." *Cell* vol. 147,3 (2011): 690-703. doi:10.1016/j.cell.2011.08.047
- Dunlevy, Kelly L et al. "The PRR14 heterochromatin tether encodes modular domains that mediate and regulate nuclear lamina targeting." *Journal of cell science* vol. 133,10 jcs240416. 27 May. 2020, doi:10.1242/jcs.240416
- Yang, M et al. "PRR14 is a novel activator of the PI3K pathway promoting lung carcinogenesis." *Oncogene* vol. 35,42 (2016): 5527-5538. doi:10.1038/onc.2016.93
- Shepard, Peter J, and Klemens J Hertel. "The SR protein family." *Genome biology* vol. 10,10 (2009): 242. doi:10.1186/gb-2009-10-10-242
- Finlan, Lee E et al. "Recruitment to the nuclear periphery can alter expression of genes in human cells." *PLoS genetics* vol. 4,3 e1000039. 21 Mar. 2008, doi:10.1371/journal.pgen.1000039
- Lim, Pek Siew et al. "Epigenetic control of inducible gene expression in the immune system." *Epigenomics* vol. 2,6 (2010): 775-95. doi:10.2217/epi.10.55
- Gaines, P., Tien, C. W., Olins, A. L., Olins, D. E., Shultz, L. D., Carney, L., & Berliner, N. (2008). Mouse neutrophils lacking lamin B-receptor expression exhibit aberrant development and lack critical functional responses. *Experimental hematology*, 36(8), 965–976. <https://doi.org/10.1016/j.exphem.2008.04.006>
- Subramanian, G., Chaudhury, P., Malu, K., Fowler, S., Manmode, R., Gotur, D., Zwerger, M., Ryan, D., Roberti, R., & Gaines, P. (2012). Lamin B receptor regulates the growth and maturation of myeloid progenitors via its sterol reductase domain: implications for cholesterol biosynthesis in

regulating myelopoiesis. *Journal of immunology* (Baltimore, Md. : 1950), 188(1), 85–102.
<https://doi.org/10.4049/jimmunol.1003804>

Wang, Y., Liu, C., & Hu, L. (2019). Cholesterol regulates cell proliferation and apoptosis of colorectal cancer by modulating miR-33a-PIM3 pathway. *Biochemical and biophysical research communications*, 511(3), 685–692. <https://doi.org/10.1016/j.bbrc.2019.02.123>

Vigouroux, C., Auclair, M., Dubosclard, E., Pouchelet, M., Capeau, J., Courvalin, J. C., & Buendia, B. (2001). Nuclear envelope disorganization in fibroblasts from lipodystrophic patients with heterozygous R482Q/W mutations in the lamin A/C gene. *Journal of cell science*, 114(Pt 24), 4459–4468. <https://doi.org/10.1242/jcs.114.24.4459>

Goelzer, M., Dudakovic, A., Olcum, M., Sen, B., Ozcivici, E., Rubin, J., van Wijnen, A. J., & Uzer, G. (2021). Lamin A/C Is Dispensable to Mechanical Repression of Adipogenesis. *International journal of molecular sciences*, 22(12), 6580. <https://doi.org/10.3390/ijms22126580>

Amendola, M., & van Steensel, B. (2015). Nuclear lamins are not required for lamina-associated domain organization in mouse embryonic stem cells. *EMBO reports*, 16(5), 610–617.
<https://doi.org/10.15252/embr.201439789>

En, A., Takauji, Y., Miki, K., Ayusawa, D., & Fujii, M. (2020). Lamin B receptor plays a key role in cellular senescence induced by inhibition of the proteasome. *FEBS open bio*, 10(2), 237–250.
<https://doi.org/10.1002/2211-5463.12775>

Fišerová, J., Efenberková, M., Sieger, T., Maninová, M., Uhlířová, J., & Hozák, P. (2017). Chromatin organization at the nuclear periphery as revealed by image analysis of structured illumination microscopy data. *Journal of cell science*, 130(12), 2066–2077.
<https://doi.org/10.1242/jcs.198424>

